Impact Assessment of Electric Vehicles and Micro-Generation Under Consideration of Domestic Household Loads in Typical Model Grids

Master Thesis

Institute of Electrical Power Systems
TU Graz

Author
Christian Flechl

Supervisor
Univ.-Prof. DI Dr.techn. Lothar Fickert

Mentor
DI Thomas Wieland

Head of the Institute: Univ.-Prof. DI Dr.techn. Lothar Fickert

A - 8010 Graz, Inffeldgasse 18-I
Telefon: (+43 316) 873 - 7551
Telefax: (+43 316) 873 - 7553
http://www.ifea.tugraz.at
http://www.tugraz.at

Graz / June - 2013

Acknowledgements

I would like to express the deepest appreciation to my supervisor Univ.-Prof. DI Dr.techn. Lothar Fickert and my mentor DI Thomas Wieland as well as the Institute of Electrical Power Systems at Graz University of Technology for their guidance and persistent help. This thesis would not have been possible without their support and engagement.

It is with immense gratitude that I acknowledge the support and help of the company Wien Energie Stromnetz GmbH, I am also exceedingly grateful to DI Dr.techn. Thomas Schuster and DDI. Andreas Bolzer.

In addition, I am indebted to my many friends, colleagues and family who supported me during this thesis.

Statutory Declaration

I declare that I have authored this thesis independently, that I have not used other than the declared sources / resources and that I have explicitly marked all material which has been quoted either literally or by content form the used sources.

Graz, 17.06.2013

Christian Flechl

Abstract

This diploma thesis is about the impact assessment of electric mobility in combination with decentralized energy production under consideration of domestic household loads onto low voltage grids. These low voltage model grids are represented by an urban, suburban and rural grid which are based on grid parameters of corresponding real grids. These model grids relate to the 20th district of Vienna (Brigittenau), Breitenfurt in Lower Austria as well as Grub, also located in Lower Austria. To examine the effects of Micro-Generation, primary photovoltaic, electric vehicles and domestic household loads onto these three types of grid areas, scenarios are established that determine the impact on the respective model grid. Therefore, three different types of scenarios are assumed that assess the year 2020, 2040 and 2060. In the scenario 2060 it is assumed that the entire individual traffic is exclusively based on electricity, photovoltaic will reach the maximum possible feed-in capacity and the domestic household loads are also increased significantly.

Kurzfassung

Diese Diplomarbeit beschäftigt sich mit der Folgenabschätzung von Elektromobilität in Kombination mit dezentraler Energieproduktion, unter Berücksichtigung von Haushaltslasten auf unterschiedliche Niederspannungsnetze. Diese Niederspannungsnetze sind Modellnetze, basierend auf realen Daten und werden durch ein städtisches, vorstädtisches und ländliches Netzgebiet repräsentiert. Diese können dem 20. Wiener Gemeindebezirk Brigittenau (städtisch), Breitenfurt (vorstädtisch) und Grub (ländlich) in Niederösterreich zugeordnet werden. Um die Auswirkungen von Mikro-Erzeugung, hauptsächlich Photovoltaik, Elektroautos und Haushaltslasten abschätzen zu können, werden drei verschiedene Szenarien entwickelt, die die Auswirkungen für das Jahr 2020, 2040 und 2060 abschätzen und die Auswirkungen im jeweiligen Netzgebiet festlegen. Im Szenario 2060 wird angenommen, dass der gesamte Individualverkehr ausschließlich auf Elektrizität basiert, Photovoltaik die maximale Einspeisekapazität erreicht und auch die Haushaltslasten deutlich zunehmen werden.

Table of Contents

1. Introduction

In the last decades decentralized energy production gained an increasing importance and the influence onto the power supply grids is growing steadily. This increase is challenging and requires amongst others the right measures to keep the quality of the voltage within their specified limits. In addition, to the increase of decentralized energy production, an increase in electric mobility will also gain further repercussions onto power supply grids. These loads cause additional loadings apart from the conventional household loads.

The aim of this master thesis is to examine the effects of a high share of decentralized energy production, primarily photovoltaic, in combination with a high share of electric mobility and conventional household loads onto power supply grids. To obtain the impact on various low voltage grids, three different types of grids are established that represent three types of areas. These areas are based on representative network structures and represent an urban, suburban and rural grid of Vienna and Lower Austria. Furthermore, three types of scenarios are applied to examine the effects in the year 2020, 2040 respectively 2060. For the scenario 2060 it is assumed that the individual traffic is entirely based on electricity, decentralized energy production will reach the maximum possible feed-in capacity under consideration of national standards (TOR - D2, EN 50160) and the household loads will also be increased significantly. For these scenarios load profiles are generated to carry out time-discrete load flow simulations for the respective model grid.

The master thesis starts with a general part about the fundamentals of electric vehicles such as types of electric vehicles, types of batteries used in these vehicles and their charging behavior. The next chapter 'Load Profile Development' is about generating load and feed-in profiles that are required for the load flow simulation. Therefore, three different types of profiles are generated that represent the conventional household-loads, the impact of electric mobility as well as the impact of decentralized energy production (micro-generation), primarily photovoltaic. The chapter 'Model Grids' deals with developing three different types of characteristic

model grids that represent an urban, suburban and rural grid. The 'Simulations' chapter deals with simulating theses three model grids (urban, suburban, rural) with different types of scenarios that assesses the year 2020, 2040 and 2060. Based on these scenarios, load flow simulations are performed by NEPLAN® to obtain the impact onto power supply grids such as voltage drops and working loads of transformers and lines. In the context of this thesis the following research questions came up:

- How massive are the transformer and line loadings due to household loads, electric mobility and micro-generation in the respective power supply grid for each scenario (2020, 2040, 2060)?
- In which range is the voltage drop/rise in the respective power supply grid for each scenario (2020, 2040, 2060)?
- Which measures can be taken into account to reduce the impact onto the low voltage grids?

Figure 1.1 gives a rough overview of this thesis.

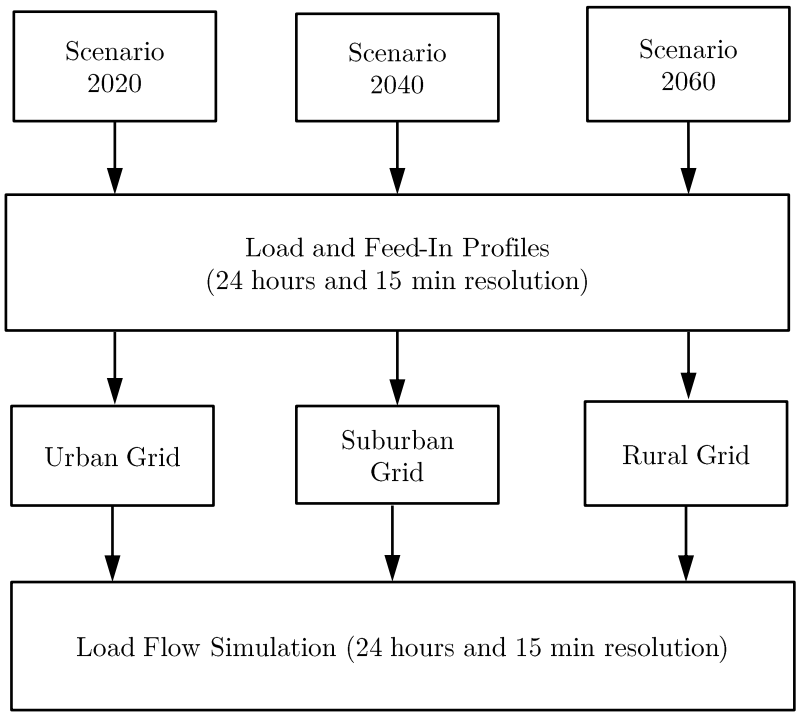

Figure 1.1.: General thesis overview with various scenarios (2020, 2040 and 2060), model grids (urban, suburban and rural) and load flow simulation

2. Fundamentals of Electric Vehicles

The following sections give an overview about the fundamentals of electric cars, starting with some important milestones in the history, followed by types and characteristics of electric cars, differences compared to conventional cars and about charging procedures. A in-depth comprehension of these fundamentals is required for building up a model to examine the impact of electric vehicles on power supply grids. The term electric vehicle (EV) refers to any type of vehicle that propulsion is powered by electricity. In this thesis the term electric vehicle only refers to road-going automobiles. These vehicles are supposed to be quite similar to internal combustion engine cars in terms of size and weight, that are used nowadays. Most of the ultra light weight concept cars of electric vehicles can not compete with conventional cars in terms of comfort and safety. In this thesis it is assumed that electric vehicles are not such ultra light-weight concept cars but have a similar actual energy consumption like conventional cars. It is also assumed that the power source of electric vehicles is primary an on-board battery and not powered by other sources like gasoline generators, sunlight (solar car) or fuel cells. The effort of other energy sources except of electricity would not cause any relevant effects onto power supply girds and therefore, it would not have any effect on this thesis. [1]

2.1. History

The history of the electric vehicle began 1834, that is, about 60 years earlier than gasoline-powered cars. In the late 19th century and early 20th century, electric vehicles gained acceptance when electricity was among the preferred methods for automobile propulsion. At that time, cars with combustion engines were not easy to use and could not provide a level of comfort that could be achieved by the first electric cars. The invention of the electric vehicle is attributed to various people and was achieved in small steps. In the early history of electric cars, they held many speed and distance records. A remarkable record was the breaking of the 100 km/h speed barrier by Camille Jenatzy on April 29, 1899.

Also notable was the world's first hybrid electric car in 1898, that was built by Dr. Ferdinand Porsche, using an internal combustion engine to spin a generator that provided power to electric motors located in the wheel hubs. Another hybrid vehicle, made by Krieger Company in 1903, used a gasoline engine to supplement the power of the electric motor which used electricity from a battery pack.

Due to advances in combustion engine technology, electric cars became less important. Considerable inventions, especially electric starters in 1911 increased the comfort of using combustion engine cars. Advantages, such as refueling time, steadily improved infrastructure for fuel as well as greater range compared to electric cars led to a worldwide decline in their use. Companies such as Ford Motor Company established the mass production of cars that enabled low prices and gained a share of the market. These mass production cars were priced at half of the price of electric cars. Additionally, rural areas had limited access to electricity to charge the batteries. As a consequence, the electric car disappeared from the market.

In the 1960s electric cars started to reappear primarily due to environmental hazards caused by emissions of gasoline-powered vehicles. The most important car manufacturers, General Motors and Ford became involved in electric vehicle research and development. As a consequence General Motors developed electric vehicles such as Electrovair and Electrovan. The Electrovair had a three-phase-induction motor with 115 hp and 13 000 rpm. The battery was a silver-zinc battery with 512 V. Electrovair reached a top speed of 129 km/h and had a range of approximately 100 km. The performance and acceleration could compete with conventional cars of that time but the battery-pack was too expensive, had a too short cycle life and required quite long for recharge. However, with the 1960s technology it was not possible to build a commercially successful electric vehicle.

In the early 1970s the gasoline price increased dramatically due to energy crises. In 1973 the Arab oil embargo increased demands for alternative energy sources. As a consequence, the interest in alternative methods for automobile propulsion increased. In addition, it became highly desirable to be less depended on foreign oil.

The 1980s and 1990s led to improvements of high power, high frequency semiconductor switches and power converter design. That improvements contributed to drive the electric motors more efficiently.

In the early 1990s electric cars were developed by most of the mayor car manufactures within a few years such as General Motors (EV1), Toyota (RAV4), Ford (Ford Ranger), Volkswagen (Volksstrom), Fiat, Citroen and Peugeot. These cars were built in tiny numbers and remained a niche product. Unfortunately the market for battery electric cars declined in the late 1990s due to the following possible reasons.

Reasons for the decline of the electric vehicle industry:

- Limited range of electric cars (most of them provided a range under 150 km) compared to conventional cars powered by gasoline
- Insufficient battery technology in terms of capacity, cycle life, weight and costs
- Long charging time of batteries (lead-acid batteries) up to 10 hours
- High purchase price
- Fuel costs of conventional cars is insignificant in comparison of the purchase price of electric cars
- Conventional cars such as pickups and SUVs were supposed to be superior in safety reasons
- Due to high development and research costs electric cars were uneconomic for car manufacturers
- Limited charging infrastructure

A greater environmental consciousness, growing concern over the problems associated with hydrocarbon fueled vehicles, including damage to the environment caused by their emissions, increasing fuel prices as well as improved technology in terms of battery and propulsion lead to a reappearance of electric cars in recent years. The higher initial costs compared to internal combustion engine cars are the major obstacles for a high penetration of electric vehicles. [2][3]

Obstacles for a succeed of electric cars:

- Breakthrough in battery technology is required for a large-scale deployment of electric vehicles
- Costs of electric vehicles have to be cut down significantly

- Rapid charging infrastructure and an appropriate grid infrastructure
- Policies according to taxation and standardization are required

2.2. Types of Electric Vehicles

A battery electric vehicle (BEV) is a car powered by an electric motor, typically powered using energy stored in batteries. To increase the maximum distance of battery electric vehicles, range extenders are used. This type of car is known as range-extender electric vehicle (REX). Electric vehicles that not exclusively use electric motors for propulsion are known as hybrid electric vehicle (HEV). These cars combine a conventional internal combustion engine propulsion system with an electric propulsion system. When the internal combustion engine and the electric motor are connected in series, the hybrid electric vehicle is a series hybrid in which only the electric motor delivers mechanical power to the wheels. When they are connected parallel, the hybrid electric vehicle is a parallel hybrid in which both the elctric motor and the internal combustion engine can provide mechanical power to the wheels. Hybrid electric vehicles can be divided in mild-hybrid electric vehicles respectively full-hybrid electric vehicles and plug-in-hybrid electric vehicles. Furthermore, they can be classified according to the way in which power is supplied to the drivetrain or by degree of hybridization. [1][4]

2.2.1. Mild-Hybrid Electric Vehicle and Full-Hybrid Electric Vehicle

Hybrid electric cars connect the advantages of combustion engine vehicles with the advantages of electric vehicles. They combine a practical long distance car for long journeys with an electric car especially for urban areas. Mild hybrids are essentially conventional vehicles with some degree of hybrid hardware, but with limited hybrid feature utilization. This cars use the combustion engine all time and cannot be used in ”electric car” only mode. Typically the structure is a parallel hybrid system with only a start-stop functionality or in combination with modest levels of engine assist or regenerative braking features. It is normally not possible with mild hybrids to propel a car entirely by electric motors. [1][4][5]

2.2.2. Plug-In-Hybrid Electric Vehicle - PHEV

A plug-in hybrid electric vehicle (PHEV) is a hybrid electric vehicle with rechargeable batteries and can be plugged into an electrical outlet to full charge the batteries. A plug-in hybrid electric vehicle shares the characteristics of both a conventional hybrid electric vehicle, having an electric motor and an internal combustion engine. They are able to run in electric-only mode as BEVs during their charge-depleting mode and have the ability to recharge from the electric power grid compared to normal hybride electric vehicles. Their main benefit is that they can be gasoline-independent for daily use, but also have the extended range of a hybrid for long distances. Plug-in hybrid electric vehicles with a series powertrain are also called range-extended electric vehicles (REEVs). The structure of REEVs is similar to battery electric vehicles but have a generator that produces electric energy to extend the maximum range limited by battery capacity. This generator can be propelled by a small combustion engine or gas turbine.[1][4]

2.2.3. Battery Electric Vehicle - BEV

The concept of battery electric vehicles is to use charged batteries for propulsion. They are increasingly more attractive with the advancement of new battery technology such as lithium-ion that have higher power and energy density. They provide greater possible acceleration and more range with fewer batteries.
Electric cars often have great acceleration and generally acceptable top speed, however, the lower specific energy of batteries compared with carbon-based fuels mean that the battery mass of electric cars is considerable greater than the mass of the entire filled tank of conventional cars and frequently provide lower range than achievable with a filled tank.
Electric cars have the potential of significantly reducing city pollution by having zero direct emissions. This reduction obviously depends on how the electricity is generated. With the current energy mix, using an electric car would results in a up to 40 % reduction in carbon dioxide emissions. If the entire electricity is provided by renewable energy sources the operation of electric cars could be completely carbon dioxide emission neutral. [1][4]

2.3. Comparison with Internal Combustion Engine Vehicles

Electric cars can offer significant benefits over conventional cars in terms of construction and power delivery thus they are not for everyone and every application. The heart of an electric car is the electric motor that provides some advantages compared to an internal combustion engine such as maximum power and a high torque from a standing start. The electric car pulls away smoothly and quickly with less vibration from the motor, is exceptionally quiet and provides a pleasant driving experience. The electric motor has an efficiency of about 90 % compared to 25 - 35 % to a combustion engine. Most of the electric cars do not have a conventional gearbox that are used in combustion engine cars. Electric cars often have a gearless or single gear design that eliminates the need for gear shifting. This delivers smoother acceleration, instant power whenever it is required and smoother braking. The torque of an electric motor is a function of current and therefore provide a high torque over a large range of speeds during acceleration compared to an internal combustion engine. The less complex design of an electric vehicle is the gearless design which requires high currents for high torques. These high currents heat up the motor and result in a lower efficiency. The torque of the electric motor is not depending on its rational speed but the output power is the product of both the torque and the rational speed. This effects a higher relatively lost in proportion to the output power at lower speeds and the electric car becomes less efficient. However, the single gear design provides a higher efficiency at lower speeds due to a gear ratio that allows the motor to turn faster than the wheel. This gear ratio translates low torque and high rotational speed of the electric motor into a higher torque and lower rotational speed at the wheels. The single gear design achieves better acceleration but lower top speed compared to the gearless design. A multiple-speed transmission combines the advantages of the gearless and the single gear design and operates efficiently at low and high speeds but is more expensive. [5]

At low speeds, electric cars are more responsive with predictable power delivery. This power reserves are useful for safer overtaking and makes it easy to drive in heavy stop-start-traffic. Especially at low speeds the electric car is very efficiently and the driver does not need to worry about the clutch or gearbox. This smooth ride can also help people which suffer from travel sickness. The braking system can contribute to recharge the battery when slowing down. The forward momentum of the electric car is used to recharge the battery. Therefore the mechanical braking

system is often only required under heavy braking. The result is a more flowing transition between accelerating and braking. [5]

Electric cars are superior in inner city use but have some disadvantages at longer and faster journeys. The actual amount of power that is needed depends on the speed. Therefore, when driving at high speeds the possible distance per charge declines significantly compared to a low speed inner city use. The most suitable fields of electric mobility are in urban and suburban environments where speed is limited with a lot of stop-start-traffic. Due to advantages in battery technology electric cars are also suitable for longer distances and higher speeds in recent years. For example the Tesla Roadster has a range of up to 380 km and a top speed of 216 km/h. The average distance of most electric cars of today is between 60 and 160 km and is far more as is actually needed for most of the travels per day. According to Statistik Austria the average distance by car and per day is about 36 km depending on the area. About two-thirds of all journeys are less than 40 km and about 90 % of all journeys is less than 100 km. Under consideration that most of the people that buy an electric car in the US replace the second car in the family and therefore the range issue has no importance anymore. [5][6]

2.3.1. Cost-Effectiveness, Running Costs and Maintenance

Due to high costs for batteries the purchase price of electric cars is significantly higher than for conventional internal combustion engine cars. The high costs are the primary obstacle of establishing electric cars.

In 2010 the results of a survey indicated, that around three quarters of American and British car buyers would consider buying an electric car, if it would not be more expensive than a conventional car. The survey showed that most of the people are not willing to pay more for an electric car above the price of a conventional car. [7] The running costs refer mainly to charging the battery. The biggest cost saving with an electrical car is a reduction in fuel costs. Instead of paying for fuel at a gas station, an electric vehicle can be charged by using off-peak electricity. To provide a complete charge, most electric vehicles use between 8 and 24 kWh of electricity.

According to a study published in 2011 the original costs of PHEVs inclusive fuel costs over their lifetimes cannot compete with normal gasoline powered cars with higher fuel consumption. This study takes no subsidies into account and estimated that battery electric vehicles are less expensive than PHEVs over their lifetimes. Due

to increasing gasoline prices and decreasing battery costs, the battery electric vehicle will even be notable more economic than conventional cars in the next decades. The maintenance costs of electric cars are very low compared to gasoline powered cars that have a lot of parts that require replacement during their lifetime. [1][4]

2.3.2. Range and Recharging Time

Electric cars can be considered to have limited range depending on the battery capacity whereas gasoline-powered cars have a indefinite range. Conventional cars can be refueled within minutes whereas the charging process of electric cars takes hours. The charging time especially depends on the battery capacity and the available charging power. Therefore, the complete recharging process fluctuates typically between half an hour at fast charging stations with a suitable high power supply and up to 15 hours with standard 230 V and 16 A outlets which corresponds to 3,7 kW at single phase outlets. In this thesis a charging power of 3,7 kW for electric cars is assumed and use a three-phase outlet with symmetric loading instead of a two-phase outlet. Nevertheless charging at fast charging stations it is still more time consuming compared to refueling a car.
Instead of charging the batteries the relatively short range of electric cars can be extended by a battery switch system. The battery change is examined at a battery switch station and replaces automatically the depleted battery with a fully charged battery. This process takes only about one minute similar to refueling a conventional car. However, this battery switch stations requires high infrastructure costs for building up such a system. [1]

2.3.3. Cabin Heating and Cooling

Due to higher efficiency of electric cars only little waste heat is generated that can be used to heat the interior. Simple heating could be provided by an electrical resistance heater. A higher efficiency can be achieved with a reversible heat pump. To avoid impacting the electric car range some models provide a pre-heating when the car is plugged in to reduce the impact on range. Other systems use auxiliary heating systems such as gasoline-fueled heaters. The cooling could be particularly achieved with solar power to avoid extreme heat buildup in the cabin. [1]

2.4. Energy Storage

Batteries are considered to be the most expensive component of battery electric vehicles and currently cost approximately half of the retail costs. The costs of batteries are substantial and despite reducing the cost through higher volumes, the costs still remain too high. The future of battery electric vehicles depends primarily upon the cost and availability of batteries with high specific energy, power density, and long life. [8]

2.4.1. Lead-Acid

Lead-acid batteries are the oldest and cheapest type of rechargeable batteries and are the most common traction batteries available. They have a very low energy-to-weight ratio and a low energy-to-volume ratio. Lead-Acid batteries maintain a relatively large power-to-weight ratio and are attractive for use in motor vehicles to provide the high current required by automobile engine starter motors. The specific energy density of 30-40 Wh/kg is quite low compared to other battery types. No lead-acid battery should be discharged below 50 % of its capacity, not to shorten the battery's life.[4][8]

2.4.2. Nickel-Metal-Hydride

The enhancements of nickel-hydrogen batteries led to the development of Nickel-Metal-Hydride batteries. The positive electrode is metal hydride and the negative electrode consists of a compressed mass of fine metal particles. The metallic alloy can absorb a large number of hydrogen molecules under certain temperature and pressure to from the metal hydride. Nickel-metal hydride batteries are now considered a relatively mature technology. The disadvantage compared to other battery types is the bad efficiency (60 - 70 %) in charging and discharging and is even worse than lead-acid but provide an energy density of 60 - 80 Wh/kg, much higher than lead-acid. The specific power of NiMH batteries can be up to 250 W/kg. These batteries can have considerably long lives if they are used properly. For example the Toyota RAV4 uses NiMH batteries and still operates well after nearly 200 000km. [3][4][8]

2.4.3. Zebra

Molten salt batteries are high-temperature electric batteries that uses molten salts as an electrolyte. The sodium or zebra battery consists of a molten chloroaluminate sodium as the electrolyte and is a relatively mature technology. The zebra battery is used where high energy density and high power density is required and has an energy density of 120 Wh/kg. Since the battery must be heated for use in any case, cold weather doesn't strongly affect its operation. Zebra batteries operate typically at a temperature range of 245 °C to 350 °C. [4][8]

2.4.4. Lithium-Ion

Lithium-ion batteries are the most recent type of battery in electric vehicles. The traditional lithium-ion chemistry involves a lithium cobalt oxide cathode and a graphite anode. Lithium has a high electrochemical reduction potential relative to that of hydrogen and the lowest atomic mass which results in 3 V cell potential. This cells have a high energy density ($>$ 200 Wh/kg) as well as high power density, and up to 90 % charge and discharge efficiency. The disadvantages of traditional lithium-ion batteries are rather short cycle lives (hundreds to a few thousand charge cycles) and significant degradation with age. Lithium-ion batteries can pose a fire safety risk if they are damaged or charged improperly. [3][4][8]

2.5. Charging Process

Batteries in electric vehicles must be periodically recharged. The charging process is most commonly performed at home. Charging time is limited primarily by the capacity of the grid connection. For most electric cars in Europe, the charging point required is normally a standard domestic power socket and delivers 3,7 kW. Many European countries feed domestic consumers with a 3 phase system fused at 16 - 25 A that allows a theoretical capacity around 11 - 17 kW. However, this capacity is also required to feed all other electric devices of this lateral. Fast charging is going to be the key for the development of a mainstream market. Even if the supply power can be increased, most batteries do not accept charging at greater than their charging rates, because that could have adverse effects on the discharge capacities of batteries. [1][3][4]

3. Load Profile Development

This chapter is about developing load profiles for electric vehicles and households respectively, feed-in profiles for photovoltaic generation to enable time-discrete load flow simulations with Neplan®. Three different types of model grids are used to represent an urban, suburban and rural grid based on real network parameters such as line lengths or types of cables. The urban grid represents the 20th district of Vienna (Brigittenau), the suburban grid represents the area around Breitenfurt and rural grid is based on the area of Grub nearby Breitenfurt. To determine the realistic impact of loads and feed-in capacities onto the model grids in the respective area, it is necessary to establish load profiles that represent the charging process of electric vehicles, load profiles that determine the impact of conventional household loads and feed-in profiles that represent the impact of decentralized energy production such as micro-generation, primary photovoltaic. For each of these loads, respectively feed-in capacities a respective profile is generated by an algorithm. The following sections gain an in-depth view about these algorithms and generating these three types of profiles.

3.1. Load Profiles for Battery Electric Vehicles (EV)

3.1.1. General about EV-profiles

Individual traffic is almost entirely carried out by combustion-engine-driven vehicles. In the next few decades it is assumed that the share of electric vehicles will increase steadily. This increase will cause a growing impact onto power supply grids, thus, today the impact of electric vehicles onto the power supply grid is insignificant. To approach a realistic simulation, three different scenarios are established that represent the usage of mobility based on electricity in the year 2020, 2040 respectively 2060. Table 3.1 depicts these assumed scenarios.
In the scenario 2020 it is assumed that electric vehicles will reach a share of 10 % according to 100 % of today's entire motor-driven individual traffic. In the year 2040

Table 3.1.: Share of electric vehicles for different scenarios

	Scenario 2020	Scenario 2040	Scenario 2060
Share of electric vehicles	10%	40%	100%

a share of 40 % is assumed, respectively, 100 % for the year 2060. A share of 100 % represents the entire change to electric mobility based on the mobility behavior of today.

In the last few decades, individual mobility increased steadily according to Statistik Austria [6]. It is assumed that this increase will be also continued for the next further decades. Therefore, the actual share of individual mobility for the scenario of 2060 could be higher than supposed in the considered simulation scenario. However, in the year 2060 it is assumed that the entire motor-driven individual traffic is exclusively based on electricity so that the assumption of 100 percent electric mobility in the year 2060 based on the data of today seems to be realistic. That is the reason why a constant and not increasing mobility behavior is the basis of these scenarios. To generate profiles that represent realistic electric vehicle loads, an in-depth appreciation of mobility behavior is required. First, a differentiation between urban, suburban and rural areas are necessary. Therefore a distinction is drawn between mobility behavior in these respective areas. Second, as accurate data as possible are required to describe the mobility behavior. Third, based on these data a stochastic usage of electric vehicles per household for a certain period of time (24 hours) with a resolution of 15 min is generated by an algorithm. A resolution of 15 min leads to 96 intervals to describe 24 h respectively an entire day. This resolution is accurate enough for the simulation to examine the impact onto power supply grids in dependency of time. The usage of electric vehicles refers to the amount of energy that is required to recharge them to 100 % SOC again. This amount of recharging energy per each household depends on various factors such as quantity and type of electric vehicles or the covered distance per day. Furthermore, the charging power, the duration of charging as well as the time of starting the charging process are relevant to examine the impact. Figure 3.1 indicates the most important factors of influence about the energy consumption of electric vehicles and interrelation onto power supply grids such as the time of starting the charging process, the charging power as well as the charging duration. The charging duration depends on the charging power and the other way round.

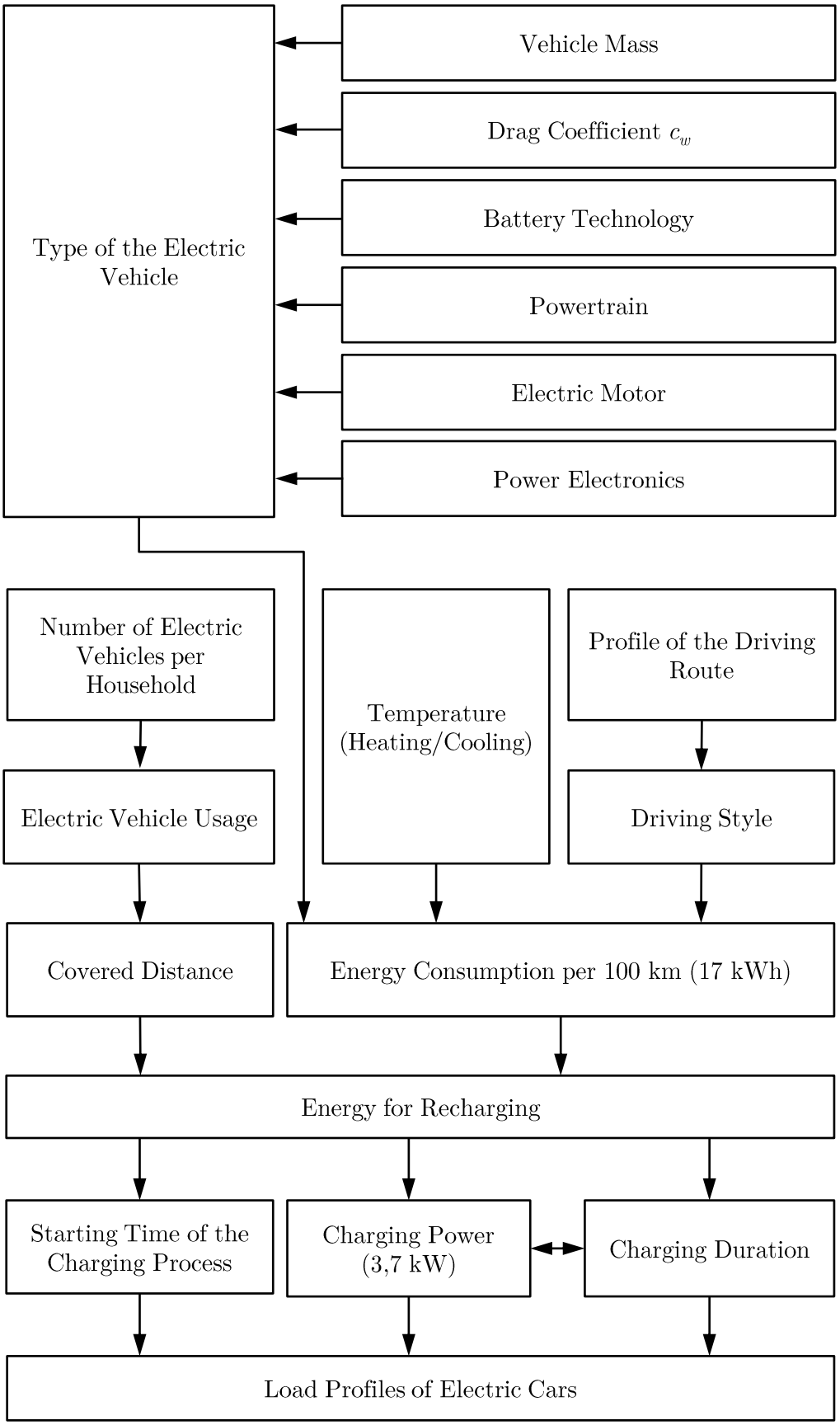

Figure 3.1.: Factors of influence for the impact onto power supply grids

To describe the mobility behavior in all three different areas as realistic as possible, accurate data about the frequency of usage, number of cars per household and driven distances per day are needed. To get these data, further information about the average size of households (occupants per household) and average distances driven by car per day as well as data about the average number of cars per 1000 inhabitants are required. The table 3.2 indicates the data obtained from Statistik Austria [6].

Table 3.2.: Data about average distances, number of cars and sizes of households

		Average distance by car per day $\bar{d}_c$	Cars/1000 inhabitants $\bar{n}$	Size of households $\bar{h_s}$
		km/day	-	-
Country	Austria	36	537	2,28
City	Vienna	35	393	1,99
State	Lower Austria	36	619	2,37
Urban	Brigittenau	35	309	1,95
Suburban	Breitenfurt	36	649	2,23
Rural	Grub	36	649	2,68

The first three data lines in table 3.2 gain an overview about the general mobility behavior in Austria, Vienna and Lower Austria. These data correspond to the more accurate data for Brigittenau, Breitenfurt and Grub. Lower Austria has one of the highest number of cars per 1000 inhabitants in Austria. Especially, the district of Mödling, in which Breitenfurt and Grub are located, has the fourth highest number of cars per 1000 inhabitants in Austria (649 cars). Unlike Mödling, the district of Brigittenau has the 2nd lowest number of cars per 1000 inhabitants in Austria (309 cars) [9]. The actual average driven 'distance by car per day' ($\bar{d}_c$) is nearly identical in urban, suburban and rural areas. The average distance in urban areas is about 35 km/day and 36 km/day in suburban and rural areas. [10] Only the number of cars per 1000 inhabitants are considerable varying. As shown in table 3.3, the 'number of households per 1000 inhabitants' ($\bar{h_i}$) is calculated by dividing 1000 by the 'average size of the household' ($\bar{h_s}$) in equation 3.1.

$$\bar{h_i} = \frac{1000}{\bar{h_s}} \tag{3.1}$$

To obtain the 'average number of cars per household' ($\bar{c_h}$), the 'number of cars per 1000 inhabitants' ($\bar{n}$), as shown in table 3.2, is divided by the result of 'number of households per 1000 inhabitants' ($\bar{h_i}$) according to equation 3.2.

$$\bar{c_h} = \frac{\bar{n}}{\bar{h_i}} \tag{3.2}$$

In the next step the result of 'cars per household' ($\bar{c_h}$) is multiplied by the 'average distance by car per day' ($\bar{d_c}$) to obtain the 'distance per household and day' ($\bar{d_h}$). This result is the most relevant data and forms the basis for the simulation algorithm of the urban, suburban and rural areas and is resulting in equations 3.3.

$$\bar{d_h} = \bar{c_h} \cdot \bar{d_c} \tag{3.3}$$

$\bar{d_c}$	Average distance by car per day
$\bar{n}$	Average number of cars per 1000 inhabitants
$\bar{h_s}$	Average size of households
$\bar{h_i}$	Number of households per 1000 inhabitants
$\bar{c_h}$	Average number of cars per household
$\bar{d_h}$	Average distance per household per day

By combining equation 3.1, 3.2, and 3.3 the 'average distance per household per day' ($\bar{d_h}$) can be calculated directly.

$$\bar{d_h} = \frac{\bar{n} \cdot \bar{h_s} \cdot \bar{d_c}}{1000} \tag{3.4}$$

The results of calculating the 'average distance per household per day' for the urban (Brigittenau), suburban (Breitenfurt) and rural (Grub) areas are depicted in table 3.3.

The average usage of cars per household differs significantly in the respective areas. In the urban area (Brigittenau) only an average distance of 21,09 km is covered per household unlike to 62,66 km in the rural area (Grub). The average covered distance in the suburban area is 52,14 km and therefore closer to the rural area.

3.1.2. Algorithm for the EV Load Profile Generation

The algorithm to generate the load profiles consists of six main steps in which partly further calculations are added. For each household in the respective area the profiles are calculated separately. Each lateral in the urban grid consists of 20 households

Table 3.3.: Distances of various areas ($\bar{d_h}$)

		Households/1000 inhabitants $\bar{h_i}$	Cars per household $\bar{c_h}$	Distance/HH per day $\bar{d_h}$
		-	-	km/day
	Austria	439	1,22	44,1
	Vienna	5031	0,78	27,4
	Lower Austria	422	1,45	52,2
Urban	Brigittenau	513	0,60	21,1
Suburban	Breitenfurt	448	1,45	52,1
Rural	Grub	373	1,74	62,7

and therefore the algorithm has to be repeated 20 times corresponding to the number of households. The results of every round are added up. Finally, after going through the algorithm 20 times, the sum refers to the amount of energy that is actually required for mobility by 20 households. In the suburban grid a single lateral corresponds to a single household. Therefore, only a single run through the algorithm is required. According to the rural grid, a single households correspond to a single lateral.

This load generation algorithm is realized with Microsoft Excel® and Microsoft Visual Basic®. The following illustration 3.2 indicates the main steps of generating the load profiles for battery electric vehicles. These profiles reflect the real mobility behavior per household in the respective areas for the scenario 2060. In this scenario it is assumed that the entire mobility based on combustion engines is transformed to mobility based on electricity. For the scenario 2020 only a share of 10 % respectively 40 % for the scenario 2040 is assumed to be based on electricity.

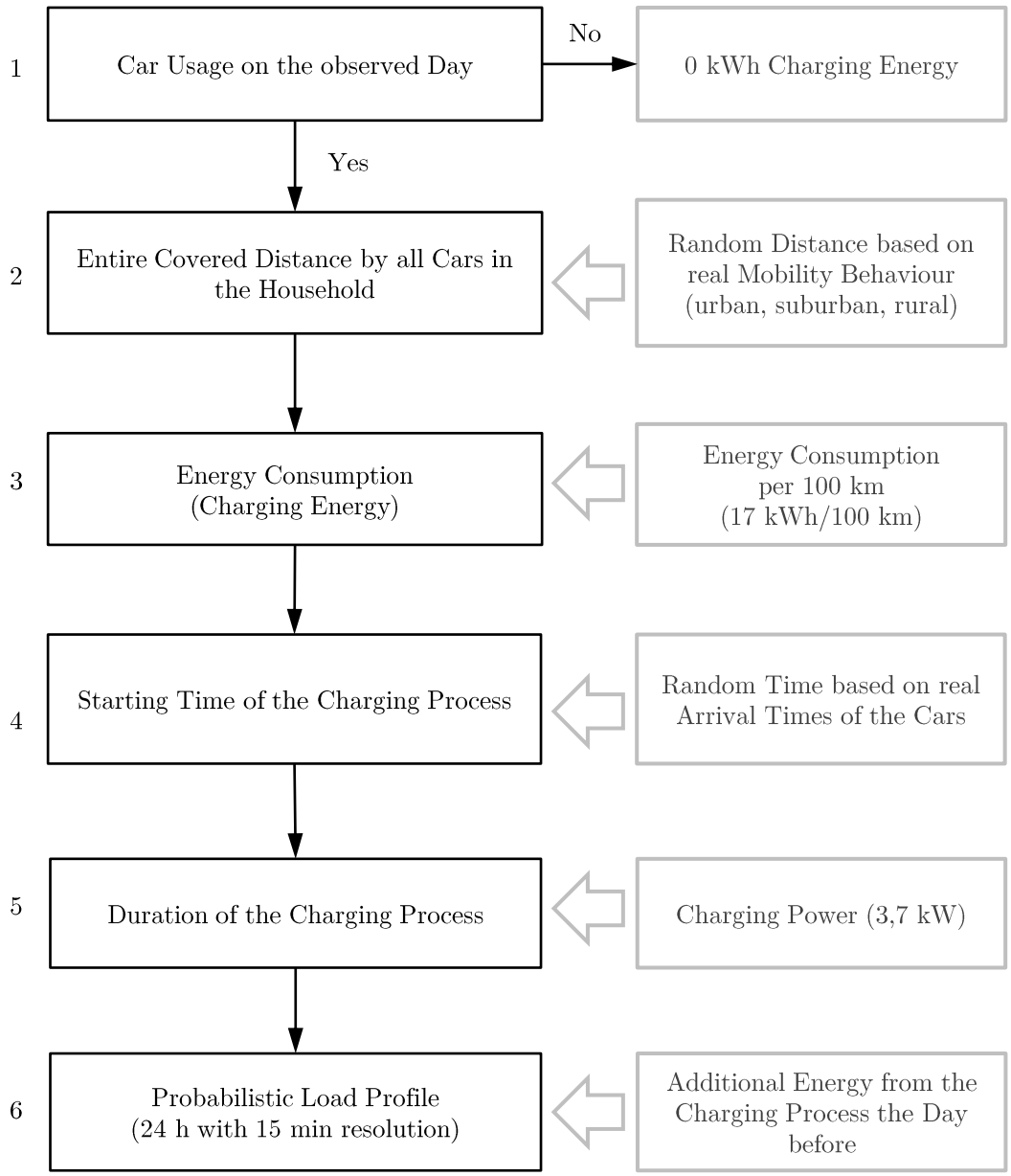

Figure 3.2.: Flow chart of the load profile generation

The first step of the algorithm refers to the usage of cars in the respective households. The average probability of using the car at a certain day is about 70 %. The entire average distance covered by all cars per household on a single day is 35 km for Vienna and 36 km for Lower Austria. The actual covered distances can be determined by the a discrete distribution in table 3.4 [11].

Table 3.4.: Probability of driven distances

range	0 - 1 km	1 - 10 km	10 - 20 km	20 - 40 km
p_i	3,5 %	24,3 %	18,0 %	20,9 %
$\bar{d}_i$	0,5 km	5,5 km	15,0 km	30,0 km
w_i	1,8	133,7	270,0	627,0
range	40 - 65 km	65 - 100 km	100 - 200 km	200 - 300 km
p_i	12,9 %	8,7 %	6,7 %	5,0 %
$\bar{d}_i$	52,5 km	82,5 km	150,0 km	250,0 km
w_i	677,3	717,8	1005	1250,0

p_i	Probability of matching the range
$\bar{d}_i$	Average distance in km
w_i	Weight that corresponds to $p_i/100 \cdot d_i$

The first line of table 3.4 depicts the range of distance with its respective probability p_i of occurrence in the second line. The average distance $\bar{d}_i$ is the average distance within its range. The weight w_i corresponds to the multiplication of p_i and $\bar{d}_i$. This discrete distribution indicates the frequency of covered distances. For example, the probability of driving a distance between 1 and 10 km is about 24,3 % on condition that at least one car in the household was used.
Calculating the expected value E(D) (equation 3.5) of the distribution shown in table 3.4:

$$E(D) = \sum_{i=1}^{8} \bar{d}_i \cdot \frac{p_i}{100} = \sum_{i=1}^{8} \frac{w_i}{100} \tag{3.5}$$

$$\begin{aligned} E(D) = 0.5 \cdot 0,035 \ + \ 5.5 \cdot 0,243 \ + \ 15 \cdot 0,18 \ + \ 30 \cdot 0,209 + \\ + \ 52,5 \cdot 0,129 \ + \ 82.5 \cdot 0,087 \ + \ 150 \cdot 0,067 \ + \ 250 \cdot 0,05 \ = \\ = \ 46,82 \ km \end{aligned} \tag{3.6}$$

$E(D)$	Expected value of the average distance referred to the distribution
$\bar{d}_i$	Average distance in km
p_i	Probability

The expected value (average distance) of the entire distribution is 46,82 km according to table 3.4.

To get the desired distance at a single day per household, a random number R1 between 0 and 100 is calculated that defines the range of distance according to the discrete distribution in table 3.4. The probability of driving a distance of less than one kilometer is 3,5 percent. If the random number R1 is less than or equal to 3,5 the distance is between 0 and 1 km. The probability of driving a distance between 1 km and 10 km is 24,3 %. Therefore the random number R1 must be greater than 3,5 and less than 27,8. The probability of 24,3 % is added to the previous probability of the range, in this case 3,5 % to define the correct range between 3.5 % and 27,8 %. This procedure is repeated analogous for the next ranges.

To obtain the distance when calculating a second random number R2 according to a higher range of distances, for example 71,32 according to the limits between 0 and 100, the matching range of distance is 40 - 65 km because $66,7 \leq 71,32 \leq 79,6$ according to table 3.4.
As mentioned before, the lower probability limit of 66,7 % is analogous to the sum of the previous probabilities such as 3,5 %, 24,3 %, 18 % and 20,9 %. This sum is 66,7 %, and when adding the next probability respectively the considered range of 12,9 %, the upper limit is 79,6 % because the sum of 66,7 % and 12,9 % is equal to 79,6 %. Table 3.5 explains this context.

Table 3.5.: Probability for driving 41,32 km with a random number R2 of 71,32

matching range	40 - 65 km
limits of probability	66,7 % - 79,6 %
probability of matching the range p_i	12.9 %
average distance of the respective range in km $\bar{d}_i$	52,5
w_i	677,25

p_i	Probability of matching the range
$\bar{d}_i$	Average distance in km
w_i	Weight that corresponds to $p_i/100 \cdot d_i$

Within the considered range of 40 km - 65 km, another random number R3 is calculated that defines the accurate distance within the limits imposed by the previous random number. The range between the limits correlates to an even distribution. Therefore, the additional random number for example is 0,578 within the limits 0

to 1. The range between 40 km and 65 km is 15 km (upper limit minus lower limit). The distance of 15 km refers to a random number of 1 because a random number of 0 refers to 0 km. It is obvious that the calculated random number R3 of 0,578 refers to a distance of 15 km multiplied by 0,578 (15 km · 0,578 = 8,67 km). The result is 8,67 km (B) and is added to the lower distance range of 40 km (A). Therefore, the actual calculated distance is the sum of the lower distance limit of the considered range (A) and the additional calculated auxiliary-distance between the range of 8,67 km (B). The result is a distance of 48,67 km (A + B = 40 km + 8,67 km = 48.67 km) for the respective household per day. This distance is quite similar to the expected value of 46,82 km and represents a typically covered distance per household within 24h.

The energy consumption of the electric vehicle depends on various factors of influence and fluctuates steadily. This fluctuations especially depend on the profile of the driving route and cooling/heating the electric vehicle. When driving only a short distance with the electric vehicle, in winter the additional amount of energy required for heating the vehicle is relatively high compared to the amount of energy that is required when driving a long distance. To keep only a constant temperature in the vehicle, less energy is required compared to heating up the vehicle. On the assumption that the vehicle has an energy consumption of 17 kWh per 100 km, the average actual mobility behavior is reflected exactly.

The calculated distance of 48,67 km is now multiplied by the energy consumption per 100 km. As mentioned in the fundamentals (chapter 2) the average energy consumption per 100 km is assumed to be 17 kWh. To obtain the actual energy consumption of the covered distance, the calculated distance of 48,67 km is multiplied with 17 kWh/100 km as shown in equation 3.7.

$$W_i = d_i \cdot \frac{W_i}{100} = 48,67\ km \cdot 17\ kWh/100\ km = 8,27\ kWh \tag{3.7}$$

W_i	Energy consumption of the electric vehicle
d_i	Traveled distance in km

The result is 8,27 kWh, this amount of energy is required to recharge the electric vehicle to 100% SOC. The efficiency of the charging process is considered by the actual energy consumption per 100 km of the electric vehicle. It is assumed that the charging power rate is 3,7 kW. The duration of the charging process is calculated

by dividing the charging energy of 8,27 kWh with the charging power of 3,7 kW (equation 3.8).

$$t_i = \frac{W_i}{P_i} = \frac{8,27\ kWh}{3,7\ kW} = 2,24\ h = 2\ h\ 15\ min \tag{3.8}$$

W_i	Energy consumption of the electric vehicle
t_i	Duration of the charging process
P_i	Power of charging

The result is 2,24 hours or 2 hours and 15 min. The charging power and duration defines the impact of the electric car onto the power supply grid.

According to a paper about 'Probabilistic load modeling and simulation for households and electric vehicles for voltage band analysis' [11] the typically power of charging is 3,7 kW, 11,0 kW, 22,1 kW or 43,5 kW assumed[11]. The power of charging is 3,7 kW for generating the load profiles. Under consideration of traveling a distance of 46,82 km in average per household and per day, this leads to an energy consumption of approximately 8 kWh. The energy consumption divided by the power of charging (3,7 kW) is the duration of the charging process. In this case the charging takes only about 2 h and 15 min. Therefore, the power of charging is mostly high enough to provide a convenient charging which can be carried out easily during the night. Due to a long traveled distance or when charging a high amount of energy, a higher power of charging could offer some benefits in terms of duration but make no odds for generating profiles of electric vehicle's charging behavior in terms of the entire impact onto power supply grids

Table 3.6 gains an overview about typically values for the power of charging and their respective parameters.

Table 3.6.: Typically charging power for electric vehicles [11]

current of charging	1 x 16A	3 x 16 A	3 x 32 A	3 x 63 A
power of charging	3,7 kW	11,0 kW	22,1 kW	43,5 kW

To determine the impact onto power supply grids of charging an electric vehicle, the duration and power of the charging process as well as the time of starting the charging process is relevant. The probability of arriving at home, respectively the

time when the car starts charging, can be determined approximately by the probability density functions in figure 3.3. These density functions are based on the arrival times of electric vehicles and can be described by equation 3.9 with the parameters μ and σ. [11]

$$f_x(\mu, \sigma) = \frac{1}{\sqrt{x\sigma 2\pi}}\, e^{-\frac{(x-\mu)^2}{2\sigma^2}},\ x > 0 \tag{3.9}$$

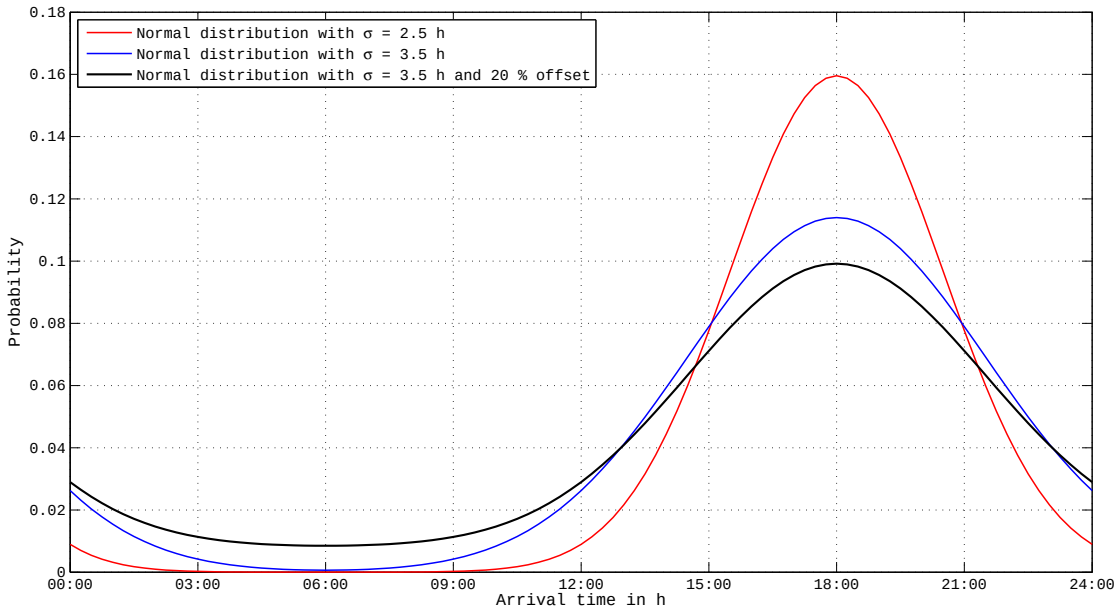

Figure 3.3.: Assumed probability density functions of the arrival time/starting the charging process

The red curve has the parameters $\mu = 72$ ($\rightarrow$ 18:00) because $\mu = 96$ would refer to 00:00 and $\sigma = 10$ ($\rightarrow \sigma = 2{,}5$ h) according to a time resolution of 15 min and 96 values for 24 h.
The blue curve has the same $\mu = 72$ but $\sigma = 14$ ($\sigma = 3{,}5$ h) respectively the black curve is also determined by $\mu = 72$ and $\sigma = 14$ but has an offset of 20 %. This offset is achieved by generating a random number between 0 and 1. If the considered random number is $< 0{,}2$ instead of the density function, the time is determined by another random number between 0 and 1. In this case, the value of 0 refers to 00:00 and the number random value of 1 refers to 24:00 with a resolution of 15 min. This corresponds to a constant probability density function. If the first random number is

$\geq$ 0,2 the density function of equation 3.9 is used. It is assumed that the probability density functions with the maximum at 18:00 and sigma 3,5 h with an 20% offset fits best to real mobility behavior. The arrival time is also the time of starting the charging process. Therefore, according to the previous example, the charging process starts at 18:00 with declining probability for earlier, respectively later beginning.

The procedure of calculating the traveled distance (duration of the charging process and time of starting to charge) is repeated as often as required for the respective lateral. The lateral in the urban model grid consists of 20 households, therefore, the procedure is repeated 20 times. The sum of theses single charging procedures corresponds to the entire impact of this lateral. In the suburban grid, laterals consist of one household and in the rural area the laterals consist of a single household.

This context is illustrated in figure 3.4 on the basis of an example with two generated load profiles of electric vehicles.

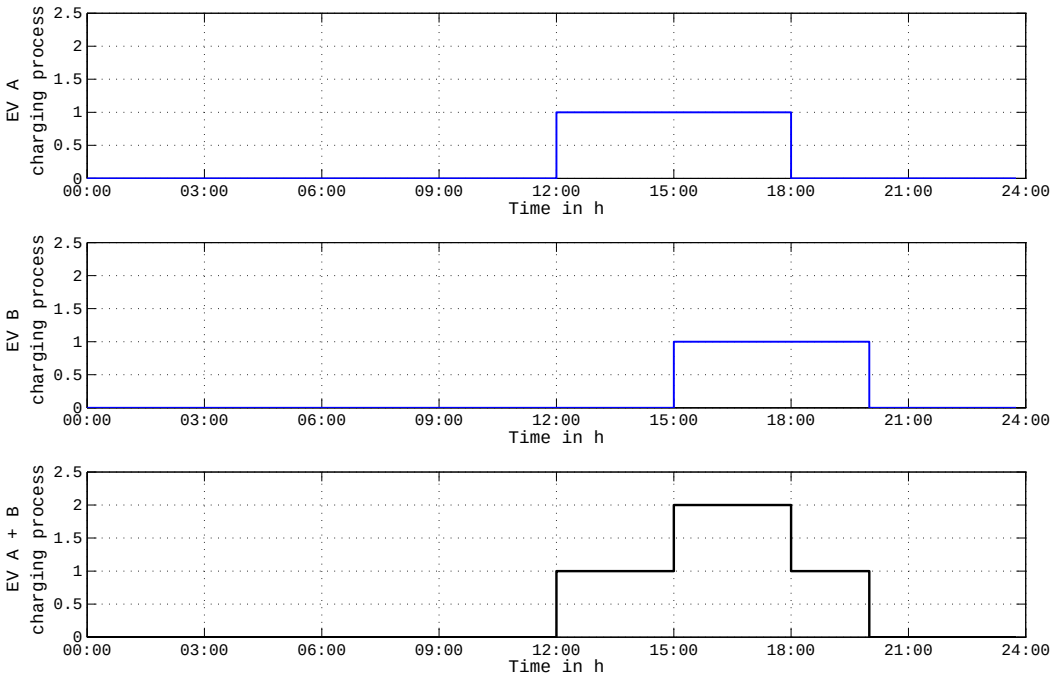

Figure 3.4.: Summing up of charging profile EV A and EV B to obtain the entire profile of EV A + EV B

In the first load profile of electric vehicle A, the charging process starts at 12:00 and has a duration of 6 h. The electric vehicle B in the second load profile starts

at 16:00 charging and ends 5 h later. The sum of these two profiles (EV A + B) is illustrated at the bottom of figure 3.4 and begins at 12:00 and ends at 20:00. At 15:00 the load profiles begin to overlap until the charging of the first profile ends.

Figure 3.5 indicates the results for 20 households. In addition, another load profile set is generated for the previous day to determine the impact of charging longer than midnight and to eliminate this error. Furthermore, it is assumed that 30% of the households do not use any car on a certain day. Therefore, the other 70% who use a car on a certain day have to travel longer with the factor of $1/0,7$ to include this circumstance. In figure 3.5 at 18:30 five electric vehicles are charging simultaneously, thus having 20 households. It is very unlikely that all electric cars of the entire households are charging exactly simultaneously.

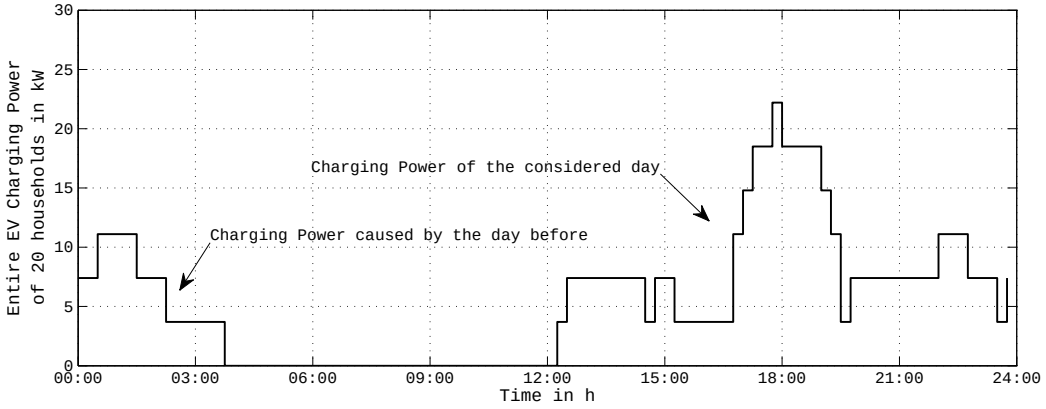

Figure 3.5.: Generated electric vehicle load profile of 20 households for the urban grid

Under consideration of these main steps to generate load profiles, the algorithm has to be adapted to the respective grid area. According to table 3.2 the average distance by car and per day is 35 km for Vienna (urban grid area) and 36 km for Lower Austria (suburban and rural grid area). Therefore, the expected value of 46,82 km has to be scaled to the 35 km according to table 3.2 for Vienna and is achieved by introducing a correction factor c_u.

$$C_u = \frac{d_c u}{E(D)} = \frac{35\ km}{46,82\ km} = 0,748 \tag{3.10}$$

$$C_s = C_r = \frac{d_c s}{E(D)} = \frac{d_c r}{E(D)} = \frac{36\ km}{46,82\ km} = 0,769 \tag{3.11}$$

C_u	Correction factor for the urban area
C_s	Correction factor for the suburban area
C_r	Correction factor for the rural area
$E(D)$	Expected value of the average distance referred to the distribution in km
$\bar{d_c u}$	Average distance by car per day for the urban area in km
$\bar{d_s u}$	Average distance by car per day for the suburban area in km
$\bar{d_r u}$	Average distance by car per day for the rural area in km

The correction factors are considered after calculating the distance based on the distribution in table 3.5. The obtained distance is multiplied by the respective correction factor.

According to table 3.6, the average power of charging in dependency of the charging power (3,7 kW, 11,0 kW, 22,1, 43,5 kW) at an infinite high number of households referred to a single household is illustrated in figure 3.6.

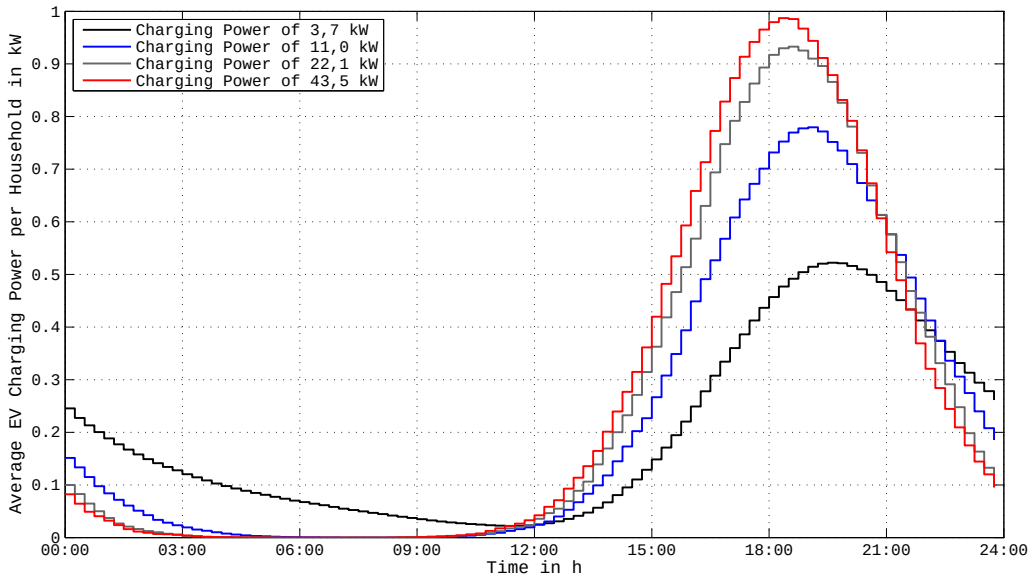

Figure 3.6.: Average power of charging at an infinite high number of electric cars

The maximum peak of the charging curves move left and the shape of the charging curve is getting sharper if the power of charging is increased.

3.2. Load Profiles for Household Loads (HH)

3.2.1. General about HH-profiles

In the last few decades the standard of living and prosperity increased steadily. This led to a higher number of electrical devices in households and therefore to a higher energy consumption. It is assumed that this increase will be continued in the next few decades but will be increasingly flattened. For the scenario of 2020 it is assumed that energy consumption of households will reach 120% based on today's 100%. Due to higher energy efficiency of electrical devices, the actual increase will be slightly lower than assumed in these scenarios, nevertheless a rate of 150% is assumed for the scenarios of 2040 and a rate of 180% for 2060. Therefore, this assumptions form the worst case scenario. These extreme assumptions demonstrate more clearly the effects onto power supply grids. Table 3.7 gains an overview about these scenarios.

Table 3.7.: Share of household loads for different scenarios

	Scenario 2020	Scenario 2040	Scenario 2060
Rate of household loads based on today	120%	150%	180%

3.2.2. Algorithm for the HH Load Profile Generation

The electrical power of loads that occur in a household can be specified by a probabilistic distribution. The difference between the standard load profile of households and the actual considered power can vary significantly when considering a small amount of households. Therefore, an algorithm is required that determines a probabilistic load profile for households based on the standard load profiles.
The distribution of loads can be determined by a log-normal distribution $\mathcal{LN}(\mu, \sigma^2)$ with the parameters $\mu \in \mathbb{R}$ and $\sigma \in \mathbb{R}, \sigma > 0$ which is depicted in equation 3.12. In a log-normal distribution X, the parameter μ denotes the expected value or mean, respectively, σ denotes the standard deviation of the variable's natural logarithm. The parameters for the log-normal density function are $\sigma = 0{,}771546$ and $\mu = 6{,}69531$. [11]

$$f(x) = \begin{cases} \frac{1}{\sqrt{2\pi}\sigma x} \exp\left(-\frac{(\ln x - \mu)^2}{2\sigma^2}\right) & x > 0 \\ 0 & x \leq 0 \end{cases} \tag{3.12}$$

The distribution function in equation 3.13 is obtained by integrating the density function in equation 3.12.

$$F(x) = \frac{1}{\sqrt{2\pi}\sigma} \int_0^x \frac{1}{t} \, \mathrm{e}^{-\frac{(\ln t - \mu)^2}{2\sigma^2}} \, \mathrm{d}\, t \tag{3.13}$$

The expected value or mean of a log-normal distribution is calculated by equation 3.14.

$$\mathrm{E}(X) = \frac{1}{\sqrt{2\pi}\sigma} \int_0^{+\infty} x \, \frac{\mathrm{e}^{-\frac{(\ln x - \mu)^2}{2\sigma^2}}}{x} \, \mathrm{d}\, x = \mathrm{e}^{\mu + \frac{\sigma^2}{2}} = 1088,93W \tag{3.14}$$

Figure 3.7 illustrates the log-normal density function of household loads of equation 3.12 with the parameters $\sigma = 0{,}771546$ and $\mu = 6{,}69531$.

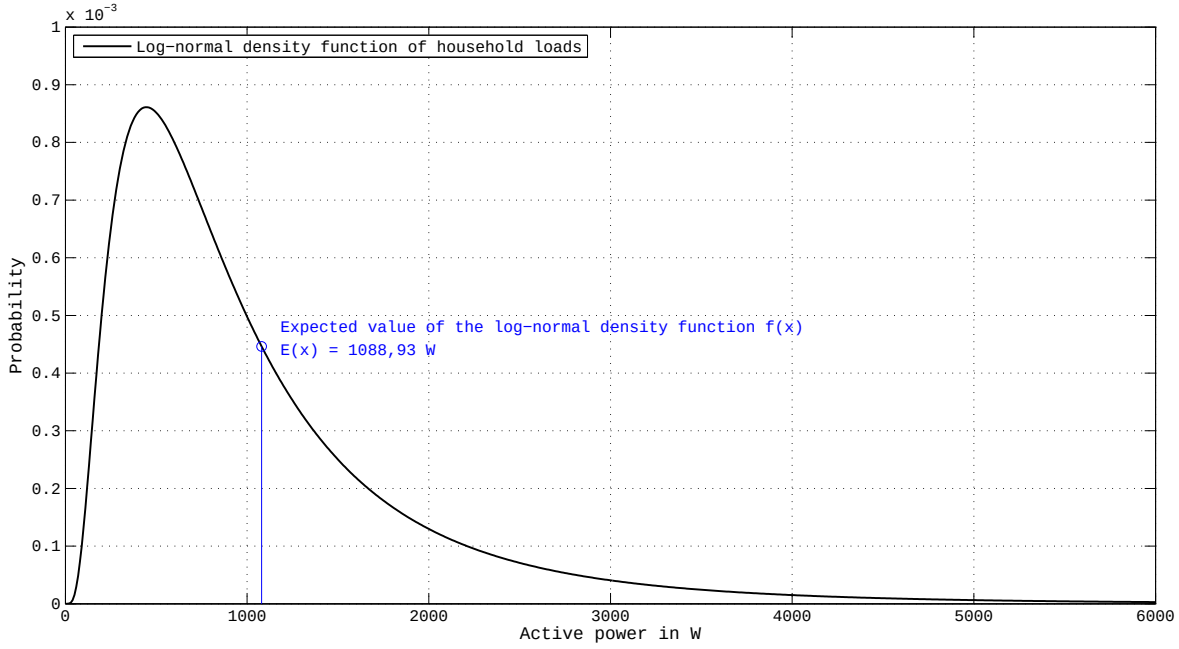

Figure 3.7.: Log-normal density function of household loads

To obtain the distribution function of household loads, the integrated density function is depicted in figure 3.8.

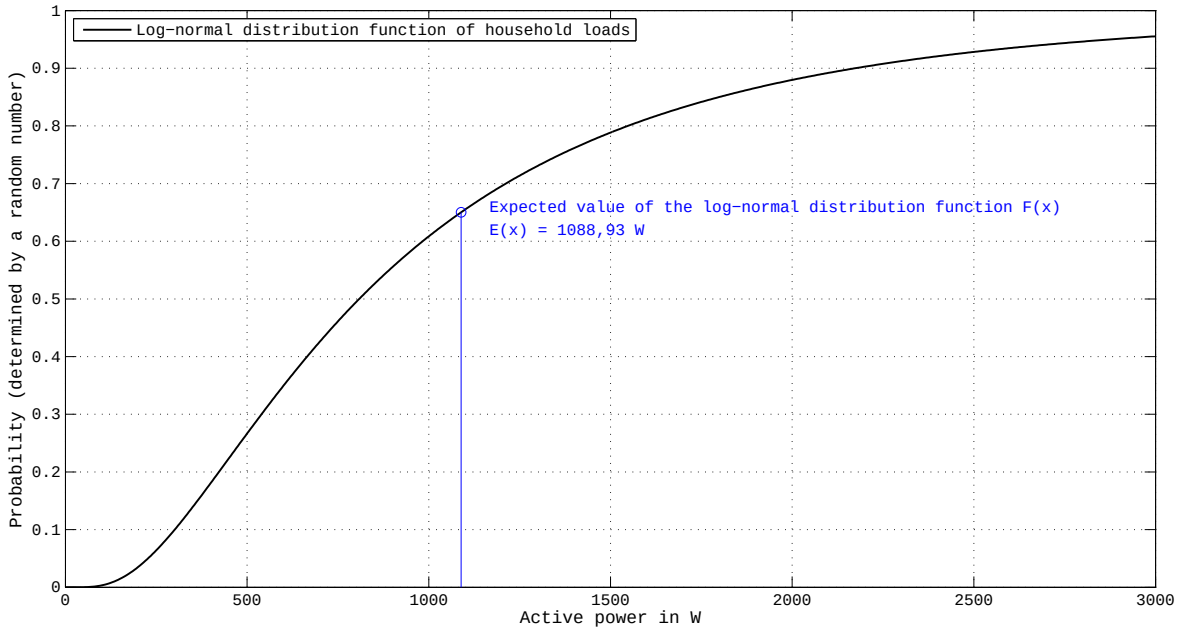

Figure 3.8.: Log-normal distribution function of household loads

The log-normal distribution function is determined by the parameters σ and μ. When the parameter μ is decreased and the parameter σ is kept constant, the curve of the distribution function gets scaled and compresses towards the left. Figure 3.9 illustrates these context for a variation of the parameter μ = 6,69531, 6,01227 and 5,0007.

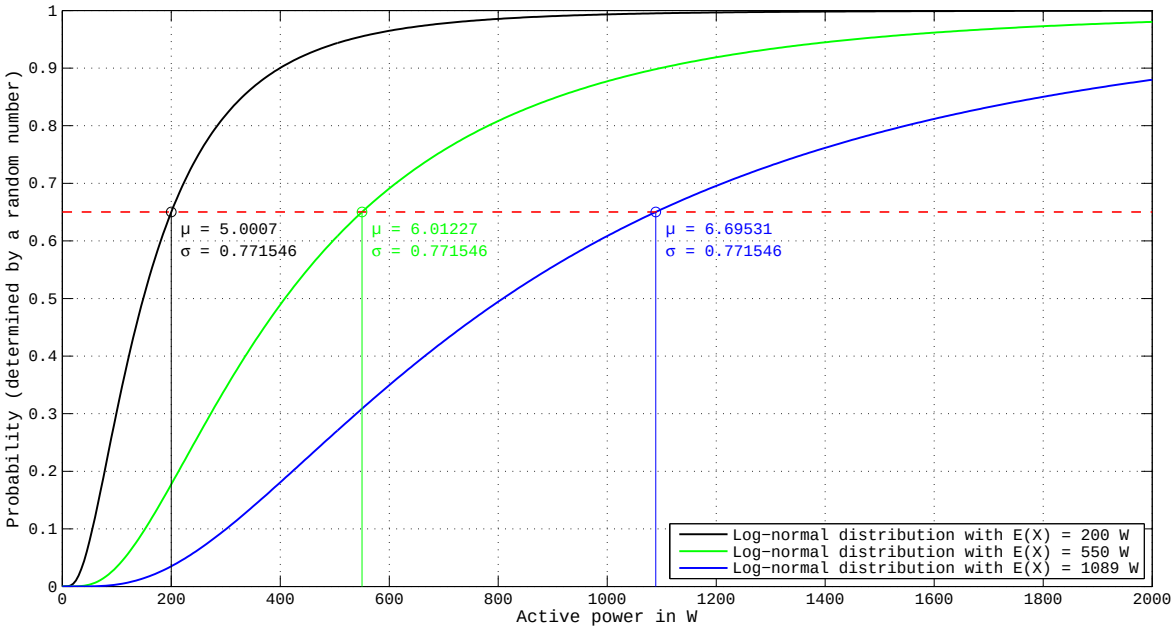

Figure 3.9.: Variation of log-normal distribution functions for different values of sigma

The expected value E(X) of the log-normal distribution moves from E(X) = 1089 W increasingly towards the left (E(X) = 200). The y-axis refers to the probability of the log-normal distribution function with a range between 0 and 1. If a random number is calculated within these limits the accompanying active power value can be obtained on the x-axis at the respective distribution function. For example, if the random number is 0,6502 the accompanying value on the x-axis is 200 W for the distribution function with $\mu = 5,0007$ (the black curve according to figure 3.9). Therefore, a probability or random number of 0,6502 implies the average active power of the household load is less than 200 W with a probability of 65,02 % at the distribution function determined by the parameter $\mu = 5,0007$.

The first step of generating the household load profiles is to obtain the desired value of E(X) = 2,9073 · 74,9 W = 217,76 W from the standard load profile for household loads H0 multiplied by a corrections factor. The considered power of 74,9 W is the first value of the standard load profile at 00:00 on the desired winter day in figure 3.10. The factor of 2,9073 is the correction factor for Vienna because the standard profile for household loads only refers to an annual energy consumption of 1000 kWh. The distribution function is scaled to the expected value of expected value of 217,76 W according to equation 3.14.

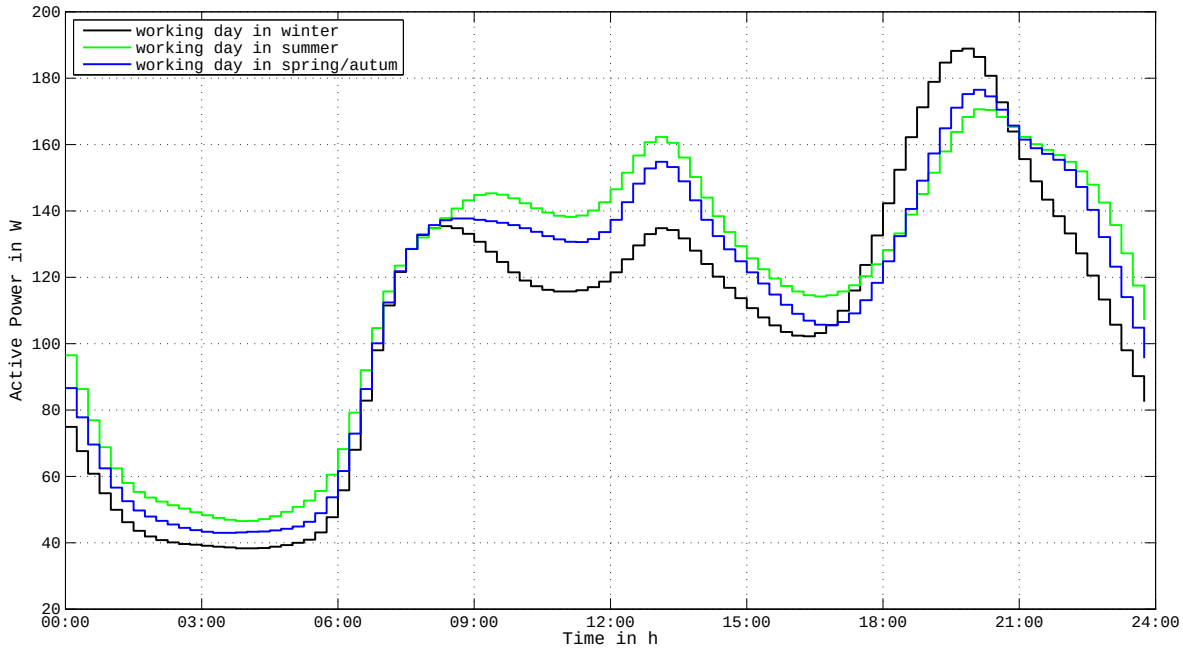

Figure 3.10.: Standard load profiles of household loads for every season at a working day

The standard load profiles in figure 3.10 represent a typically working day in winter, spring/autumn as well as summer. The values in the entire standard load profile set refer to an annual energy consumption of 1000 kWh.

This first step is equivalent to scale the log-normal distribution function by changing the parameter μ to involve an expected value of the distribution function that is equal to the value obtained by the standard load profile multiplied by the correction factor to determine the actual energy consumption per year.
Under consideration of an average energy consumption of 2907,3 kWh/year per household for Vienna and 3252,8 kWh/year for Lower Austria, the values of the standard load profiles are scaled to determine the respective energy consumption. The values obtained by the standard load profile are based on an annual energy consumption of 1000 kWh and therefore, every value of the calculated profile is multiplied by a factor of 2,9073 for Vienna, respectively 3,2528 for Lower Austria.

Figure 3.11 shows the scaled distribution function to the desired value of E(X) = 217,76 W.

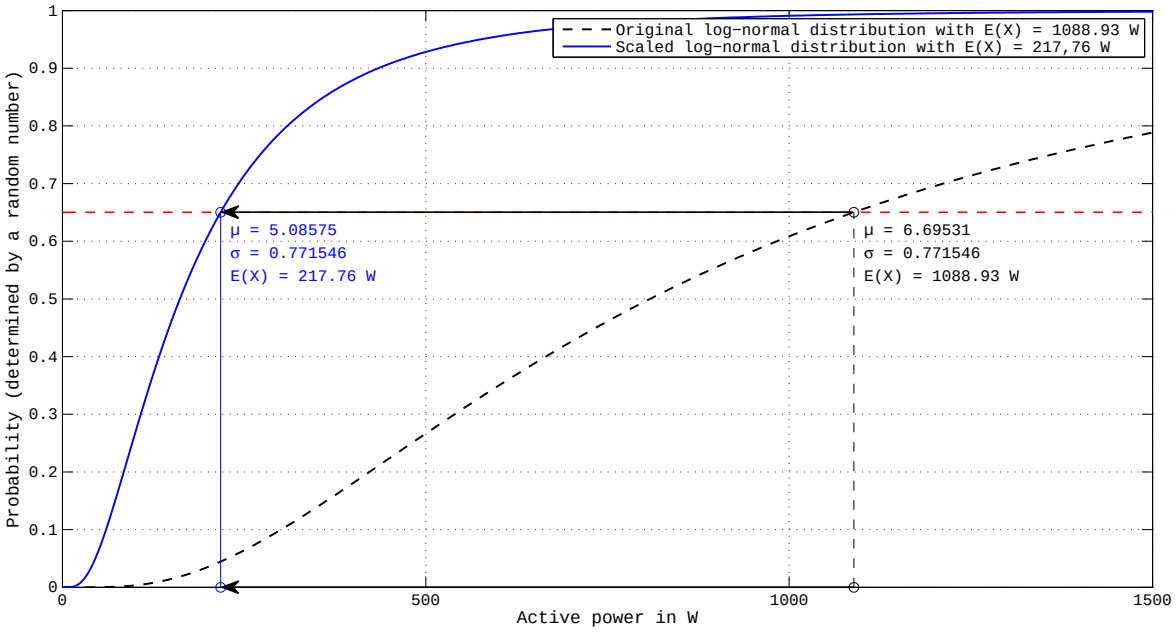

Figure 3.11.: Scaled distribution function to the desired value of the standard load profile

In the next step a 4th random number R4 is calculated within the limits 0 and 1. For example, this random number R4 is assumed to be 0,32. This number refers to the y-axis of the scaled distribution function and determines the power value on the x-axis. Therefore, the log-normal distribution is scaled by changing the parameter μ to entail the expected value of the distribution function to the scaled value (to the respective energy consumption of the considered area) of standard load profile values.

Therefore the initial $\mu = 6{,}69531$ is changed to $\mu = 5{,}08575$. The calculated random number R4, in this case 0,32, denotes the probability on the y-axis of the distribution function with the parameter $\mu = 5{,}08575$ and $\sigma = 0{,}771546$ and determines the accompanying power value on the x-axis. In this case, the obtained value is 112,72 W according to figure 3.12 and refers to a current active power of 112,72 W of a single household in the generated load profile for urban grids. In this case, the active power of 112,72 W would be the first value in the final probabilistic load profile at 00:00 based on the first value of the standard load profile at 00:00.

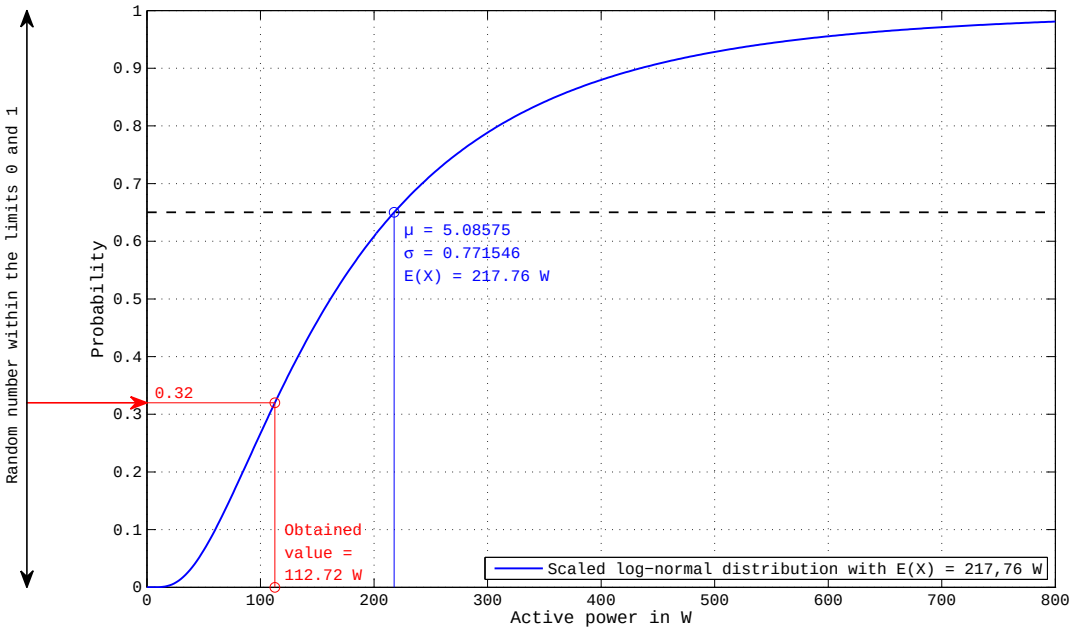

Figure 3.12.: Determine the power value of the household load profile H0

This sequence is repeated for every value of the standard load profile to obtain the entire probabilistic power characteristic of a single household.
This context is depicted in figure 3.13, the load profile of a single household seems to be determined only in a probabilistic way. The red curve in figure 3.13 indicates the difference to the respective standard load profile.

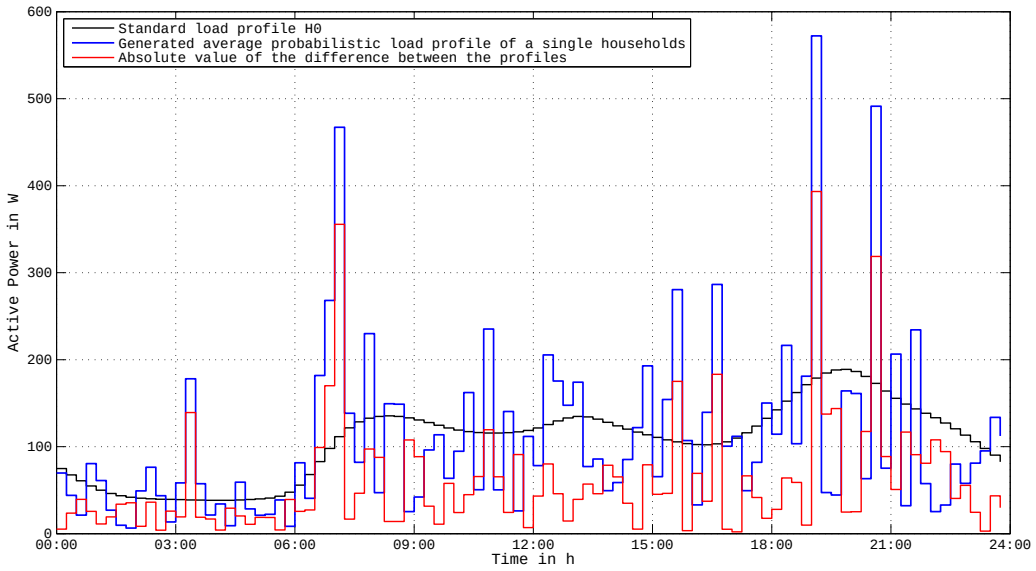

Figure 3.13.: Average profile of a single household and differences to the standard load profile H0

The generated load profile of 20 households in figure 3.14 is correlating more precisely with the standard load profile, although some freak values are existing. This profile represents a single lateral in the urban grid structure. Therefore, the sum of 20 single profiles is generated and then divided by the number of households to obtain the average power characteristic of a single household under consideration of 20 households.

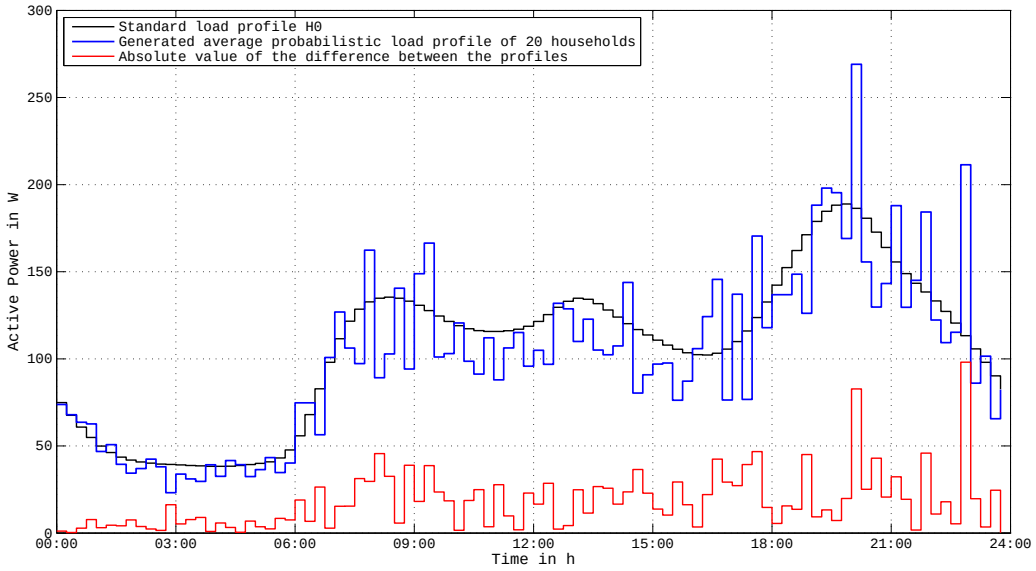

Figure 3.14.: Average profile of 20 households and differences to the standard load profile

Figure 3.15 reveals the similarity to the standard load profile due to 420 households that represent a single subgrid in the urban grid according to the chapter 4 (Model Grids).

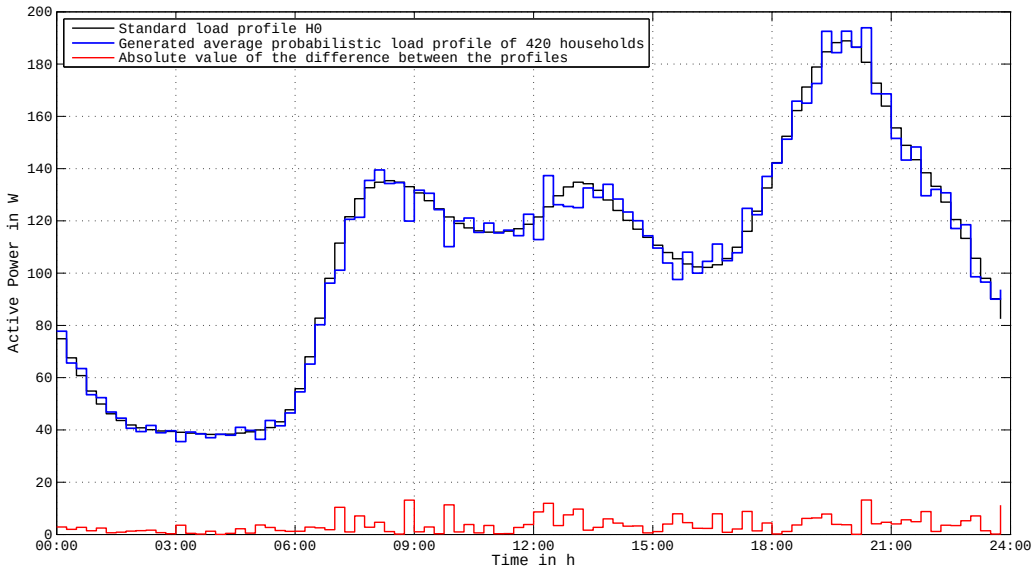

Figure 3.15.: Average profile of 420 households and differences to the standard load profile H0

It is obvious that the differences between the generated profile and the standard load profile declines to a minimum. These differences are depicted in figure 3.15 by the red curve. This considered profile of 420 households is also divided by the number of households to obtain the average load profile per household.

3.3. Load Profiles for Micro-Generation (Photovoltaic PV)

3.3.1. General about PV-profiles

To generate feed-in profiles of micro generation in this thesis it is assumed that only photovoltaic represents the decentralized energy production. Therefore, a photovoltaic profile is generated based on real data recorded on a winter day. The usage of a winter day allows to examine the worst case scenario of standard profiles for household loads with a high peak in the evening in combination with a volatile photovoltaic profile. Additionally, the profiles overlap hardly and therefore, they cannot compensate each other (feed-in and load profiles). The break-in of the photovoltaic profile according to figure 3.16 before midday offers the opportunity to examine the effects of rapid load changes. Due to this distinctive profile shape the decision of applying this profile gains an interesting perspective.

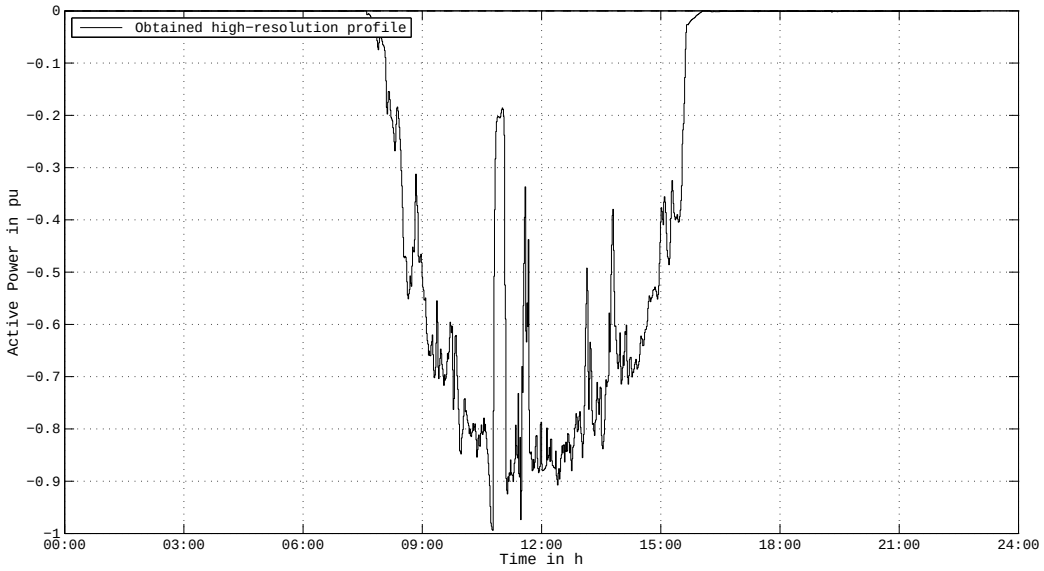

Figure 3.16.: Obtained high resolution photovoltaic profile

Unlike electric mobility, decentralized energy production such as photovoltaic is assumed to reach more rapid higher shares. A share of 100% refers to the maximum feed-in capacity that is possible to limit the voltage rise to specified thresholds. For the scenario 2060 a share of 100 % is assumed, 80 % for the year 2040 and only 20 % for the year 2020.

Table 3.8.: Share of photovoltaic for different scenarios

	Scenario 2020	Scenario 2040	Scenario 2060
Share of photovoltaic	20%	80%	100%

3.3.2. Algorithm for the PV Feed-in Profile Generation

To generate the photovoltaic profiles, the obtained high-resolution profile is divided into intervals with 15 min duration. Within these sections the average value is calculated. The result is a photovoltaic profile with a 15 min time resolution. This profiles are also scaled to the desired maximum value required in the respective area. Table 3.9 indicates these maximum values [12].

Table 3.9.: Peak values of the photovoltaic profiles

	Urban area	Suburban area	Rural area
Peak values	26 kW	2,5 kW	1,5 kW

Due to feed-in properties of these profiles, the signs of the power values are negative. To obtain slightly different values for the individual profiles, a noise is added. This noise represents fluctuations in terms of power caused by influences such as clouds, that move over in the considered area and particular shade some rooftop modules. The efficiency of photovoltaic rooftop systems also depends on the azimuth/angle of the modules to the sun and the temperature coefficient. Therefore, the power of single modules on different rooftops does not have exactly the same power values and does not fluctuate simultaneously. To take these slight differences into account, for every calculated value, an additional random number R5 is calculated between 0 and 1. The range of 0 to 1 is scaled to -1 and +1 by multiplying with a factor of 2 and adding the value -1. The obtained random number R5 between -1 and +1 is multiplied by the calculated value of the photovoltaic profile. In the next step, the result is multiplied by the factor of 0,15 to generate a noise with a maximum peak of +/- 15%. The calculated noise value is added to the original value of the profile to generate a profile with 15% of noise.
Figure **??** indicates the finally generated photovoltaic profile of 20 households for the urban grid.

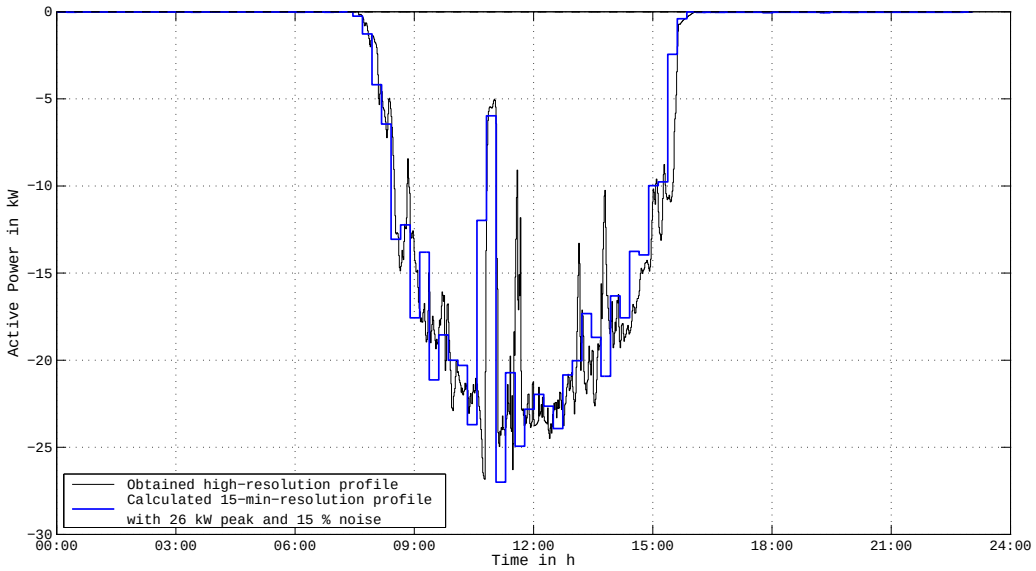

Figure 3.17.: Generated photovoltaic profile for urban grids with 26 kW peak, 15 min resolution and 15 % of noise overlay

4. Model Grids

To determine the effects of decentralized energy production such as photovoltaic in combination with household loads and electric mobility, three different model grids were developed. According to the diploma thesis about 'Impact Assessment for a High Penetration of Distributed Generators in Medium and Low Voltage Grids' [12] this three model grids represent an urban, suburban and rural grid. The urban model grid is based on the area of Brigittenau, the 20th district of Vienna. The suburban model grid refers to the area Breitenfurt in Lower Austria and the rural model grid refers to Grub near Breitenfurt, also located in Lower Austria. Based on real grid parameters these three model grids were developed. The following sections give an overview over these grid structures. These three different types consist both of a medium voltage and a low voltage grid structure.

4.1. Urban Model Grid

The urban grid consists of the medium voltage transformer No. 0 (110/10 kV, 40 MVA). This branch leads after a distance of a = 422 m to the first of nine distribution transformers (10/0,4 kV, 1000 kVA) and is made of an aluminum cable with a cross section of 240 mm^2 with a maximum (nominal) current of 244,8 A for 60% load (Figure 4.1). All transformers (No. 0 and No. 1 - No. 9) are assumed to be regulating transformers. After two further line sections with a transformer in the middle, which has the same specifications, a further feeder branches off at the busbar No. 3. This further feeder consists of two further distribution transformers (No. 4 and No. 5) after a line section of also 422 m, respectively 844 m. The main feeder of busbar No. 3 has four line sections with transformer No. 6, No. 7, No. 8 and No. 9 towards the end of each line section. Due to the longest distance to transformer No. 9 of 2954 m (7 x 422 m) the main focus of interest is on the low voltage grid No. 9.

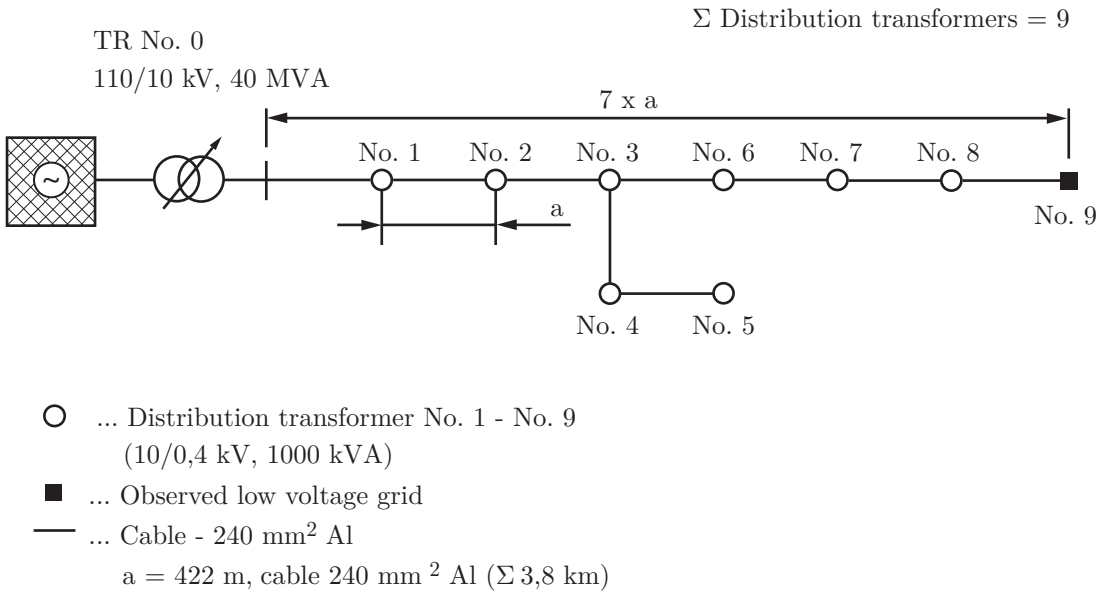

Figure 4.1.: Urban grid structure at medium voltage level

At each of these nine low voltage transformers (substations) identical low voltage subgrids branch off and consist of five feeders (Figure 4.2). The first four of these five branches (No. 9.1 - No. 9.4) consist of five b = 25 m long line sections, made of aluminum with a cross section of 150 mm^2. At every end of these line sections a lateral (No. 9.X.1 - No. 9.X.5) is located which consists of each 20 households. The fifth branch consists of only one line section with also 25 m and one lateral with 20 households (No. 9.5.1). Therefore, the low voltage subgrid consists of 21 laterals, respectively 420 households. The entire considered grid structure has 189 (21 x 9) laterals or 3969 (189 x 20) households (figure 4.2). Every lateral requires three types of profiles that represent the conventional household and electric mobility loads as well as feed-in profiles for photovoltaic. All together 567 (3 x 189) profiles are required for the urban grid for each of the three established scenarios (2020, 2040, 2060).

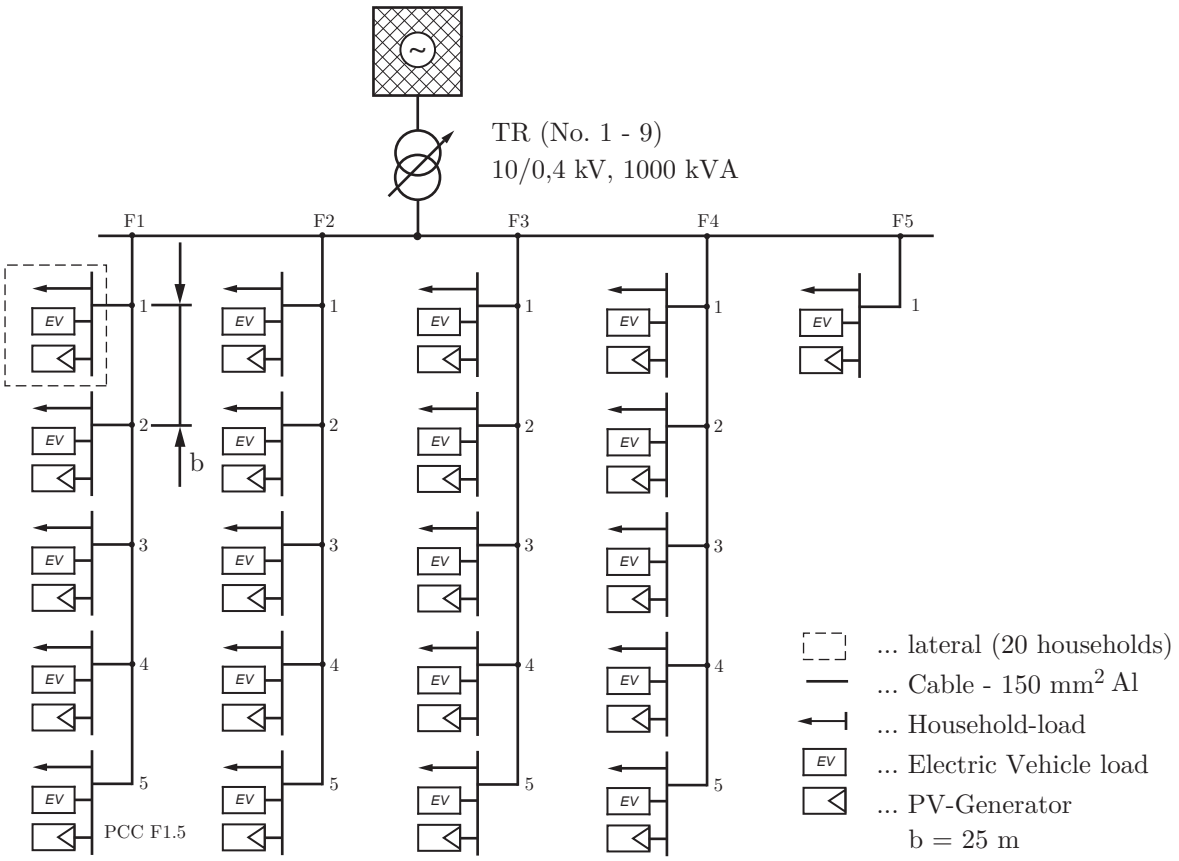

Figure 4.2.: Urban grid structure at low voltage level

4.2. Suburban Model Grid

The medium voltage grid structure of the suburban grid is similar to the urban grid structure at medium voltage level but with a different voltage level (20 kV) and is also fed by a medium voltage transformer Nr. 0 (110/20 kV, 40 MVA). Due to the substation arrangements and similar properties of this network, also nine distribution transformers are used but with different ratings (20/0,4 kV, 400 kVA).

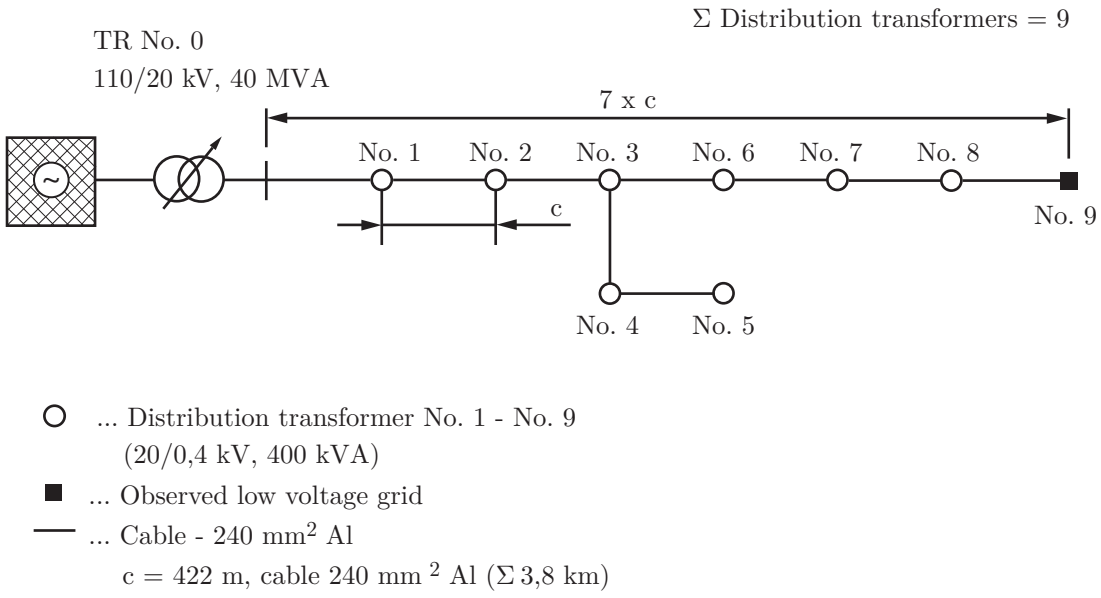

Figure 4.3.: Suburban grid structure at medium voltage level

The entire low voltage structure consists of two feeders which supply two low voltage feeders of equal arrangement (figure 4.4. Every branch consists of 20 laterals and line sections of 35 m between the detached houses. The line sections No. 1 - No. 10 are made of aluminum cables with cross sections of 150 mm^2. However, the line section No. 11 - No. 20 are overhead lines which are made of steel reinforced aluminum with cross sections of 95 mm^2. Each of the 20 laterals refer to a single household. Therefore, the entire subgrid structure consists of 40 (2 x 20) households and 120 (3 x 20) profiles. The entire suburban grid structure requires 1080 profiles and is depicted in figure 4.4.

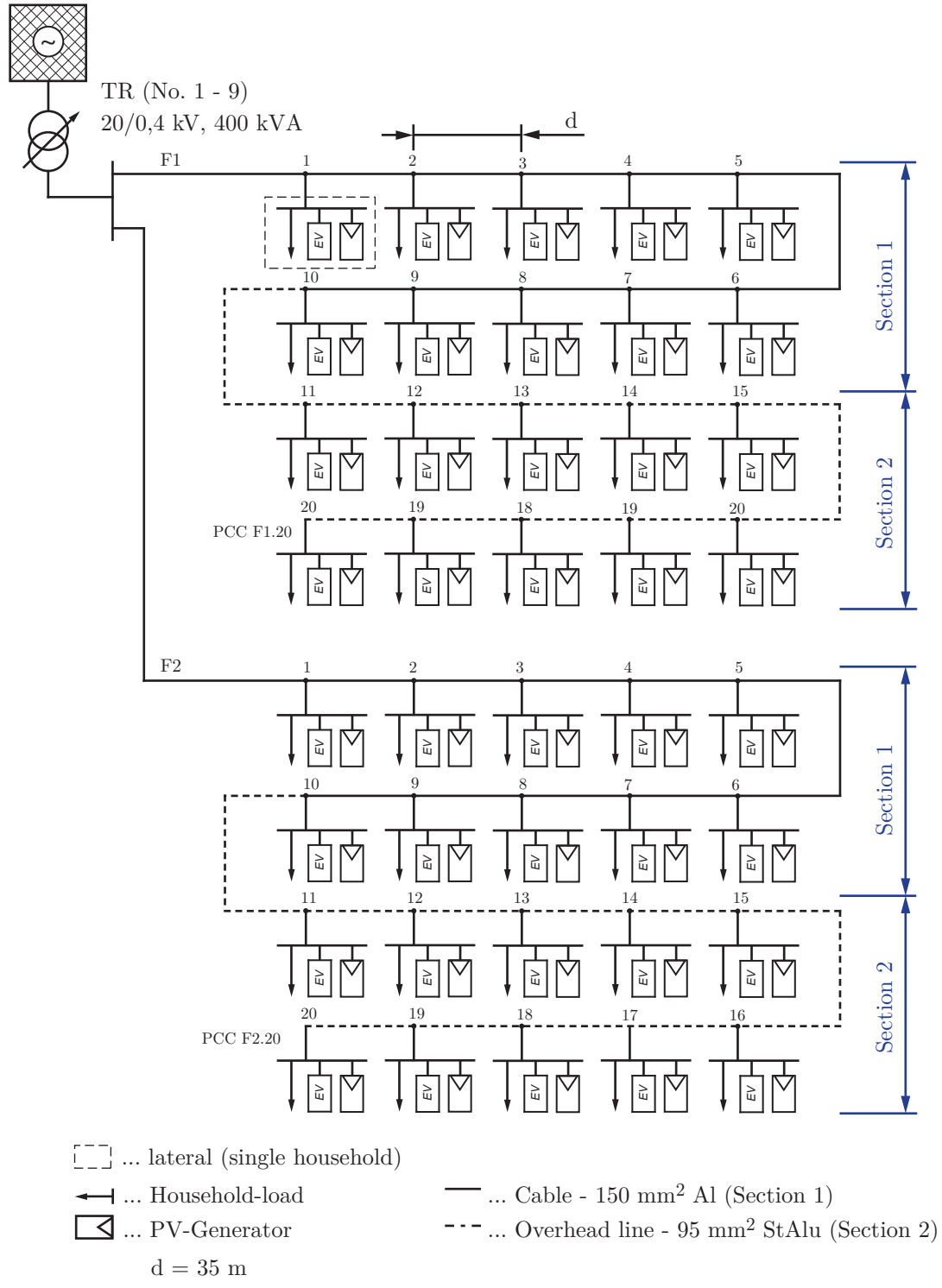

Figure 4.4.: Suburban grid structure at low voltage level

4.3. Rural Model Grid

The rural medium voltage grid structure consists of the same medium voltage transformer No. 0 as used in the suburban grid (110/20 kV, 40 MVA) with a single feeder. This main branch is divided into two main sections which have a branched structure. The first section consists of 19 distribution transformers (20/0,4 kV, 400 kVA) and are connected with 150 mm^2 aluminum cables. The distance between the substations in the first main section is stated with e = 840 m. The second main section consists of 39 substation and are connected with steel reinforced aluminum overhead lines with cross sections of 95 mm^2. The distances between the substations in the second main section is f = 280 m. The resulting grid structure is depicted in figure 4.5.

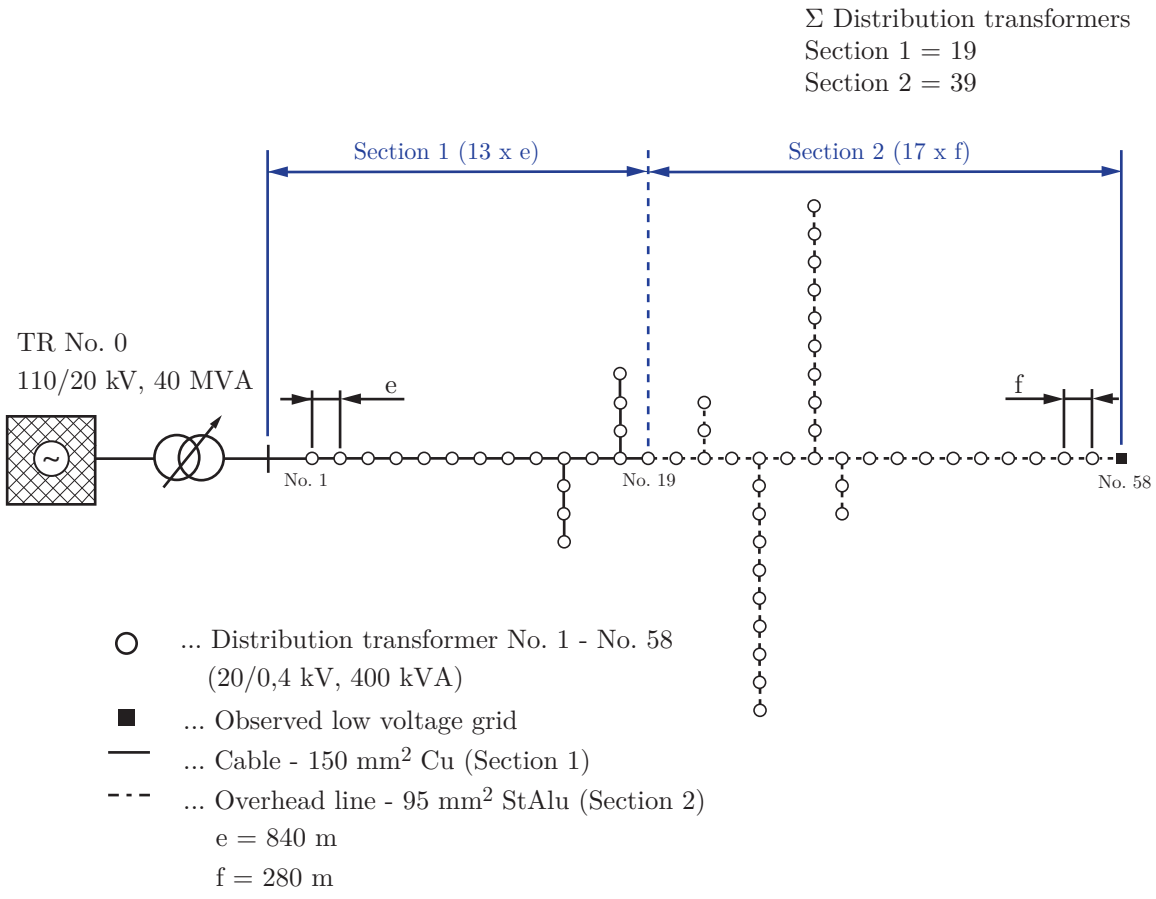

Figure 4.5.: Rural grid structure at medium voltage level

The low voltage grid structure shown in figure 4.6 consists of 10 single laterals

with an average distance of g = 144 m. These detached houses are connected with a steel reinforced aluminum overhead line with a cross section of 95 mm^2. It is assumed that every single house has its own rooftop photovoltaic generation to feed in electrical energy. For every lateral which represent a single household, three profiles are required to assess the impact of photovoltaic, household loads as well as electric mobility. For the entire low voltage grid are 30 (3 x 10) profiles required. Therefore the load flow simulation of the entire medium voltage structure requires 1740 (58 x 30) profiles.

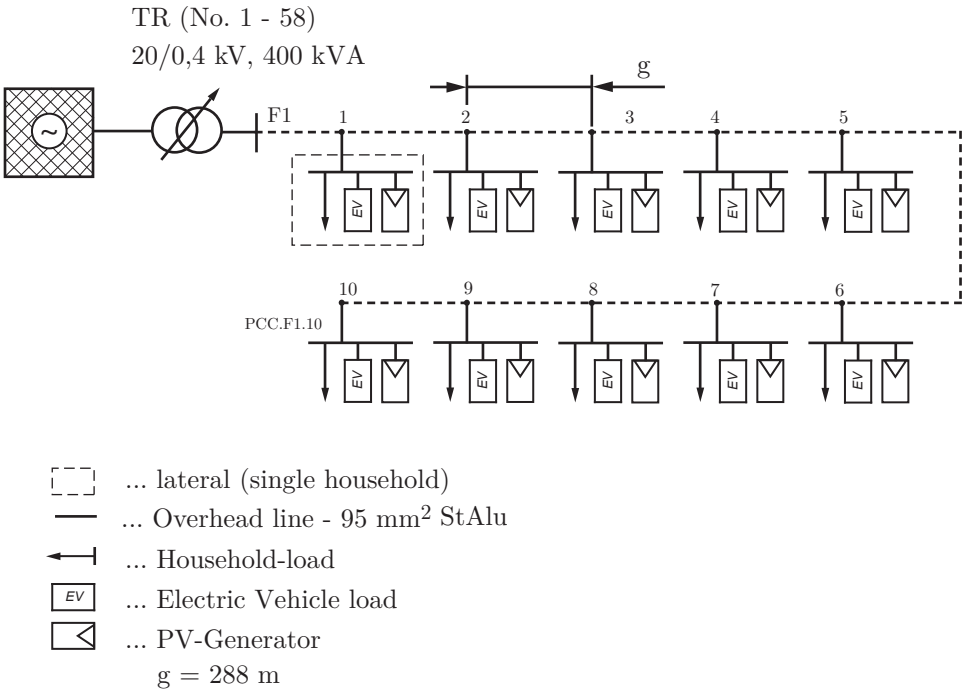

Figure 4.6.: Rural grid structure at low voltage level

5. Simulations

To determine the impact of decentralized energy production in combination with electric mobility onto power supply grids, load flow simulations are performed. These simulations are carried out by Neplan® and the analysis with MathWorks® MATLAB®. For every lateral in the respective grid, load and feed-in profiles are established which involve a realistic image of loads and feed-in capacities. These load flow simulations are accomplished for three different types of scenarios that assesses the year 2020, 2040 and 2060. Every scenario is applied on three different types of model grids that represent an urban, suburban and rural grid. The detailed explanation of the model grid structures and about generating these profiles is in chapter 3 and 4. This current chapter only gains a rough overview about the most relevant grid elements that are required for comprehending the simulation.

5.1. Urban Model Grid

The entire urban model grid structure at middle and low voltage level is illustrated in figure 5.1. The main focus of interests is on the middle voltage transformer No. 0 (110/10 kV, 40 MVA), the low voltage transformer No. 9 (10/0,4 kV, 1000 kVA) at subgrid 9 (maximum distance to transformer No. 0), the line sections (No. 0, No. 9.1.1, No. 9.1.5 and No. 9.2.1) to examine the power respectively the load and busbar No. 0, No. 1 and 9. Furthermore, the busbar No. 9.0 at the low voltage grid with its feeder No. 1 (F1) and their laterals at the beginning (No. 9.1.1) respectively at end of the branch (No. 9.1.5). Both of the transformers are regulating transformers that are remote controlled by voltage nodes.
For all scenarios a similar approach in simulation procedures is carried out to facilitate comparing the simulation results.

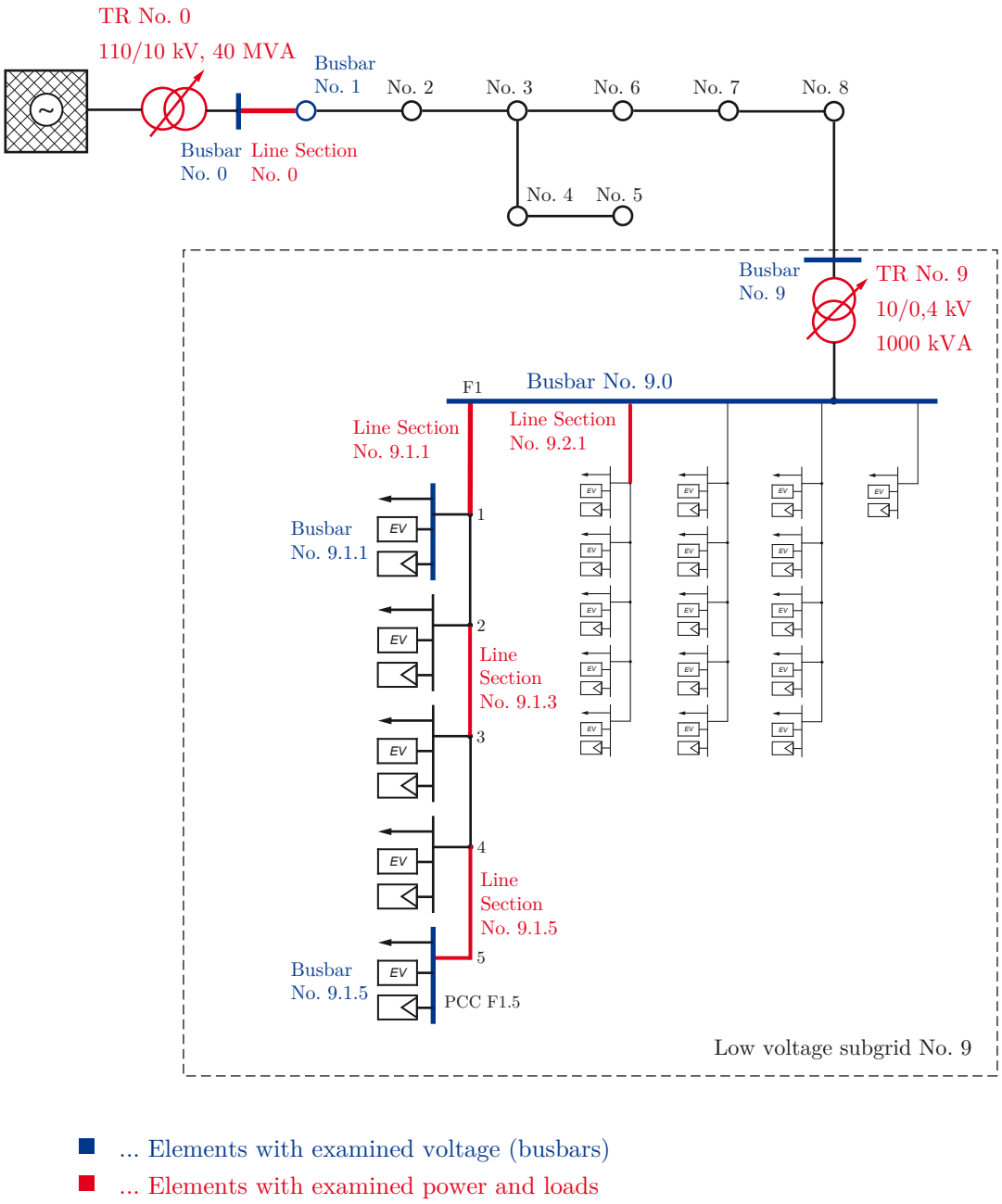

Figure 5.1.: Entire urban grid structure with emphasized simulation-relevant structures are marked red and blue

5.1.1. Scenario U-2060

The scenario 2060 is the worst case scenario and determines the impact of 100 % electric mobility, a 80 % increase in domestic energy consumption compared to the

year 2012 and the maximum feed-in capacity of photovoltaic. In addition, a typically winter day is chosen to analyze the impact with a high peak in the standard load profile for households.

According to figure 5.1 the voltage characteristic along the main line sections beginning at busbar No. 0 and ending at busbar No. 9 at every 15 min within a 24 h day is depicted in figure 5.2 as a three-dimensional surface. Load flow simulations are performed to obtain the voltage at every busbar (No. 0 to No. 9) and the values between these busbars are linearly interpolated to get a continuous surface. In this case, all transformers such as the medium voltage transformer No. 0 (110/10 kV, 40 MVA) as well as the distribution transformer No. 9 (10/0,4 kV, 1000 kVA) are not regulated to illustrate the voltage drop/rise along the line. To gain a better overview about the shape of the surface, figure 5.2 shows a slanted view to this surface. The color of the surface represents the voltage in pu, therefore, a dark red color corresponds to a slight voltage rise and a dark blue color corresponds to a voltage drop of even nearly 2 %.

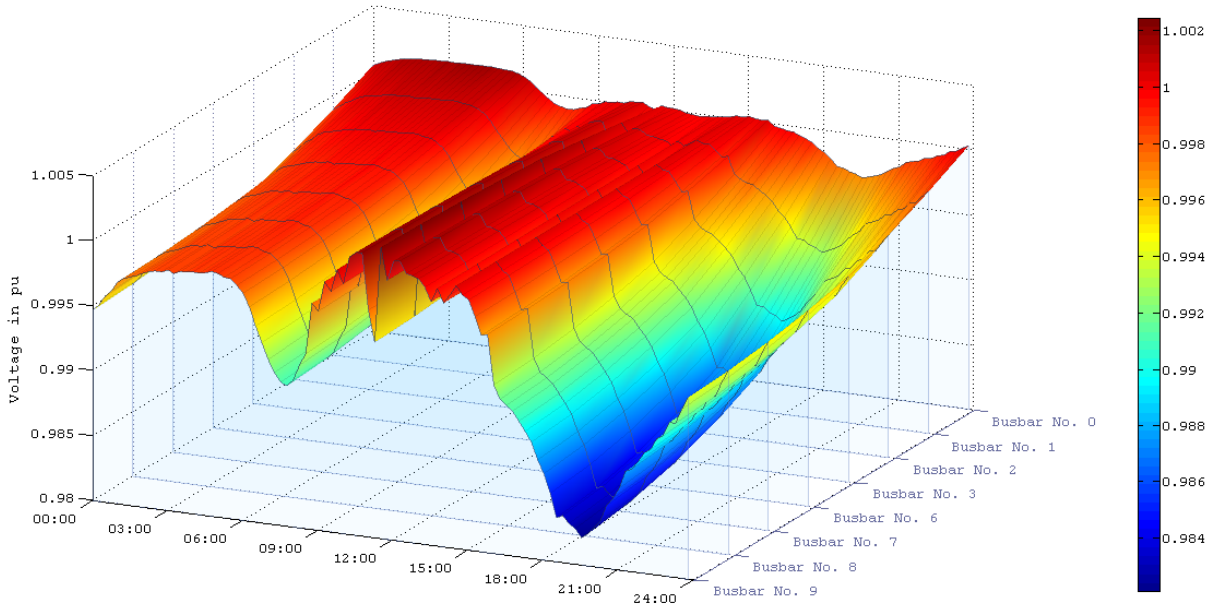

Figure 5.2.: U2060 - Medium voltage surface plot along the main line section from busbar No. 0 to No. 9

To examine the complete surface without hidden edges, figure 5.3 depicts the view from above. The black horizontal lines mark the positions of the respective busbars.

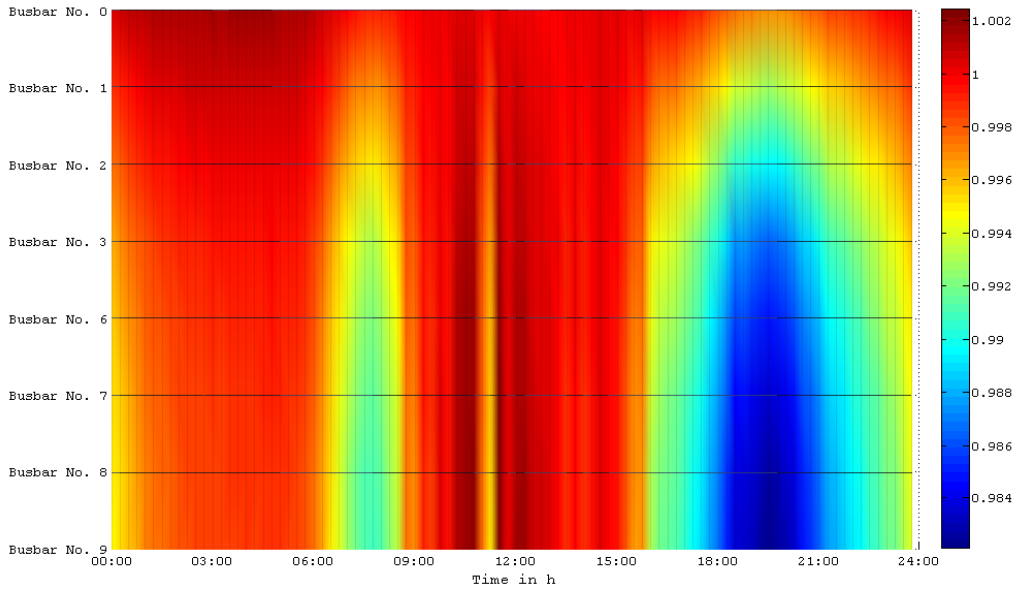

Figure 5.3.: U2060 - Medium voltage surface plot along the main line section (view from above)

As shown in figure 5.4 the voltage characteristic at busbar No. 0 (beginning of the main line section) is rather constant and is increasingly more volatile towards busbar No. 9 (end of the main line section). In the evening between 18:00 and 20:00 the voltage drop reaches its maximum and is depicted as the dark blue area. Figure 5.4 shows the surface plot at the front to examine the voltage drops. The maximum voltage drop is in the evening 1,5 pu between busbar No. 0 and No. 9.

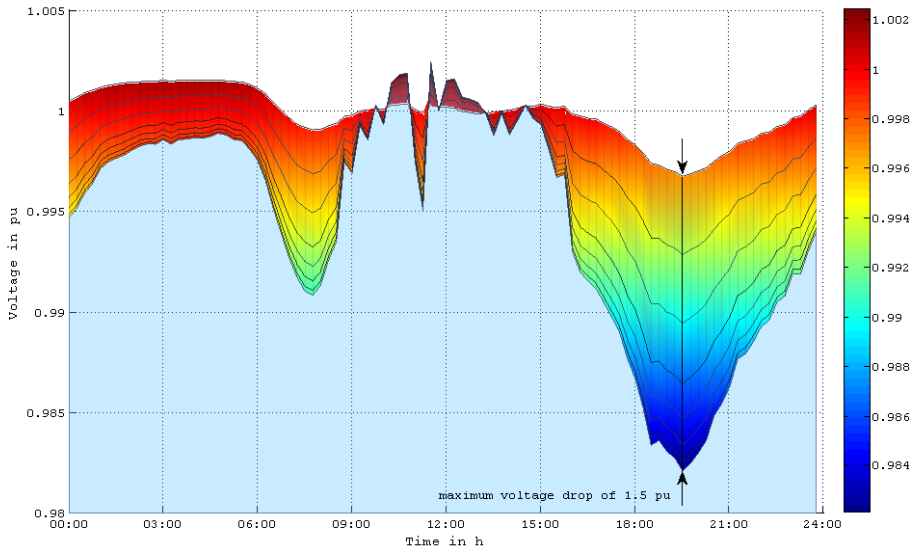

Figure 5.4.: U2060 - Medium voltage surface plot along the main line section (view from the front)

The considered surface at the side view in figure 5.5 shows a kink at the busbar No. 3. This higher gradient is resulted due to an additional feeder at this busbar with two low voltage grids No. 4 and No. 5 and therefore, additional loads, according to figure 5.1.

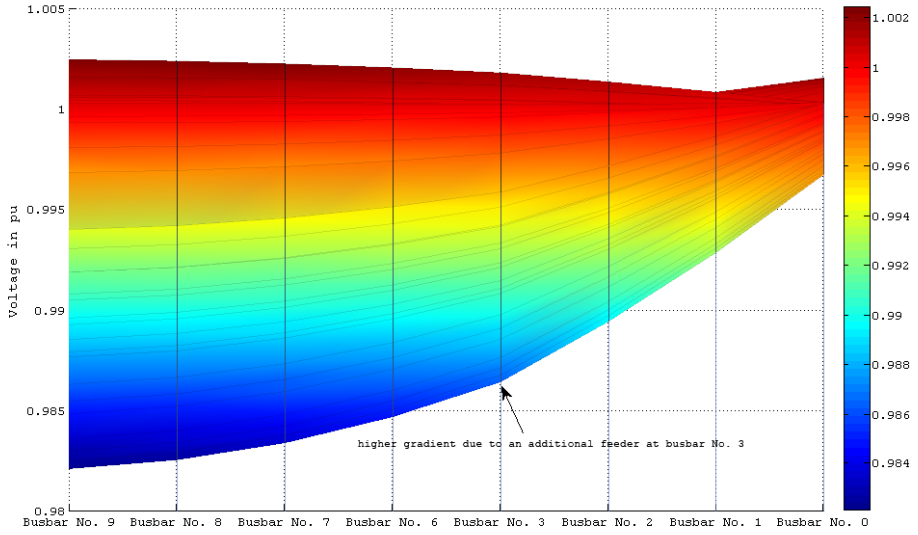

Figure 5.5.: U2060 - Medium voltage surface plot along the main line section (view from the side)

A similar three-dimensional surface plot is carried out for the low voltage grid No.

9. Beginning at busbar No. 9.0 along the first line section to lateral No. 9.1.1 respectively, busbar No. 9.1.1 at feeder No. F1 to the end of this branch to busbar No. 9.1.5 the voltage characteristics are depicted in figure 5.6 from a slanted perspective. The values between the busbars are interpolated to obtain a smoother surface.

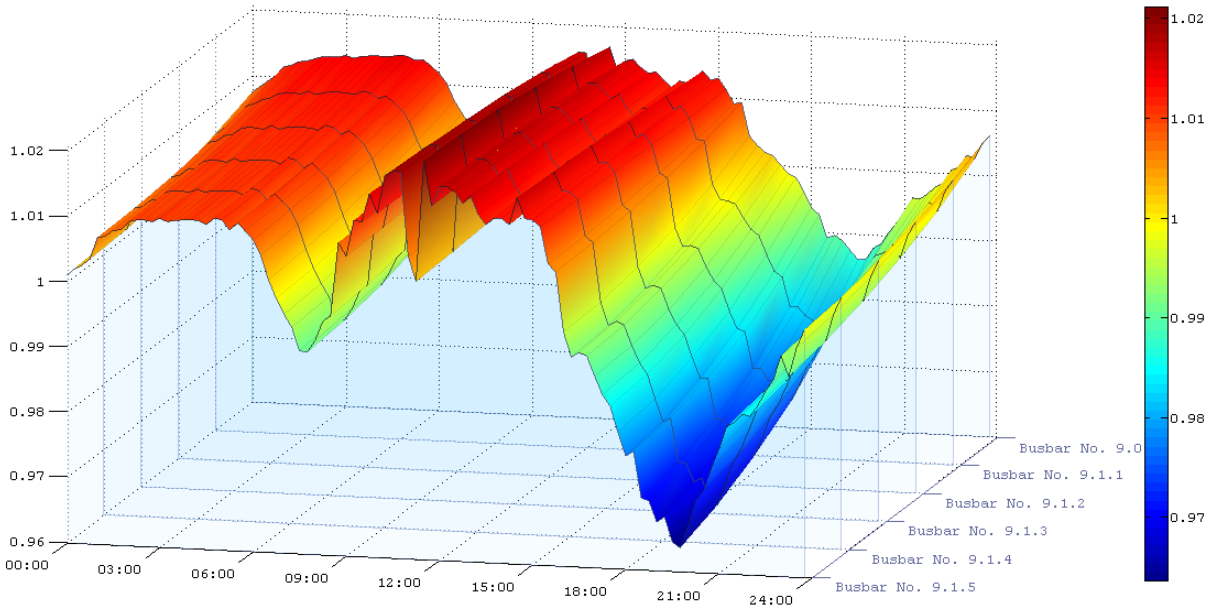

Figure 5.6.: U2060 - Low voltage surface plot along the line sections of feeder No. 1 from busbar No. 9.0 to No. 9.1.1

The main difference to the surface plot to the medium voltage line is in this case the voltage characteristic at busbar No. 9.0 at low voltage level. This voltage characteristic is similar to the voltage of busbar No. 9 at medium voltage level in figure **??**. Figure 5.7 depicts this surface plot from the above's perspective to examine the entire plot without hidden edges. In the low voltage surface plot along feeder F1, the voltage characteristic at the beginning (busbar No. 9.0) is much more volatile compared to the voltage characteristic at busbar No. 0 in figure 5.3. That is obvious, because the voltage at busbar No 9 (medium voltage level) corresponds to the voltage of busbar No. 9.0 (low voltage level).

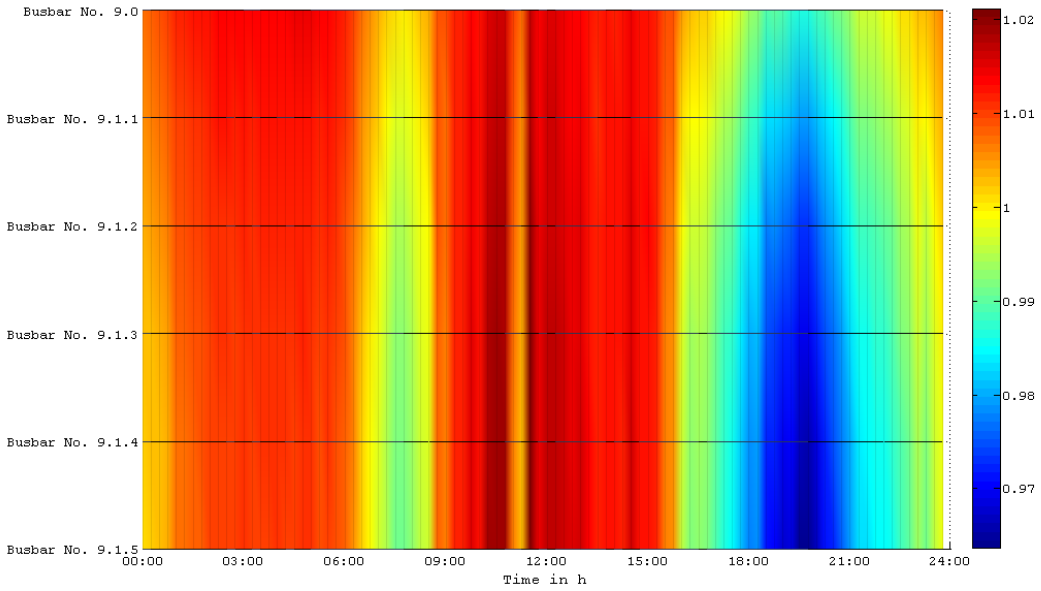

Figure 5.7.: U2060 - Low voltage surface plot along the main line section (view from above)

The voltage drop at the front's perspective is depicted in figure 5.8 from busbar No. 9.0 to No. 9.1.5. The maximum voltage drop is 2,3 % referred to busbar No. 9.0. The entire maximum voltage drop from busbar No. 0 at medium voltage level to Busbar No. 9.1.5 at low voltage level is approximately 5,5 % referred to the busbar No. 0 with 100 % or 1 pu.

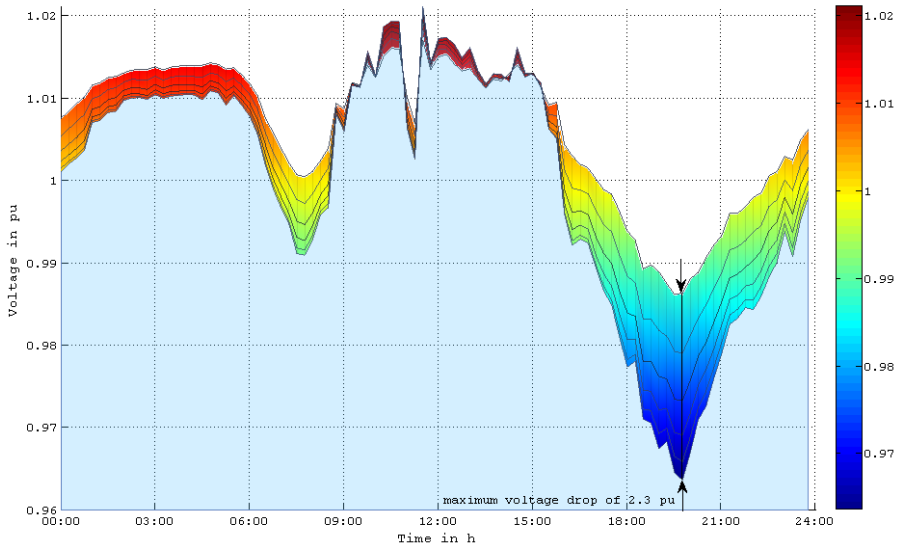

Figure 5.8.: U2060 - Low voltage surface plot along the main line section (view from the front)

The following simulations are performed with regulating transformers. Figure 5.9 indicates the power characteristic of transformer No. 0 (110/10 kV, 40 MVA) and transformer No. 9 (10/0,4 kV, 1000 kVA). The red dashed line is the 60% load threshold of transformer No. 9 (10/0,4 kV, 1000 kVA).

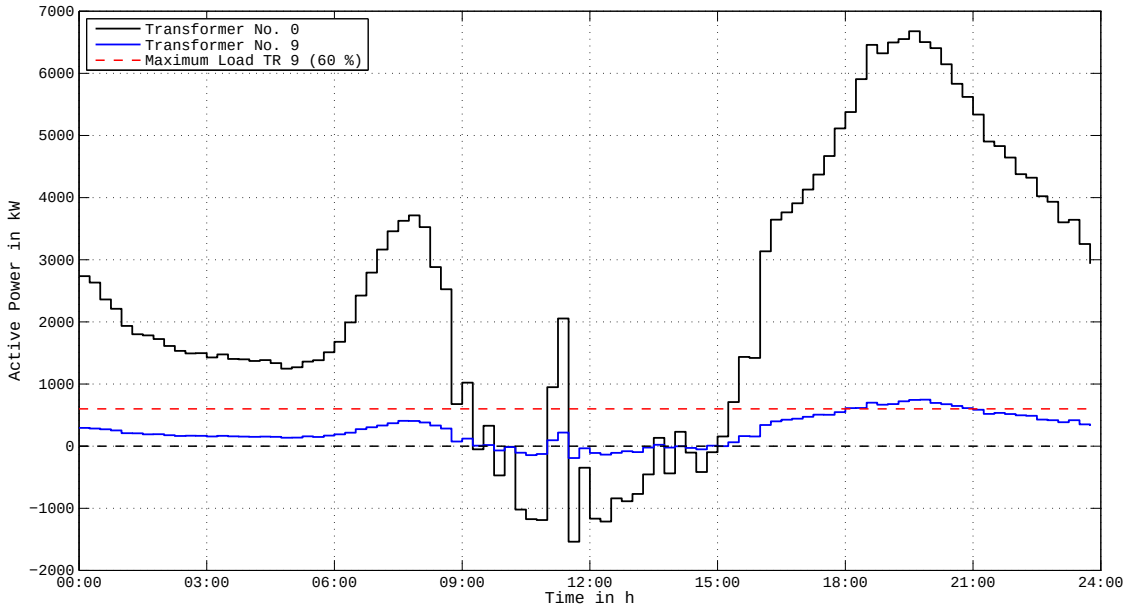

Figure 5.9.: U2060 - Active power of transformer No. 0 (110/10 kV, 40 MVA) and No. 9 (10/0,4 kV, 1000 kVA)

This threshold is slightly violated in the evening. The power peak at 20:30 of transformer No. 0 (110/10 kV, 40 MVA) is nearly exactly nine times higher than for the considered transformer No. 9 (10/0,4 kV, 1000 kVA). This is due to nine identical subgrids and therefore nearly nine identical power values, thus the load profiles are probabilistic generated. The power characteristic is rather continuous due to the high amount of households ($9 \cdot 420 = 3780$) except the influence of photovoltaic is distinctly apparent because of the similar characteristic of each photovoltaic profile. Figure 5.10 compares the power values along the feeder No. 1 of subgrid No. 9. The power values are summed up towards transformer No. 9 (10/0,4 kV, 1000 kVA).

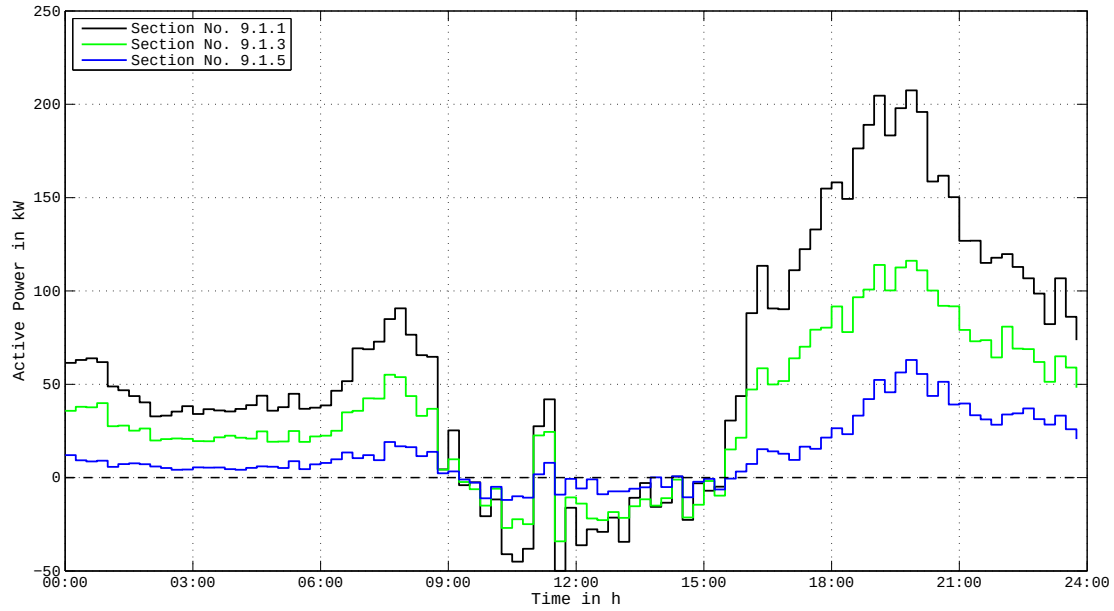

Figure 5.10.: U2060 - Active power of section No. 9.1.1, No. 9.1.3 and No. 9.1.5

In figure 5.11 the first and second feeder of subgrid No. 9 are compared. Due to the high number of households there is only a slight difference between them.

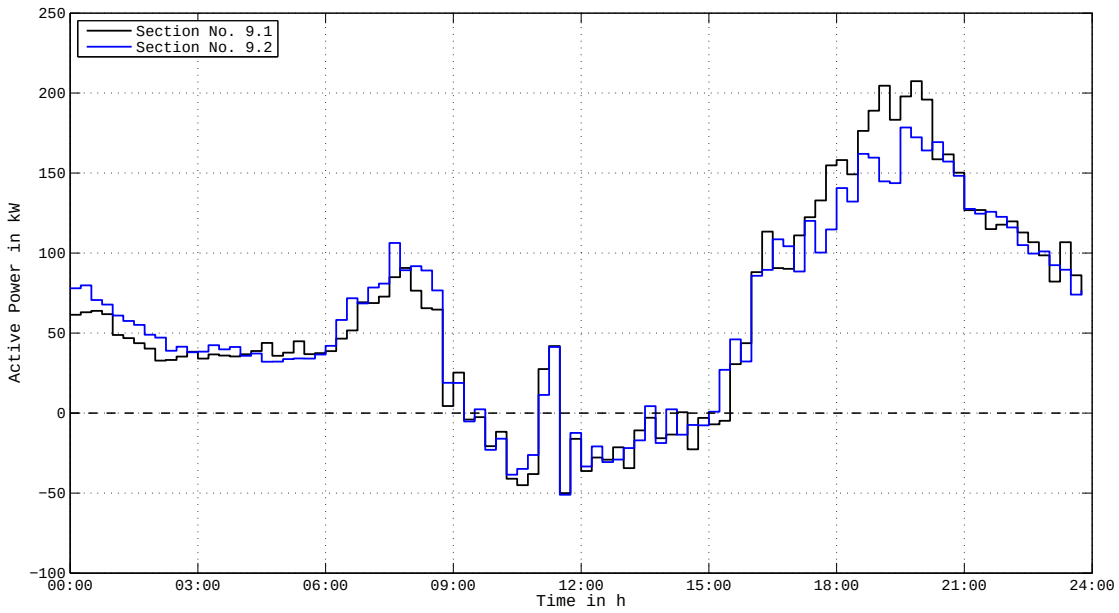

Figure 5.11.: U2060 - Active power of feeder No. 9.1 and No. 9.2

Figure 5.12 and 5.13 illustrates the the voltage characteristics along the middle

voltage line beginning at transformer No. 0 (110/10 kV, 40 MVA) and ending at transformer No. 9 (10/0,4 kV, 1000 kVA) and along the first feeder of subgrid 9. The voltage rise/drop reaches its maximum at the open end of the line. At 17:30 the tap change of the regulating transformer No.0 is clearly visible that added an additional voltage.

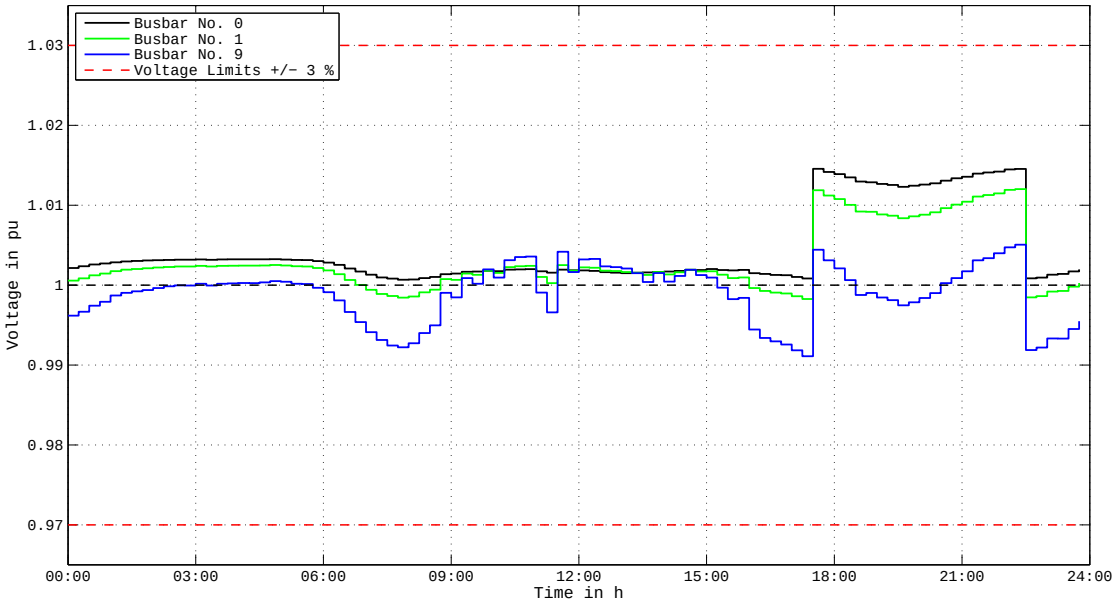

Figure 5.12.: U2060 - Voltage of busbar No. 0, No. 1 and 9

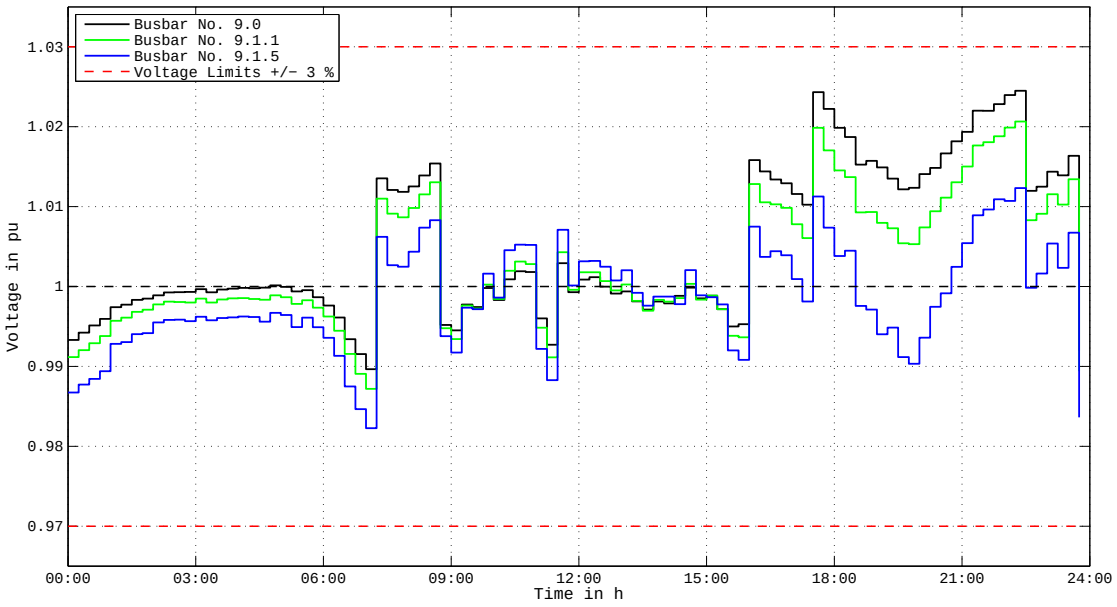

Figure 5.13.: U2060 - Voltage of busbar No. 9.1., No. 9.1.1 and No. 9.1.5

However, they don't violate the voltage thresholds given with +/-3% even at the scenario 2060. The tap position of the regulating transformers is illustrated in figure 5.14. It is obvious, that for example, if the regulating transformer No. 0 (110/10 kV, 40 MVA) changes its tap-position at 17:30 h in figure

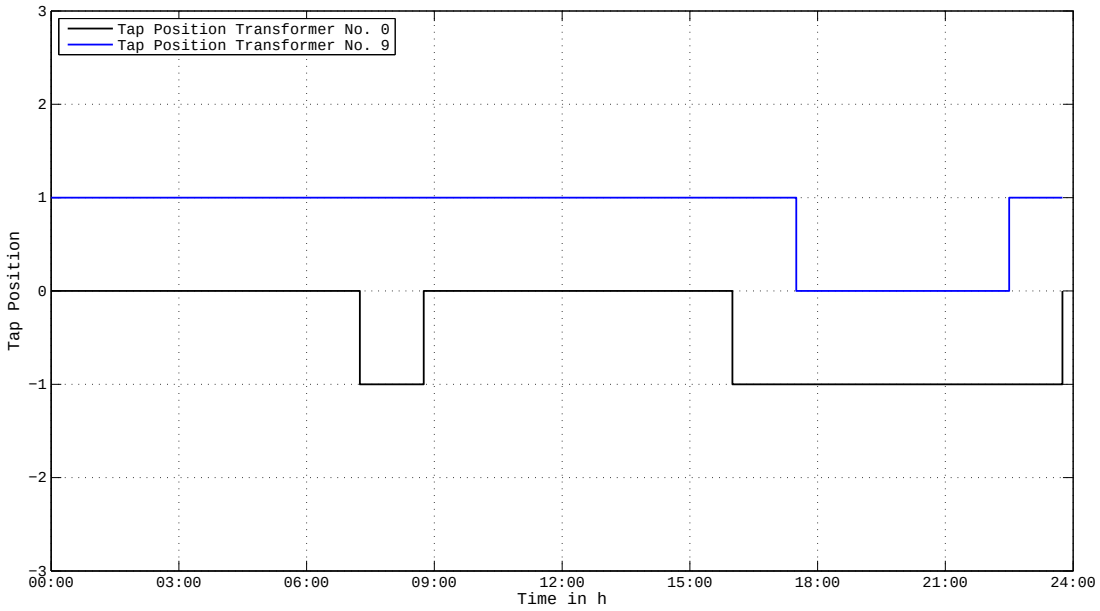

Figure 5.14.: U2060 - Tap positions of transformer No. 0 (110/10 kV, 40 MVA) and No. 9 (10/0,4 kV, 1000 kVA)

The load of the low voltage transformer No. 9 (10/0,4 kV, 1000 kVA) violates the 60% threshold according to figure 5.15 in the evening. Line No. 0 which is located near the middle voltage transformer as well as line No 9.1.1 at the first section of feeder No. 1 in subgrid No. 9 violate the 60% limit massively. In this worst case scenario that assesses the scenario 2060, it is not possible to keep the transformer and line loads under the 60% threshold.
Table 5.1 give an overview about all relevant data of this simulation scenario.

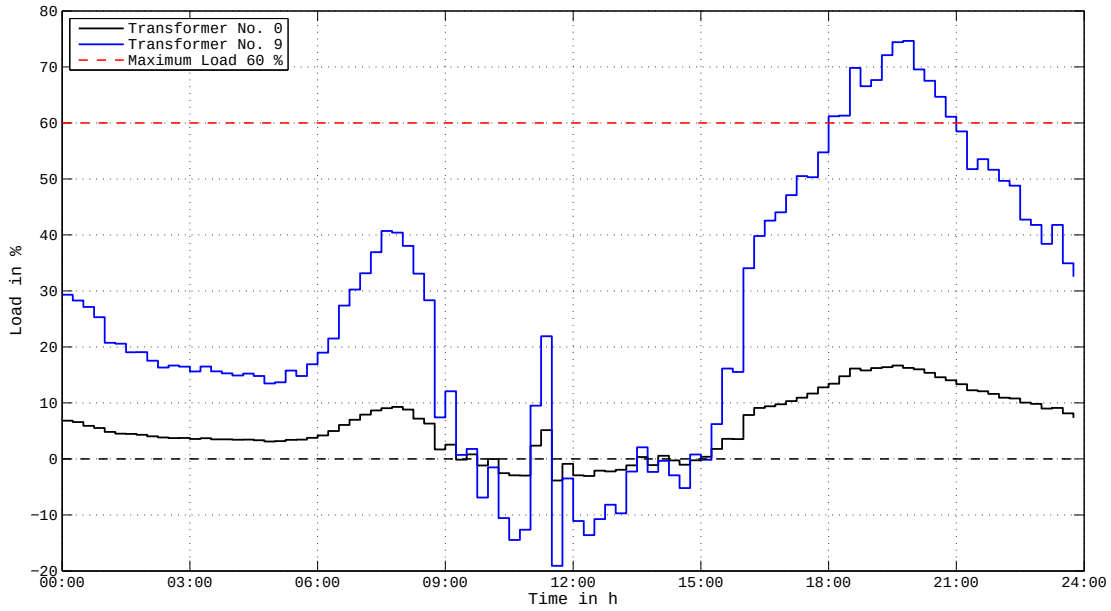

Figure 5.15.: U2060 - Load of transformer No. 0 (110/10 kV, 40 MVA) and No. 9 (10/0,4 kV, 1000 kVA)

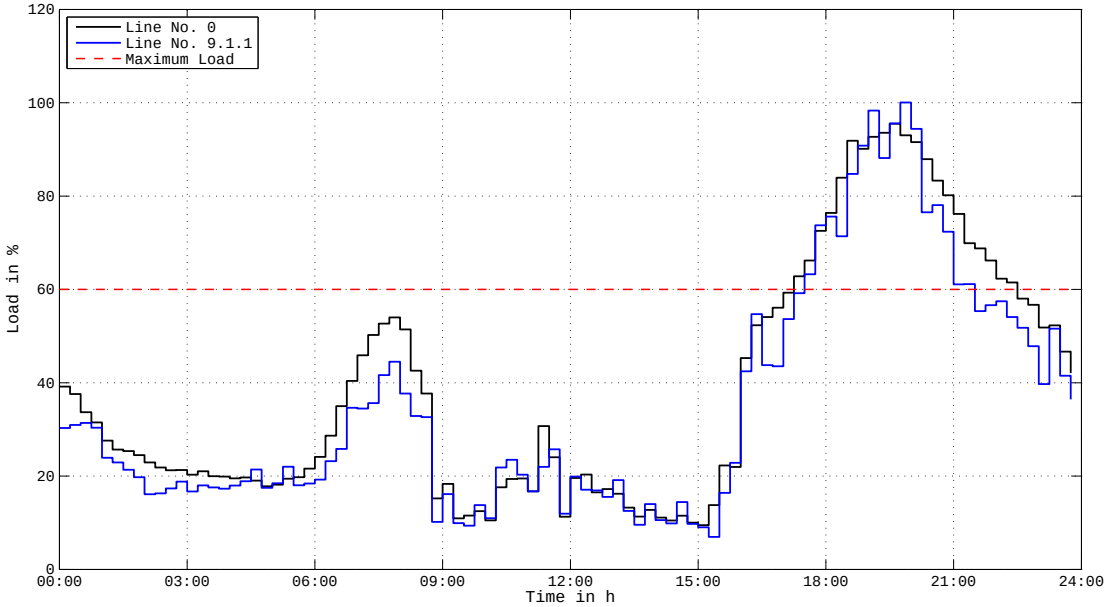

Figure 5.16.: U2060 - Load of line No. 0 and No. 9.1.1

The most relevant simulation results are depicted in table 5.1.

Table 5.1.: Simulation results for the urban grid - scenario 2060

		Transformer No. 0	Line No. 0	Transformer No. 9
Active power in kW	min	-2000 (11:30)	-2000 (11:30)	-210 (11:30)
	max	5800 (19:30)	5801 (19:30)	650 (19:30)
Voltage in %	min	99,1 (11:30)	99,1 (11:30)	99,4 (11:30)
	max	101,7 (17:45)	101,7 (17:45)	100,67 (17:45)
Maximum load in %		25 (19:30)	140 (19:30)	180 (19:30)
Tap changes		4	-	4

		Lateral 9.1.1	Line No. 9.1.1	Lateral 9.1.5
Active Power in kW	min	-60 (10:15)	-60 (10:15)	-13 (11:30)
	max	190 (19:30)	191 (19:30)	50 (20:15)
Voltage in %	min	99,5 (23:00)	99,5 (23:00)	98,16 (23:30)
	max	102,5 (17:45)	102,5 (17:45)	101,3 (21:15)
Maximum load in %		-	150 (19:30)	-
Tap changes		-	-	-

5.2. Suburban Model Grid

The entire suburban grid structure with its middle voltage and low voltage structures is depicted in figure 5.17. With main emphasis on transformer No. 0 (110/20 kV, 40 MVA), the distribution transformer No. 9 (20/0,4 kV, 400 kVA) at subgrid 9, the line sections (No. 0 and No. 9.1.1), busbar (No. 0, No. 1, No. 9) and busbar respectively, laterals (No. 9.0, No. 9.1.1 and 9.1.20) as well as the feeder No. 9.1 and No. 9.2.

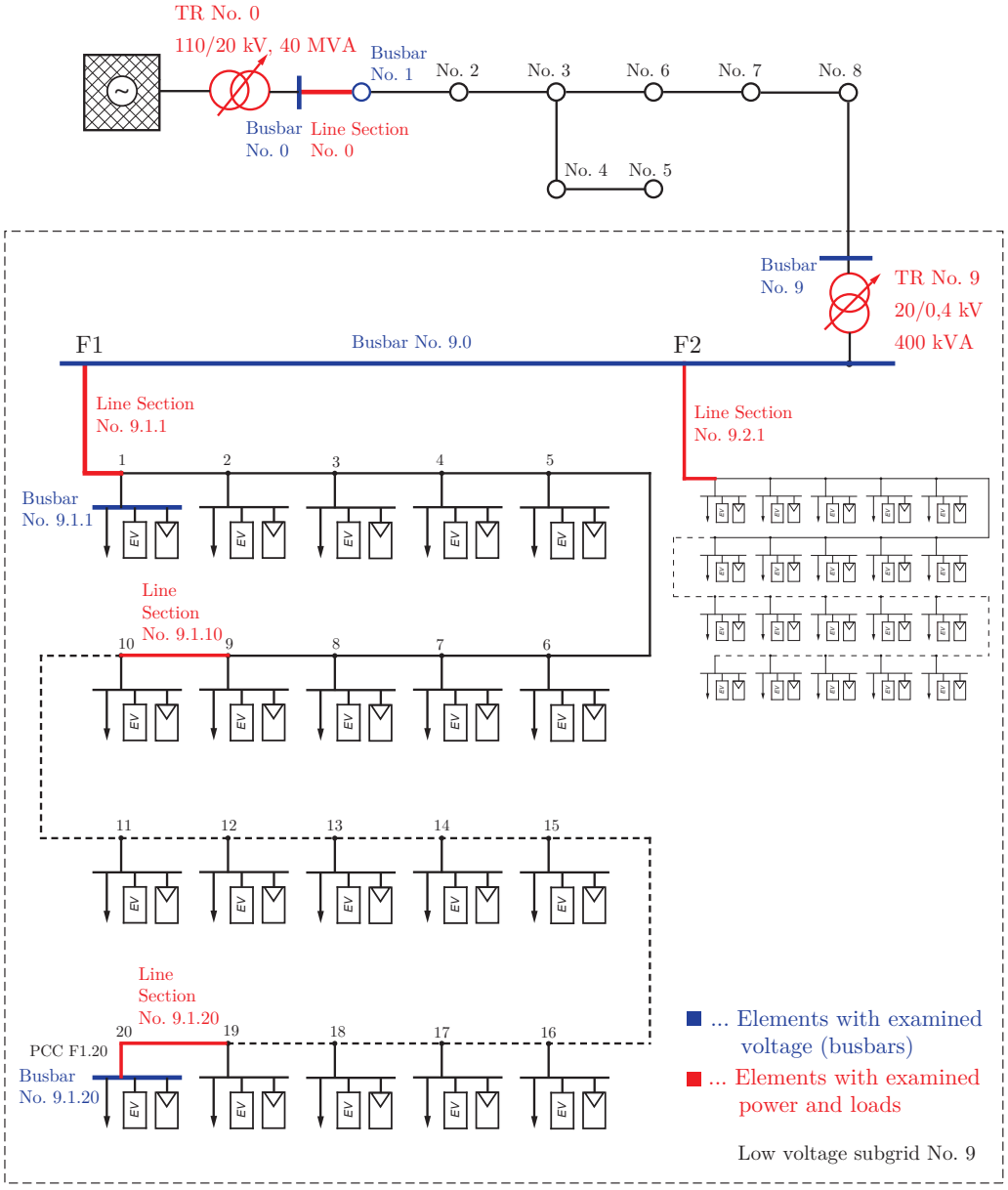

Figure 5.17.: Entire suburban grid structure with emphasized simulation-relevant structures are marked red and blue

5.2.1. Scenario S-2060

The scenario 2060 indicates the worst case with the highest impact onto power supply grid. The share of photovoltaic is assumed to reach its maximum feed-in capacity, the entire mobility is exclusively based on electric mobility and the conventional household loads are increased up by 80% above today's energy consumption. In figure 5.18 the power of the transformer No. 0 reaches at its maximum 750 kVA, that is approximately nine times of transformer No. 9 with a maximum power of 80 kVA. The 60% threshold of transformer No. 9 and therefore for all substations is not violated at any time. Figure A.18 in the appendix shows the power characteristic at different distances on the line sections of feeder No. 1 at subgrid No. 9. The power characteristic of feeder No. 1 and No. 2 are unsurprisingly rather similar. Transformer No. 0 does not change the tap position at any time (figure 5.23). That is because of a very constant and only slightly changing voltage in figure 5.21 at medium voltage level. Due to a low load of transformer No. 0 (figure 5.24) the voltage fluctuates in figure 5.21 minimal. The voltage in figure 5.22 fluctuates obviously and violates just the limits of +/- 3%. Table 5.2 gives an overview about the relevant simulation results.

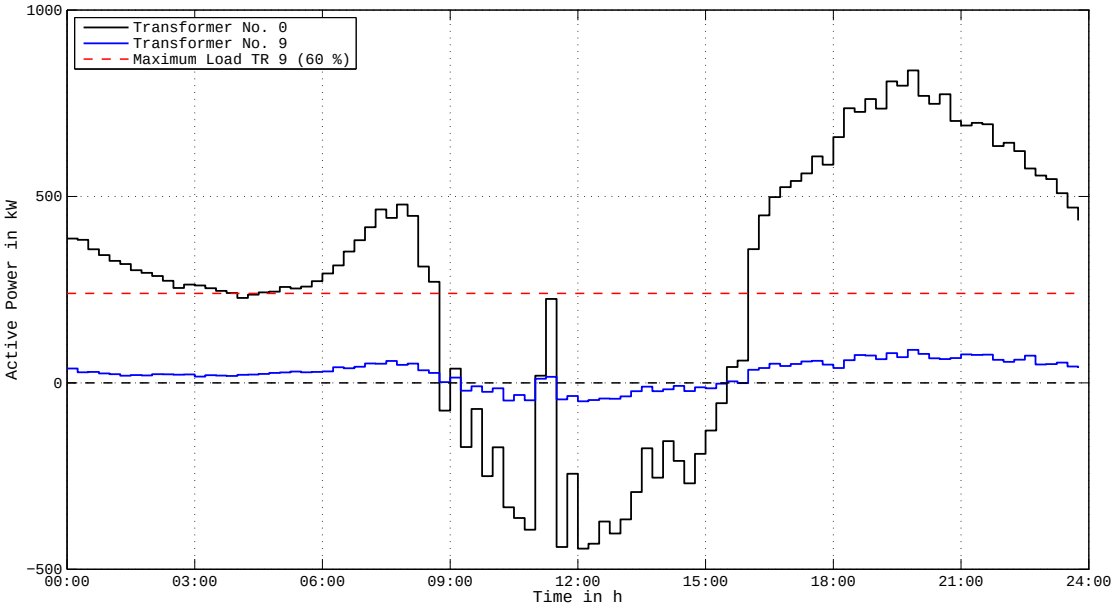

Figure 5.18.: S2060 - Active power of transformer No. 0 (110/10 kV, 40 MVA) and No. 9 (20/0,4 kV, 400 kVA

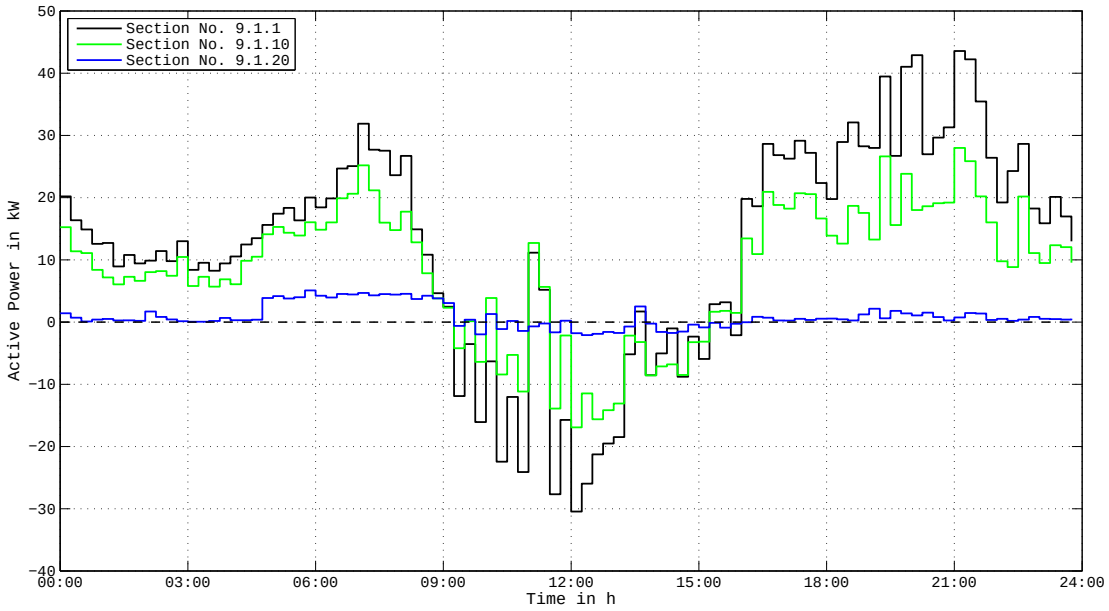

Figure 5.19.: S2060 - Active power of section No. 9.1.1, No. 9.1.10 and No. 9.1.20

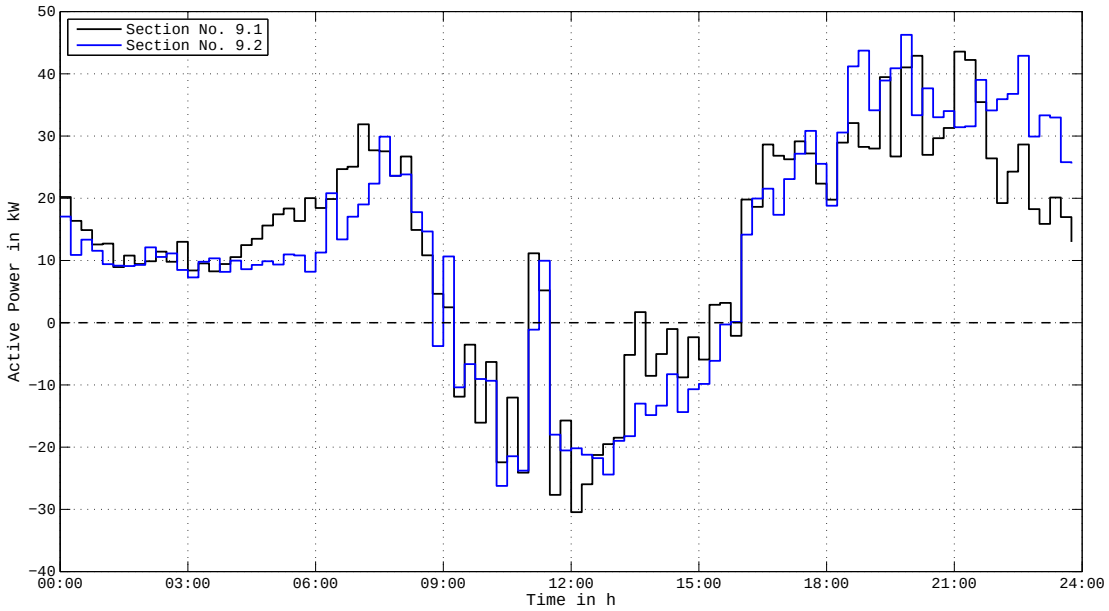

Figure 5.20.: S2060 - Active power of feeder No. 9.1 and No. 9.2

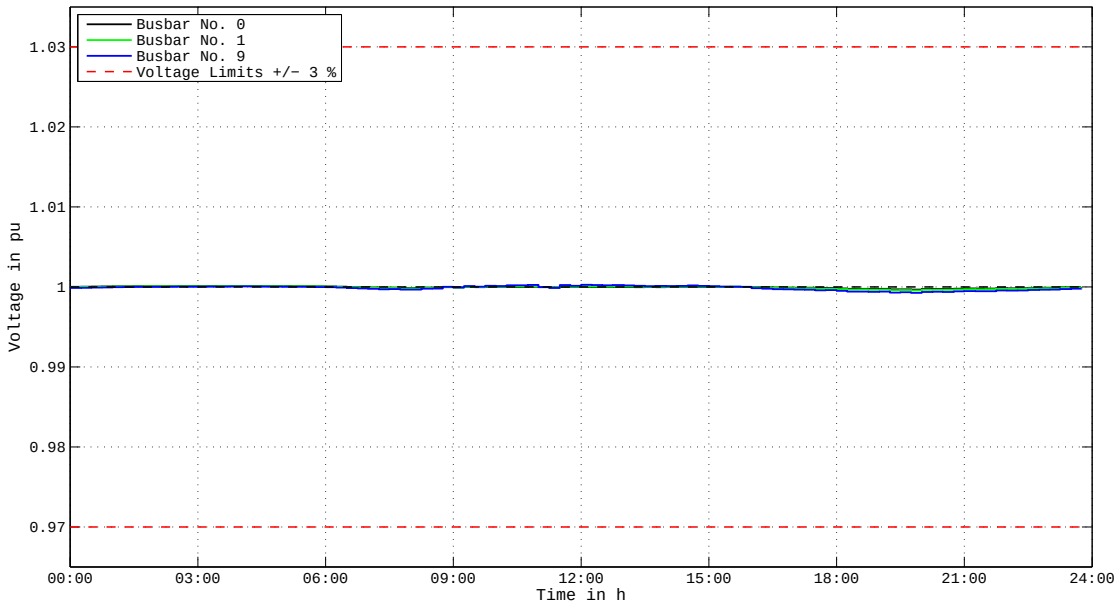

Figure 5.21.: S2060 - Voltage of busbar No. 0, No. 1 and 9

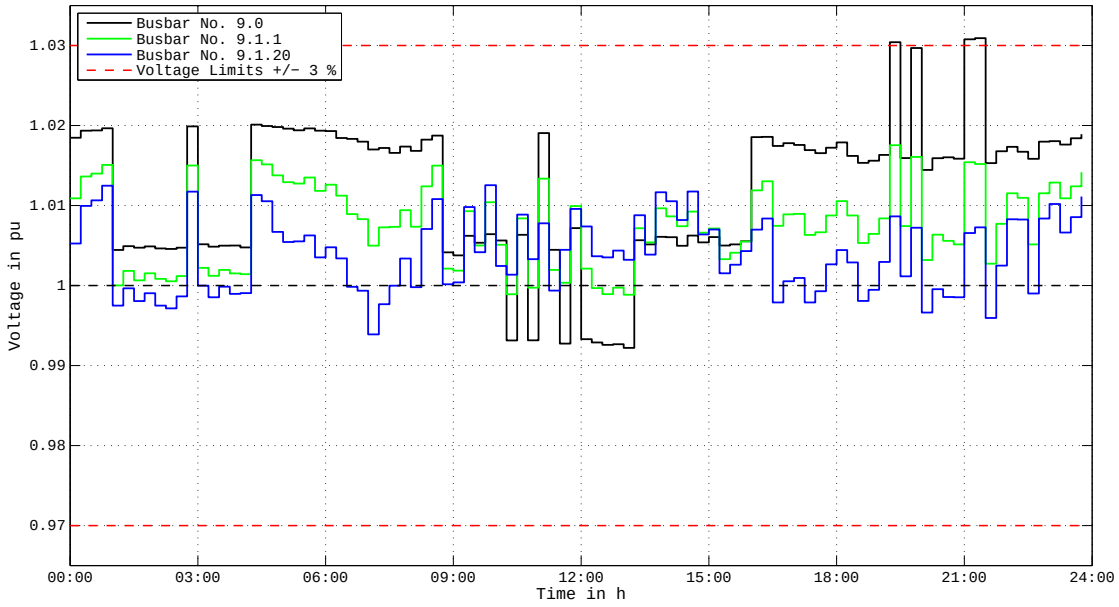

Figure 5.22.: S2060 - Voltage of busbar No. 9.1., No. 9.1.1 and No. 9.1.20

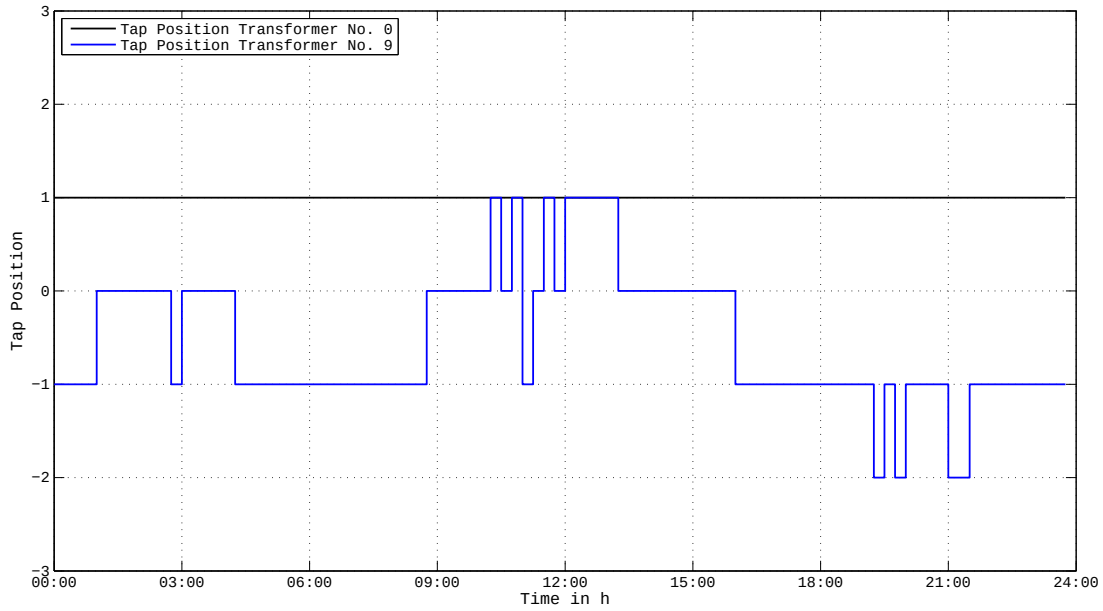

Figure 5.23.: S2060 - Tap positions of transformer No. 0 (110/10 kV, 40 MVA) and No. 9 (20/0,4 kV, 400 kVA

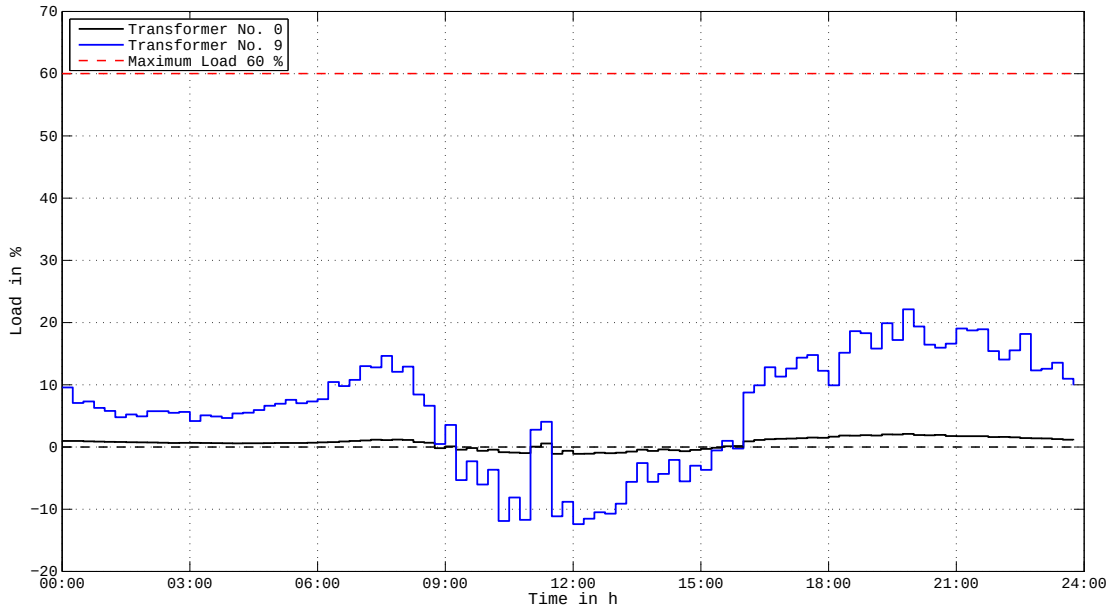

Figure 5.24.: S2060 - Load of transformer No. 0 (110/10 kV, 40 MVA) and No. 9 (20/0,4 kV, 400 kVA

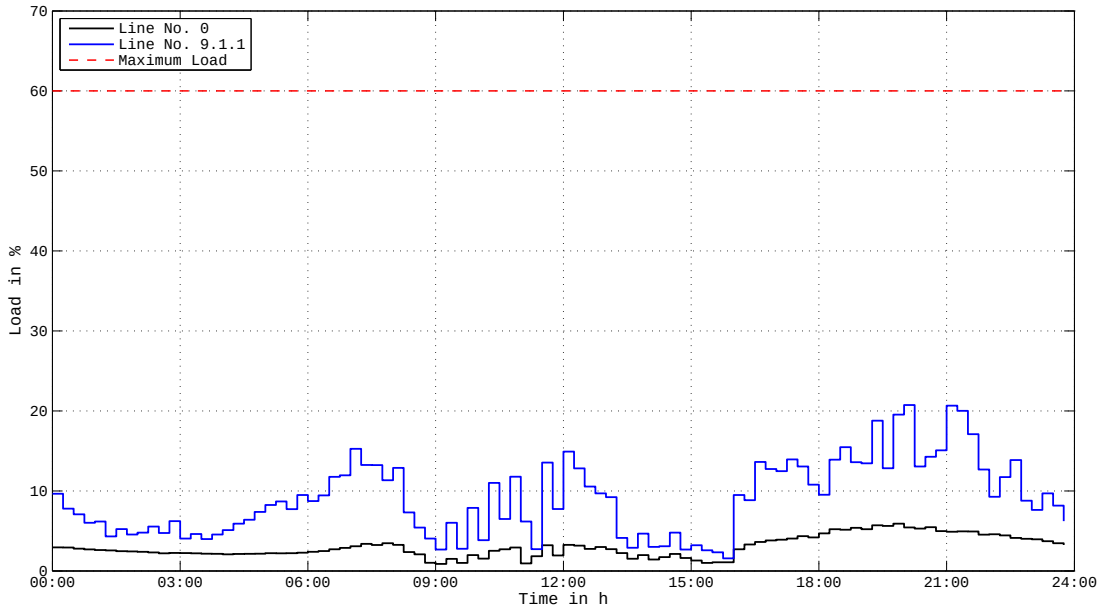

Figure 5.25.: S2060 - Load of line No. 0 and No. 9.1.1

The most important simulation results are depicted in table 5.2.

5.3. Rural Model Grid

The entire rural grid structure (middle voltage and low voltage structure) is depicted in figure 5.26. The main focus is again on the middle voltage transformer No. 0 (110/20 kV, 40 MVA), the low voltage transformer No. 58 (110/20 kV, 400 kVA), the line sections (No. 0 and No. 58.1.1), busbar (No. 0, No. 1 and No. 58) and busbar respectively lateral (No. 58.0, No. 58.1 and 58.10). The power comparison between the first of two feeders is not possible because only a single feeder at the busbar No. 58 branches off.

Table 5.2.: Simulation results for the suburban grid - scenario 2060

		Transformer No. 0	Line No. 0	Transformer No. 9
Active power in kW	min	-508 (11:15)	-508 (11:15)	-55 (11:15)
	max	742 (19:30)	743 (19:30)	80 (19:30)
Voltage in %	min	100,625 (19:30)	100,625 (19:30)	100,59 (19:30)
	max	100,663 (02:30)	100,663 (02:30)	100,68 (11:15)
Maximum Load in %		3,2 (19:30)	9 (19:30)	35 (19:30)
Tap changes		0	-	12

		Lateral 9.1.1	Line No. 9.1.1	Lateral 9.1.20
Active Power in kW	min	-32 (12:00)	-32 (12:00)	-2,1 (10:45)
	max	38 (18:15)	39 (18:15)	4,6 (07:30)
Voltage in %	min	99,22 (12:30)	99,22 (12:30)	99,42 (07:15)
	max	101,93 (04:45)	101,93 (04:45)	101,59 (13:45)
Maximum load in %		-	31 (18:15)	-
Tap changes		-	-	-

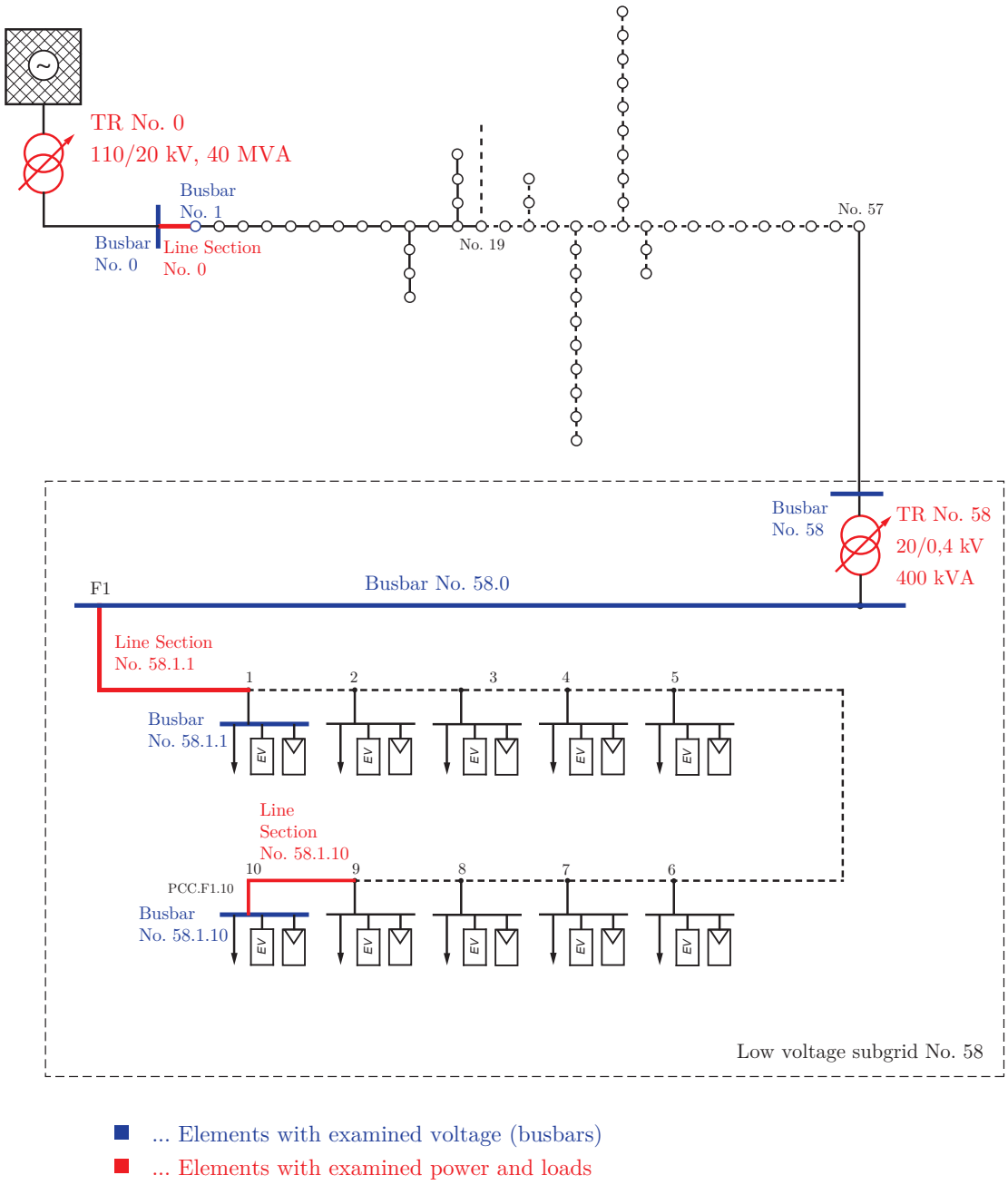

Figure 5.26.: Entire rural grid structure with emphasized simulation-relevant structures are marked red and blue

5.3.1. Scenario R-2060

The scenario 2060 represents the worst case with maximum feed-in capacities, 100% shares of electric mobility and and massively increasing household loads up to 180%.

The low voltage transformer No. 58 reaches only a small load, even in this worst case scenario (figure 5.27). Transformer No. 0 reaches a maximum power of nearly 1200 kVA and is far away of its maximum power of 40 MVA. The strong probabilistic influence of the load profile generation at a few laterals is shown in figure 5.28 with rather fluctuating values. The voltage at medium voltage level is due to the small load at transformer No. 0 only changing about 1%. In the low voltage structure at transformer No. 58, the +/- 3 % voltage thresholds are violated significantly at 19:30. Simultaneously, the tap position of the regulating transformer No. 58 is changing to -2. This tap position prevents at 19:30 from violating the lower voltage threshold, but violates the upper limit. The maximum load of transformer No. 0 and No. 58 is far away of the 60% load threshold (figure 5.32) as well as the line load No. 0 and No. 58.1.1 (figure 5.33). The summary of the simulation results are depicted in table 5.3.

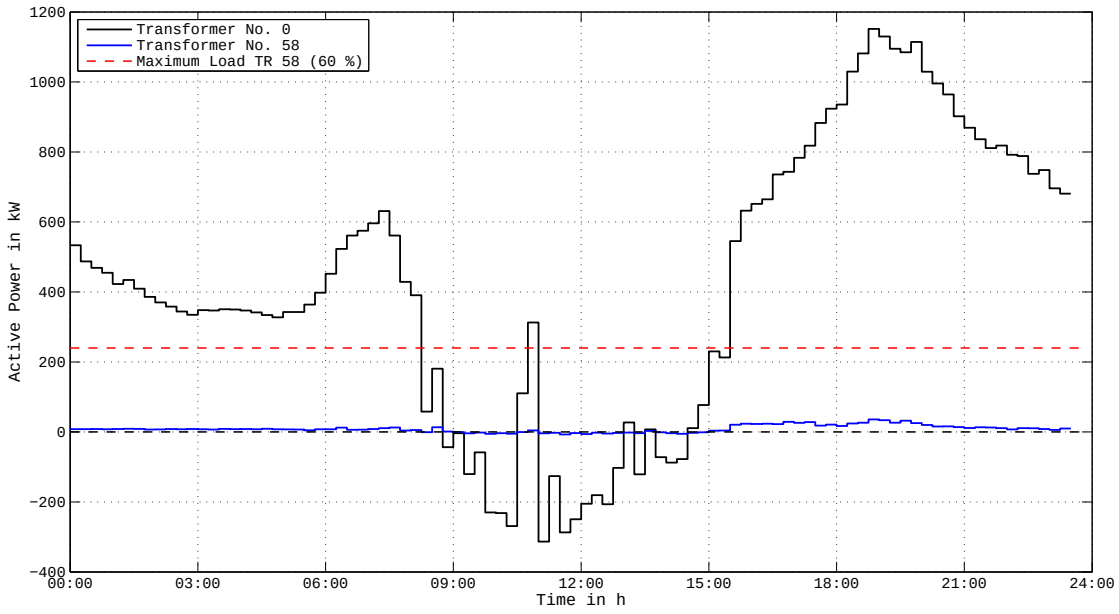

Figure 5.27.: R2060 - Active power of transformer No. 0 (110/10 kV, 40 MVA) and No. 58 (110/20 kV, 400 kVA)

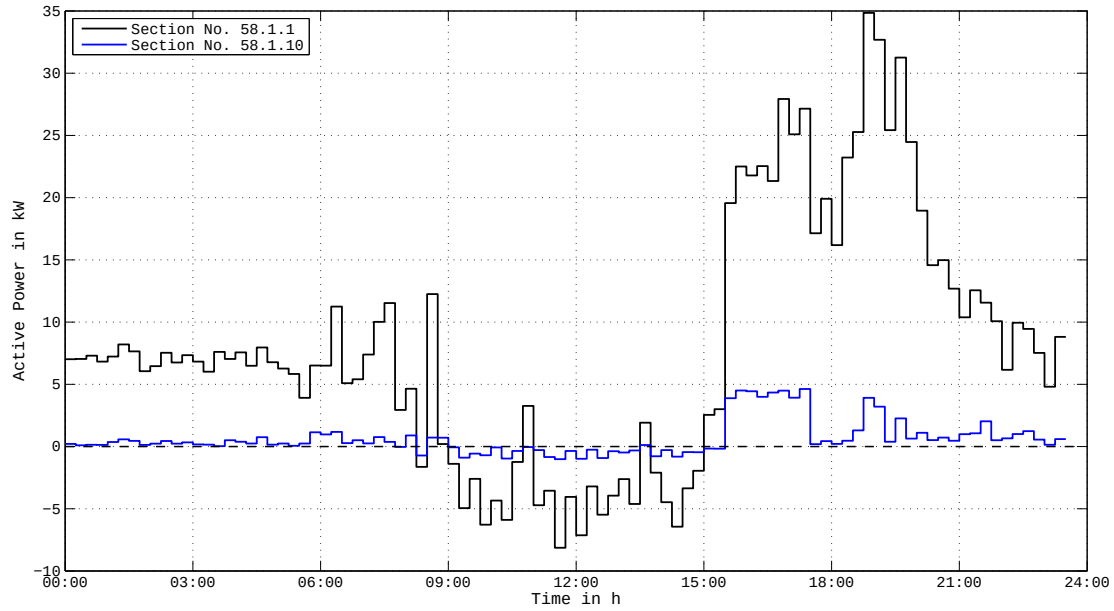

Figure 5.28.: R2060 - Active power of section No. 58.1.1 and No. 58.1.10

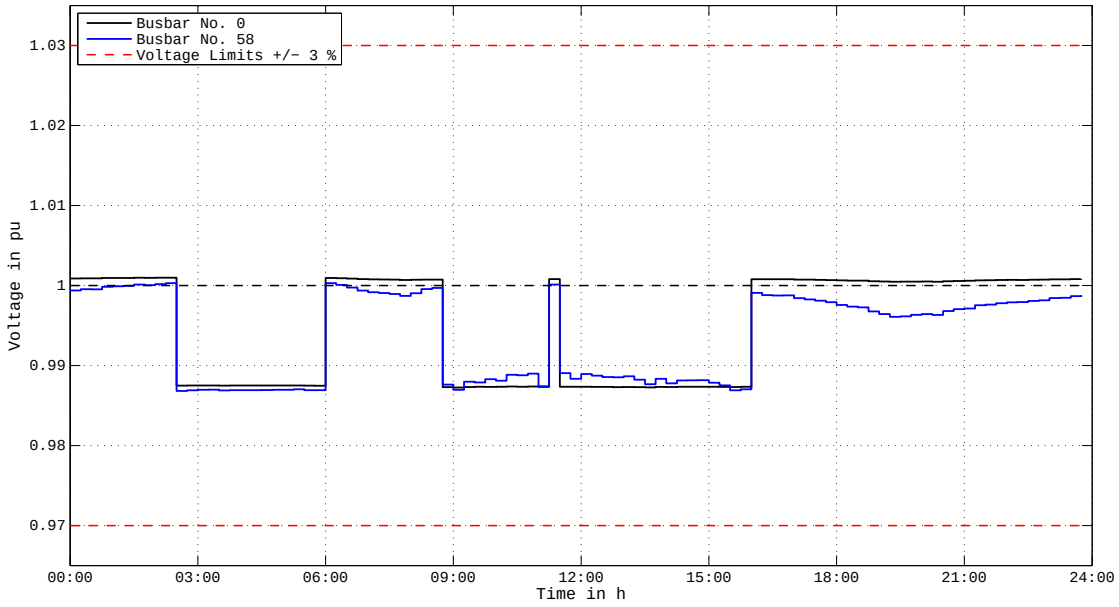

Figure 5.29.: R2060 - Voltage of busbar No. 0, No. 58

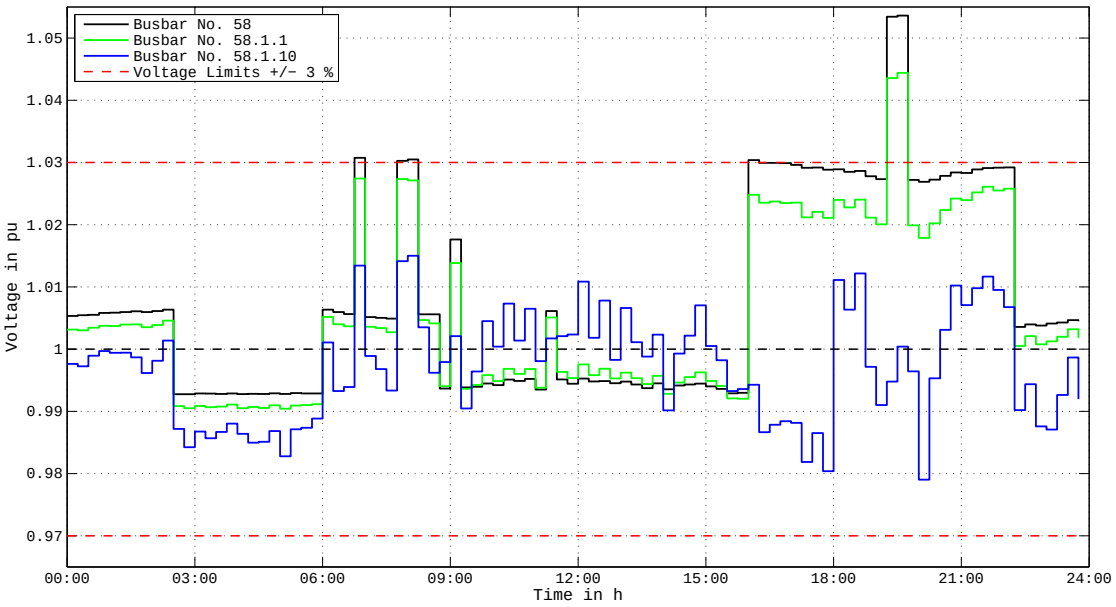

Figure 5.30.: R2060 - Voltage of busbar No. 58.1., No. 58.1.1 and No. 58.1.10

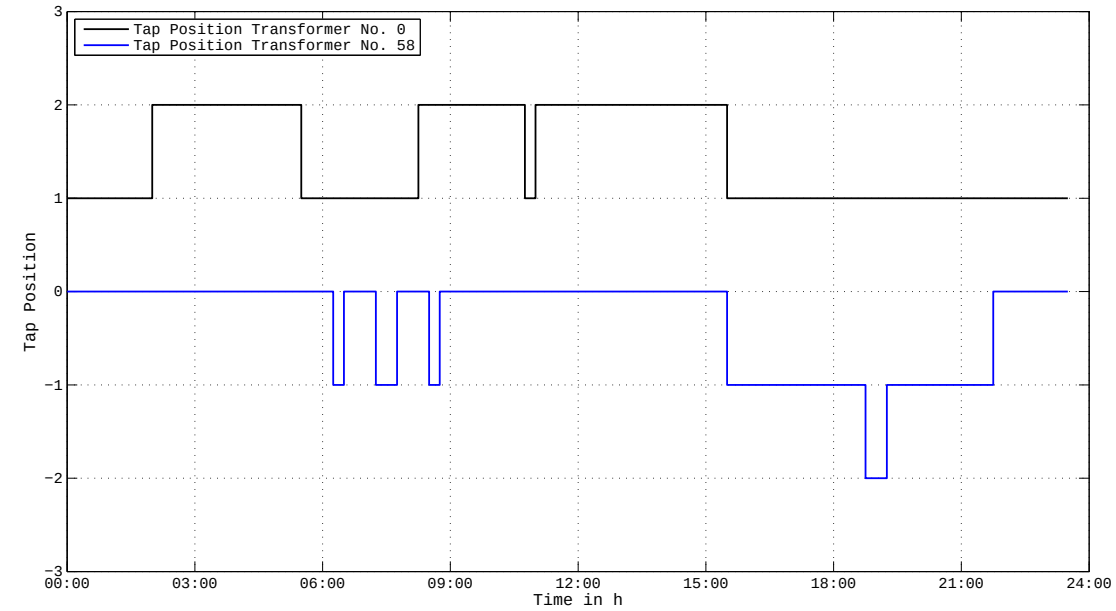

Figure 5.31.: R2060 - Tap positions of transformer No. 0 (110/10 kV, 40 MVA) and No. 58 (110/20 kV, 400 kVA)

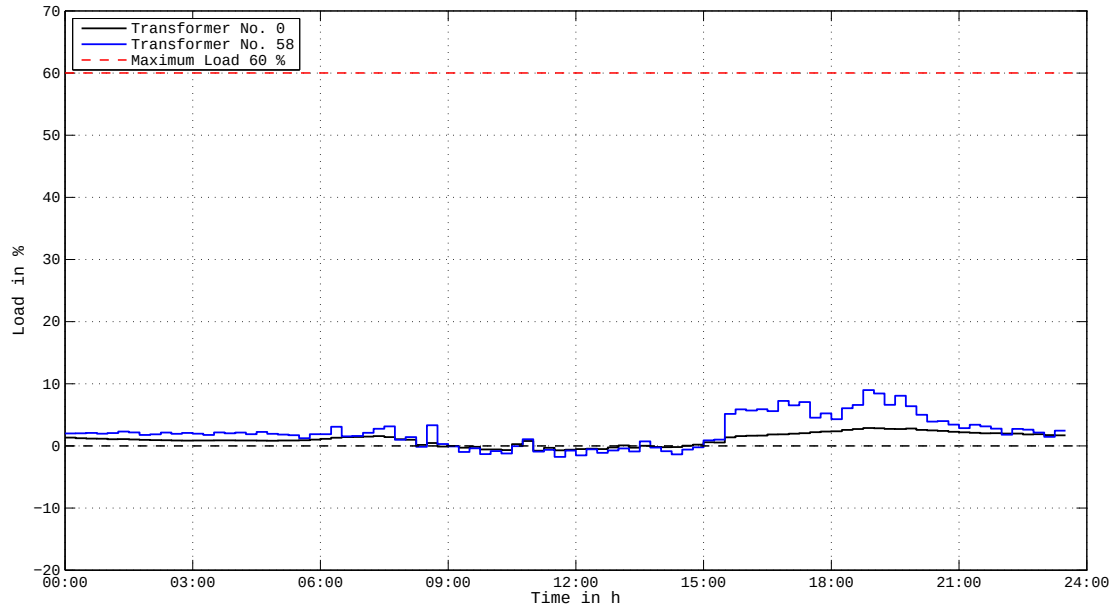

Figure 5.32.: R2060 - Load of transformer No. 0 (110/10 kV, 40 MVA) and No. 58 (110/20 kV, 400 kVA)

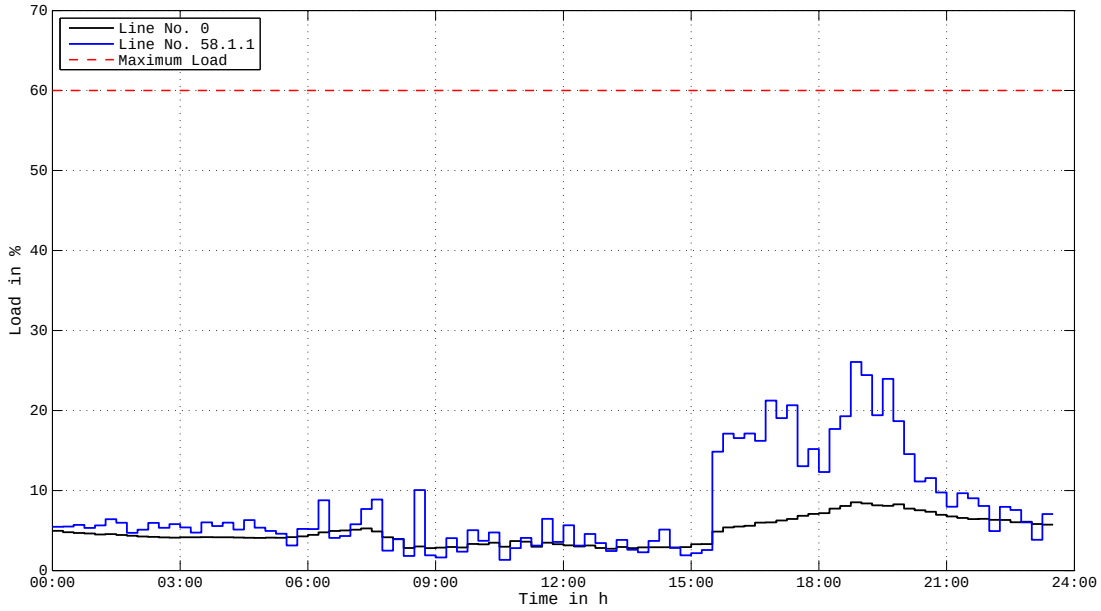

Figure 5.33.: R2060 - Load of line No. 0 and No. 58.1.1

The most relevant simulation results are shown in table 5.3.

Table 5.3.: Simulation results for the rural grid - scenario 2060

		Transformer No. 0	Line No. 0	Transformer No. 58
Active power in kW	min	-280 (11:30)	-7700 (12:15)	-5 (14:45)
	max	1230 (20:00)	1231 (20:00)	38 (19:30)
Voltage in %	min	99,36 (13:30)	99,36 (13:30)	99,32 (04:00)
	max	100,75 (02:00)	100,75 (02:00)	100,7 (05:30)
Maximum Load in %		5,3 (19:15)	15 (19:15)	16 (19:15)
Tap changes		10	-	14

		Lateral 58.1.1	Line No. 58.1.1	Lateral 58.1.10
Active Power in kW	min	-7,7 (12:00)	-7,7 (12:00)	-1 (12:00)
	max	37 (19:15)	38 (19:15)	5 (16:30)
Voltage in %	min	99 (04:00)	99 (04:00)	97,8 (17:45)
	max	104,4 (19:00)	104,4 (19:00)	101,35 (08:00)
Maximum load in %		-	46 (19:15)	-
Tap changes		-	-	-

6. Conclusion

The load flow simulation for the urban, suburban and rural model grids indicate the transformer and line sections with the highest loads as well as the busbars with the highest voltage drops/rise. Generally, the impact of conventional household loads and electric mobility in combination with photovoltaic onto power supply grids is massively in the scenario 2060 and violates the permitted transformer and line loadings in the evening when the highest loads occur. The voltage drop is due to the usage of regulating transformers in no scenario a serious problem. The load profiles of the photovoltaic and the load profile of the electric vehicle do not really overlap significantly to compensate each other, but the maximum electric vehicle loads occur together with the conventional household loads in the evening and reinforce the impact onto power supply grids. In the scenario 2040 and 2020 all relevant grid parameters are within specified limits and do not violate any thresholds.

How massive are the transformer and line loadings due to household loads, electric mobility and micro-generation in the respective power supply grid for each scenario?

As a summery the results of the performed load flow simulations with respect to the transformer and line loadings for the three scenarios (2020, 2040, 2060) are depicted in table 6.1.

Table 6.1.: Conclusion of transformer and line loadings for each scenario

	2020		2040		2060	
	Transformers	Lines	Transformers	Lines	Transformers	Lines
Urban	✓	✓	✓	✓	×	×
Suburban	✓	✓	✓	✓	✓	✓
Rural	✓	✓	✓	✓	✓	✓

Only in the urban model grid the limits of transformer and line loadings are violated for the scenario 2060.

In which range is the voltage drop/rise in the respective power supply grid for each scenario (2020, 2040, 2060)?

The summery of the simulation results according to the voltage rise/drop for each scenario and for every three types of model grids is shown in table 6.2.

Table 6.2.: Conclusion of voltage drop/rise for each scenario

	2020	2040	2060
	Busbars/Laterals	Busbars/Laterals	Busbars/Laterals
Urban	✓	✓	✓
Suburban	✓	✓	✓
Rural	✓	✓	✓

In every scenario for all three model grids the voltage drop/rise is within specified limits due to the usage of regulating transformers .

Which measures can be taken into account to reduce the impact onto low voltage grids?

The following measures can be taken into account:

- Usage of regulating transformers
- Grid reinforcement
- Intelligent charging management to reduce the peak caused by the electric mobility in the evening
- Better overlapping of PV and EV/HH to compensate each other is due to high load peaks in the evening hardly possible

Bibliography

[1] M. Boxwell, *The 2011 Electric Car Guide*, A. Boxwell, Ed. Greenstream Publishing, 2011, vol. 2.

[2] I. Husain, *Electric and Hybrid Vehicles, Design Fundamentals*. Taylor and Francies Group, 2011, vol. 2.

[3] C. Anderson, *Electric and hybrid cars: a history, Design Fundamentals*. McFarland and Company, Inc., 2010, vol. 2.

[4] K. C. C.C. Chan, *Modern Electric Vehicle Technology*. Oxford University Press, 2001, vol. 1.

[5] M. Boxwell, *Owning an electric car*. Greenstream Publishing, 2010, vol. 1.

[6] S. Austria, *KFZ - Bestand*, Statistik Austria, 2012.

[7] F. Times, "Buyers loath to pay more for electric cars," *Financial Times*, Sep 2010.

[8] S. Dahameja, *Electric Vehicle Battery Systems*. Newnes, Reed Elsevier, 2002, vol. 1.

[9] VCÖ, *VCÖ-Untersuchung: Wo es in Österreich die meisten und die wenigsten Autos gibt - 29.07.2011*, VCÖ, http://www.vcoe.at/de/presse/aussendungen-archiv/details/items/Ausgabe2011-100, Ausgabe 2011-100.

[10] ——, *Österreichs Autofahrer fahren 36 Kilometer pro Tag - 20.02.2012*, VCÖ, http://www.vcoe.at/de/presse/aussendungen-archiv/details/items/Ausgabe2012-33, Ausgabe 2012-33.

[11] D. A. Probst, *Erstellung und Simulation probabilistischer Lastmodelle von Haushalten und Elektrofahrzeugen zur Spannungsbandananlyse*.

[12] F. Otto, "Impact assessment for a high penetration of distributed generators in medium and low voltage grids," Master's thesis, University of Technology Graz, 2012.

A. Appendix

A.0.2. Scenario U-2040

In this scenario 2040 the the household loads are reduced from 80% above today's energy consumption in scenario 2060 to 50% above today's consumption. The photovoltaic reaches 80% of the possible feed-in capacity and the electric mobility share rates at 40% of a entire transformation from combustion engine based mobility towards electric mobility. Figure A.1 indicates the power characteristics of transformer No. 0 and No. 9. In this scenario the power characteristic of transformer No. 9 stays under the threshold of 60% (figure A.1 and A.7). Also the line loads of line No. 0 and No 9.1.1 do not violate the 60% threshold in figure A.8.

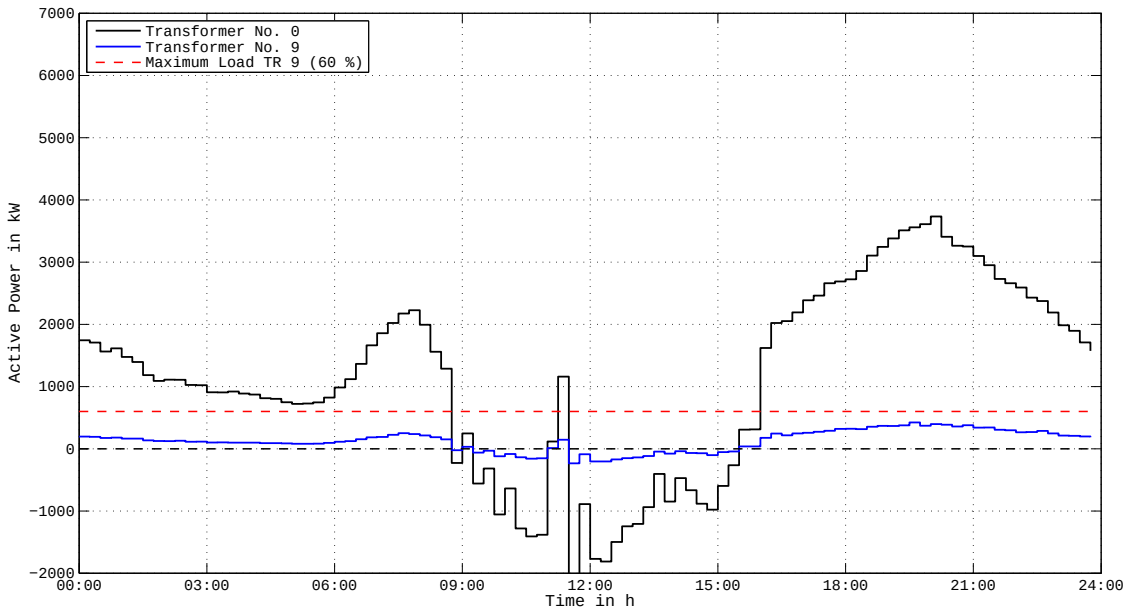

Figure A.1.: U2040 - Active power of transformer No. 0 (110/10 kV, 40 MVA) and No. 9 (10/0,4 kV, 1000 kVA)

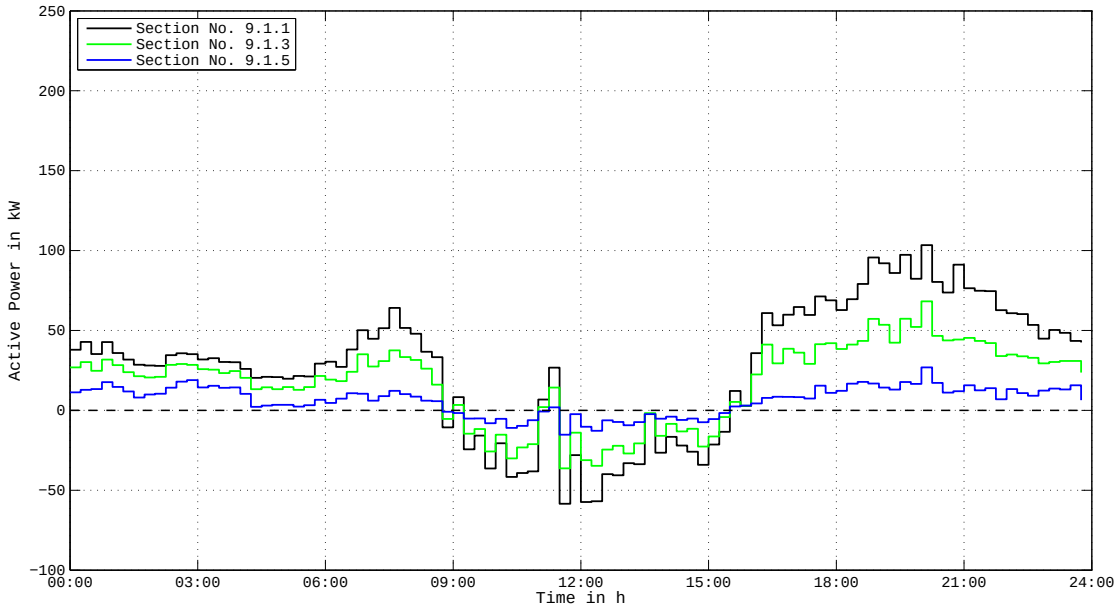

Figure A.2.: U2040 - Active power of section No. 9.1.1, No. 9.1.3 and No. 9.1.5

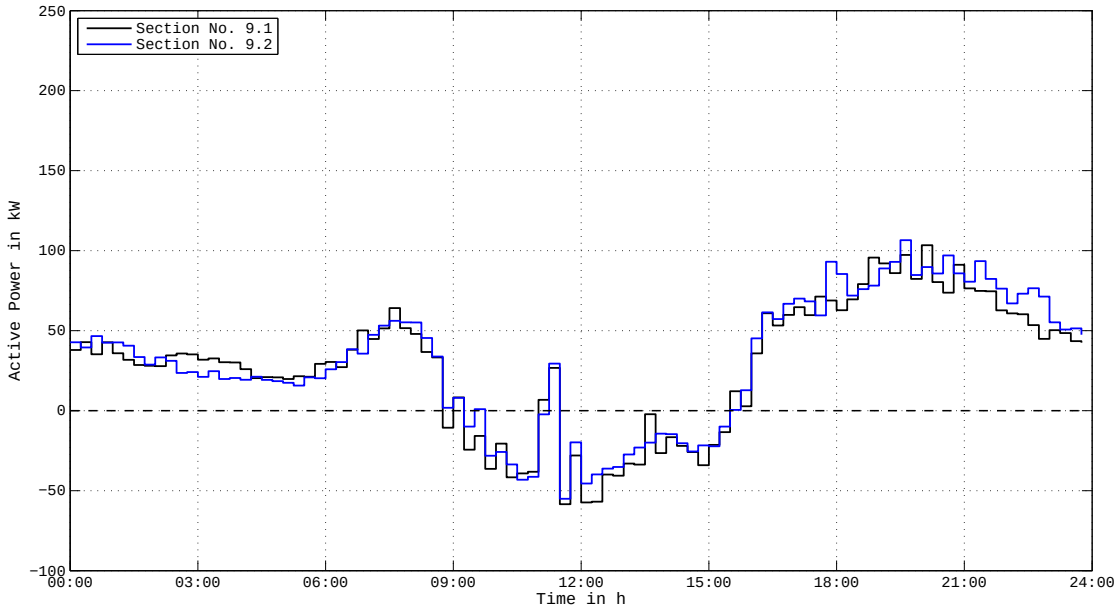

Figure A.3.: U2040 - Active power of feeder No. 9.1 and No. 9.2

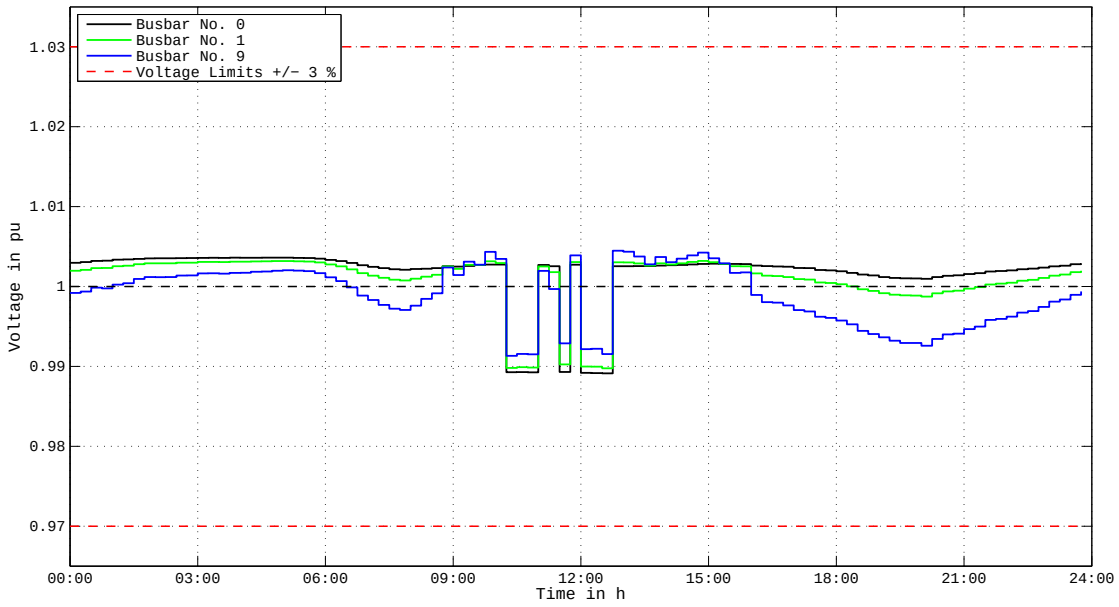

Figure A.4.: U2040 - Voltage of busbar No. 0, No. 1 and 9

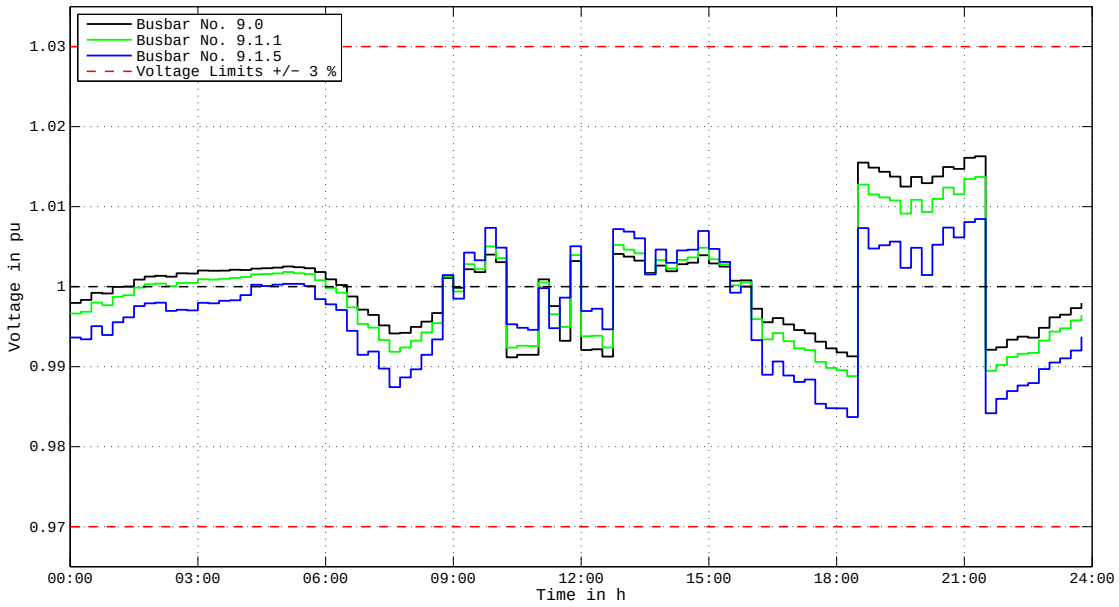

Figure A.5.: U2040 - Voltage of busbar No. 9.1., No. 9.1.1 and No. 9.1.5

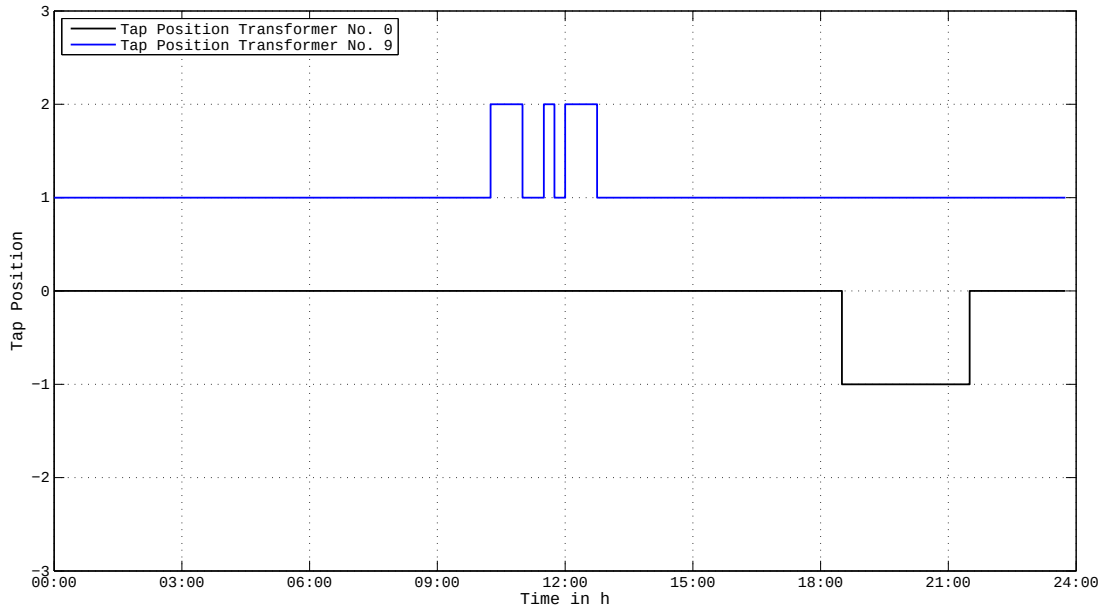

Figure A.6.: U2040 - Tap positions of transformer No. 0 (110/10 kV, 40 MVA)and No. 9 (10/0,4 kV, 1000 kVA)

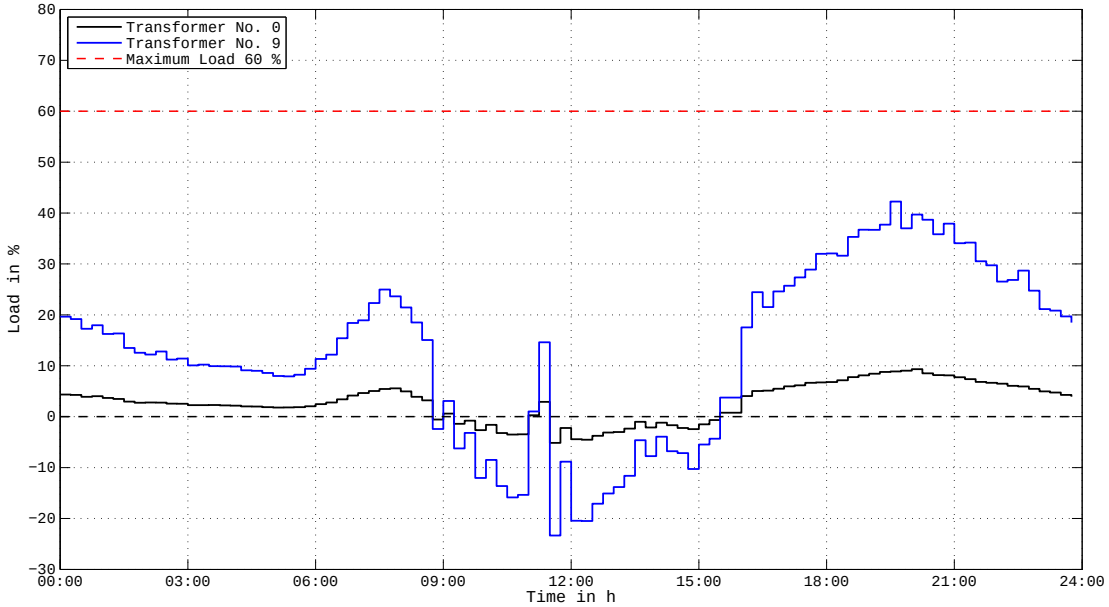

Figure A.7.: U2040 - Load of transformer No. 0 (110/10 kV, 40 MVA)and No. 9 (10/0,4 kV, 1000 kVA)

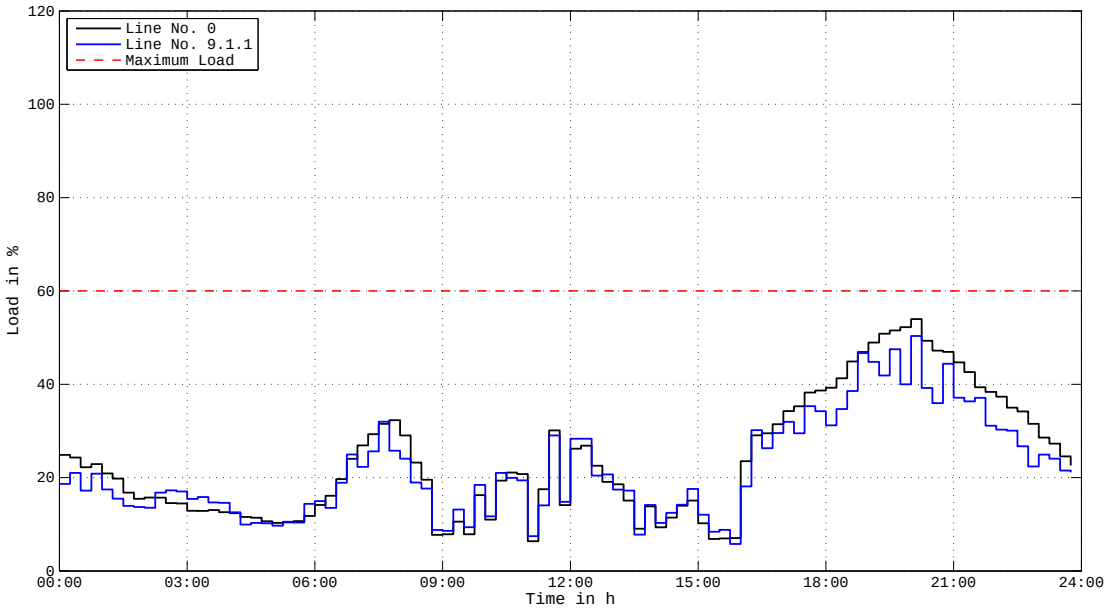

Figure A.8.: U2040 - Load of line No. 0 and No. 9.1.1

A.0.3. Scenario U-2020

In the scenario 2020 the decentralized energy production (photovoltaic) only gains a share of 20% of the possible feed-in capacity. The electric mobility shares only reach 10% and the household loads only increase to 120% of today's share. It is obvious that this impact is less significant than in scenario 2040 and therefore the transformer and line loads do not violate any specified thresholds. Even the regulating transformers No. 0 and No. 9 do not change any tap position (figure A.14).

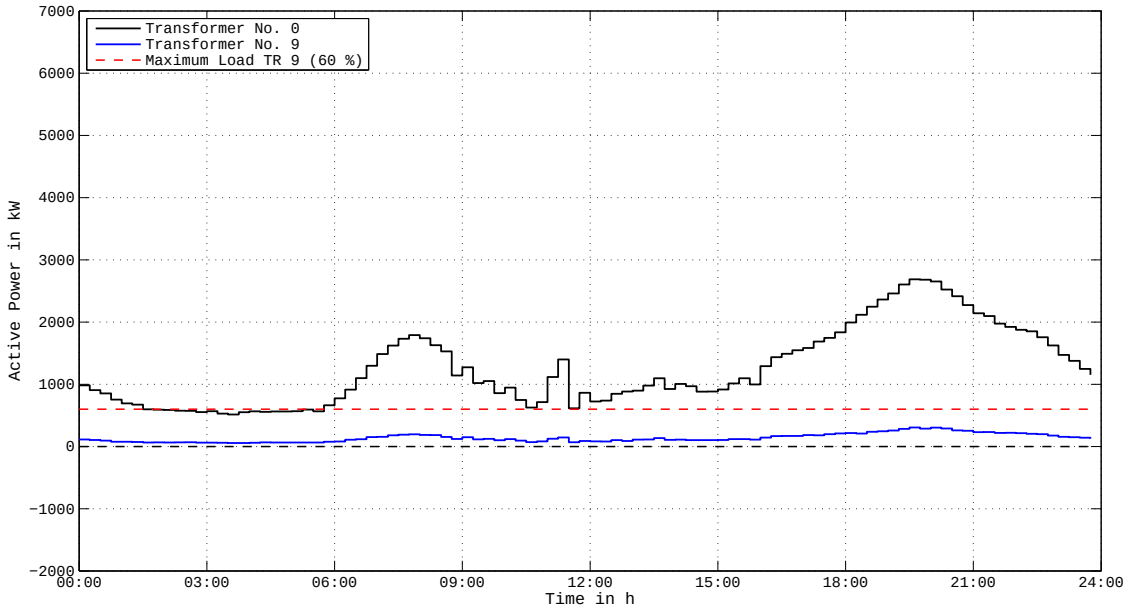

Figure A.9.: U2020 - Active power of transformer No. 0 (110/10 kV, 40 MVA) and No. 9 (10/0,4 kV, 1000 kVA)

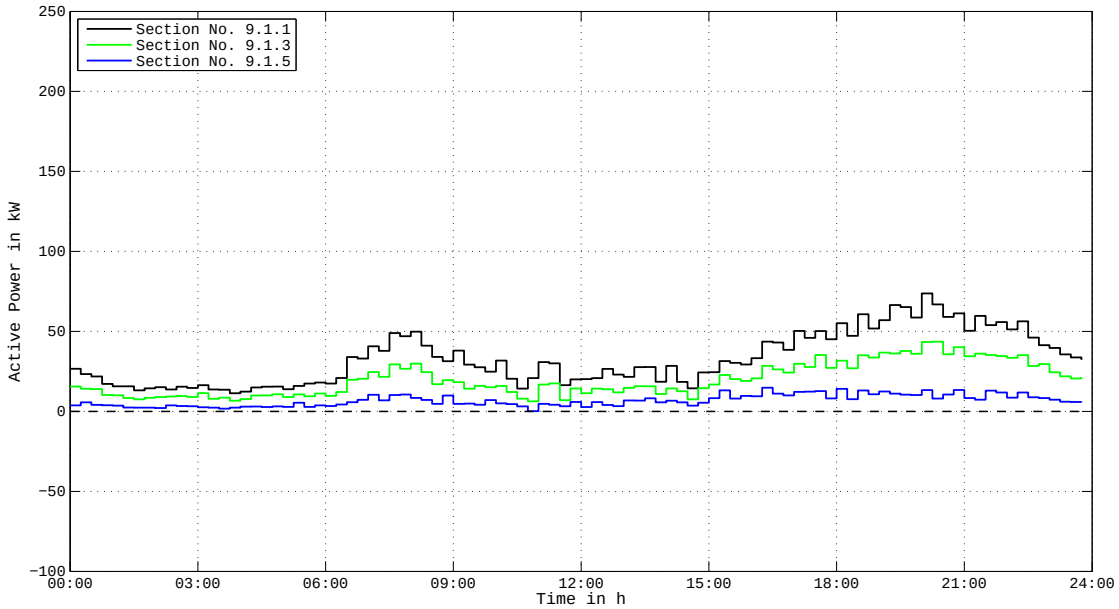

Figure A.10.: U2020 - Active power of section No. 9.1.1, No. 9.1.3 and No. 9.1.5

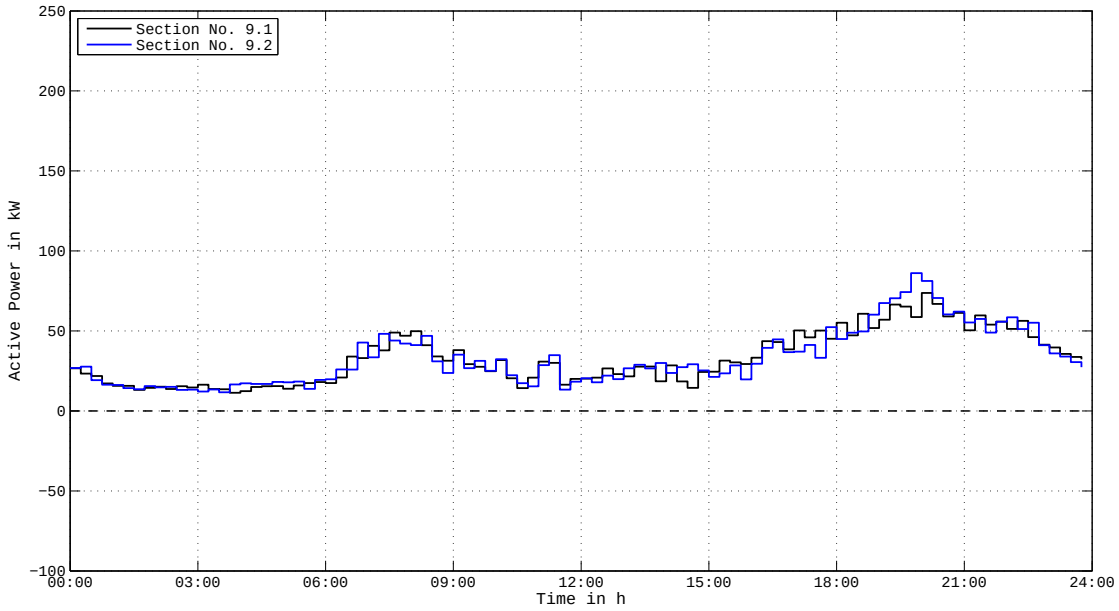

Figure A.11.: U2020 - Active power of feeder No. 9.1 and No. 9.2

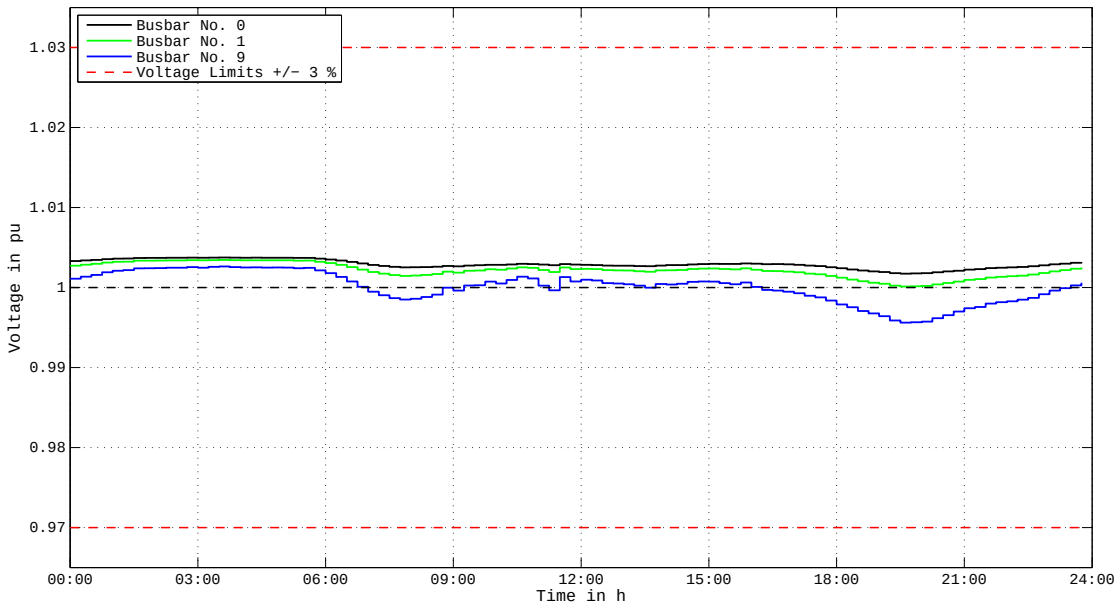

Figure A.12.: U2020 - Voltage of busbar No. 0, No. 1 and 9

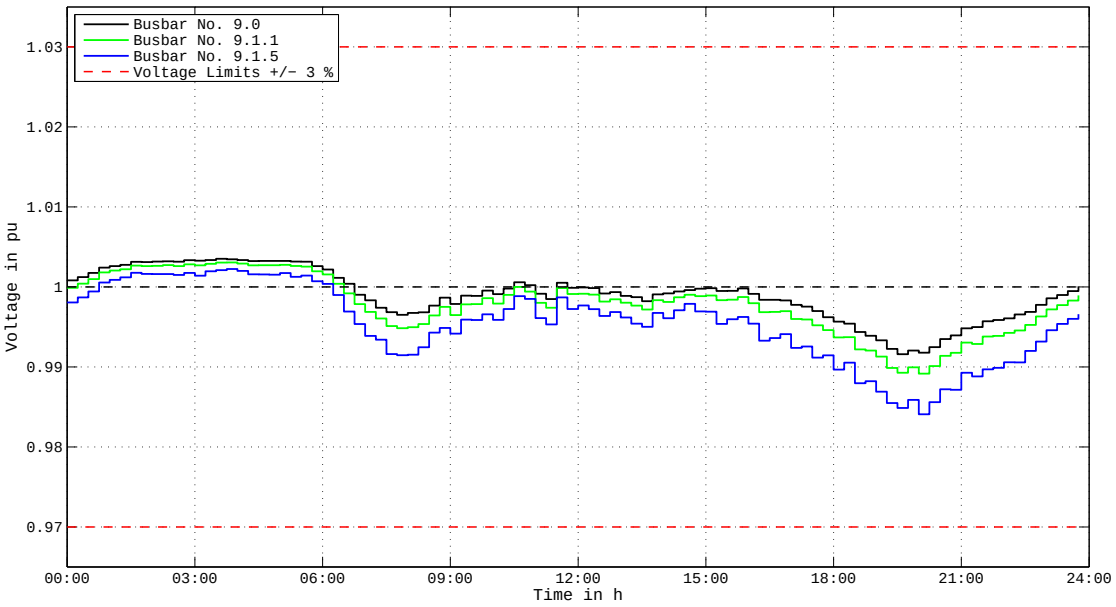

Figure A.13.: U2020 - Voltage of busbar No. 9.1., No. 9.1.1 and No. 9.1.5

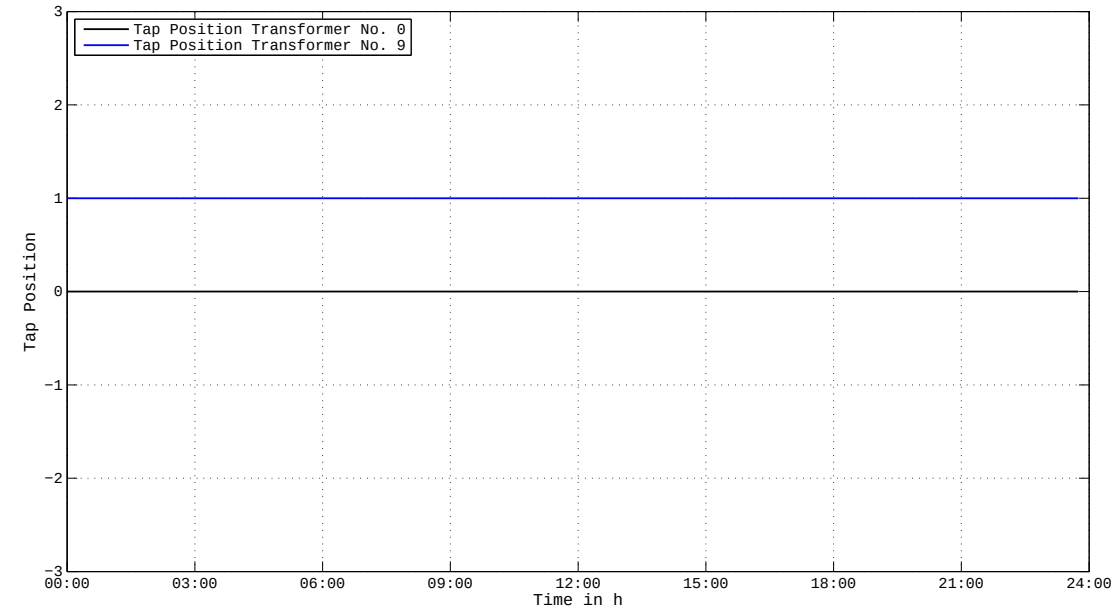

Figure A.14.: U2020 - Tap positions of transformer No. 0 (110/10 kV, 40 MVA) and No. 9 (10/0,4 kV, 1000 kVA)

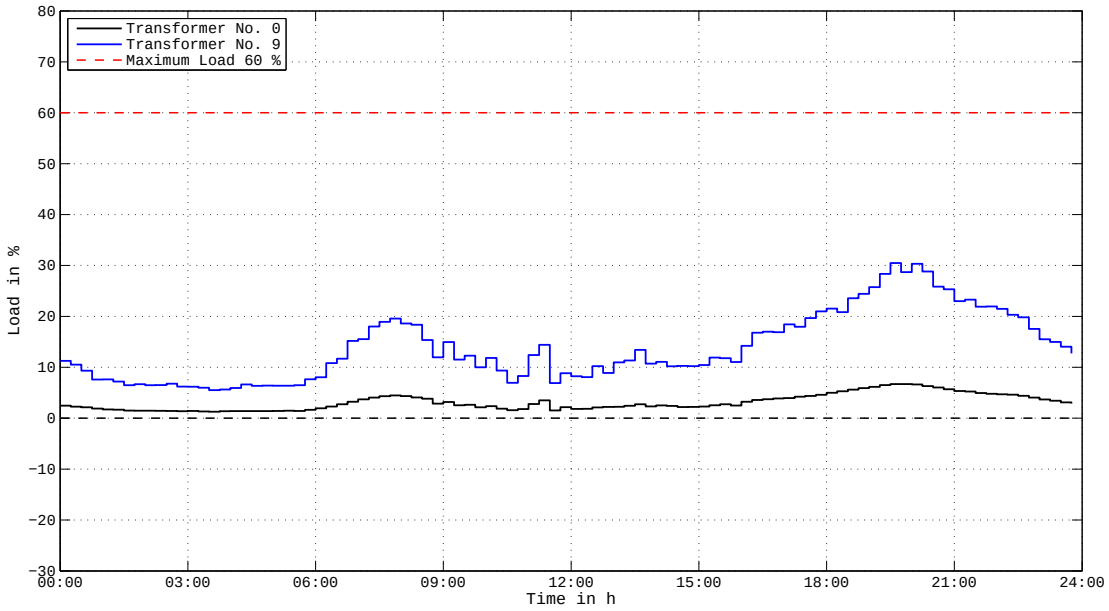

Figure A.15.: U2020 - Load of transformer No. 0 (110/10 kV, 40 MVA) and No. 9 (10/0,4 kV, 1000 kVA)

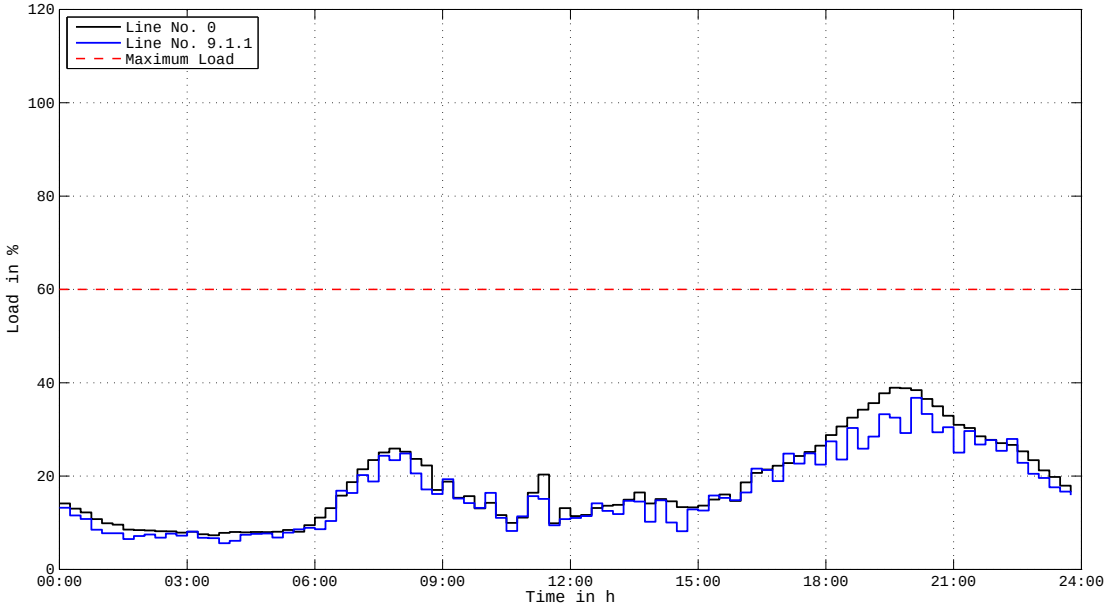

Figure A.16.: U2020 - Load of line No. 0 and No. 9.1.1

A.0.4. Scenario S-2040

In this scenario photovoltaic gains a share of 80%, electric mobility 40% and the household loads gain 50% above today's values. The simulation shows, that no limits are violated.

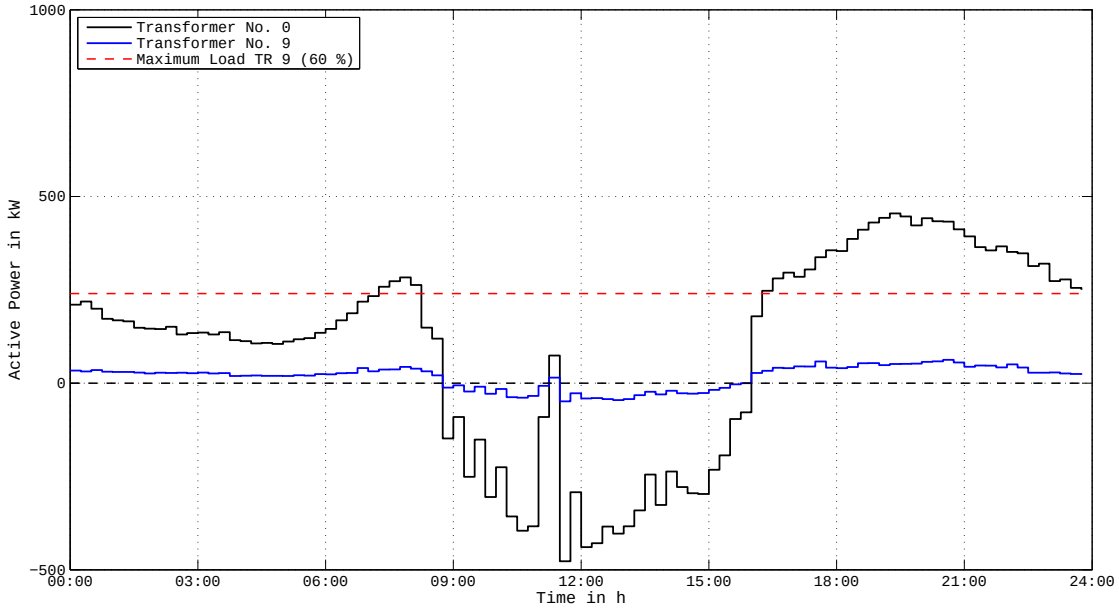

Figure A.17.: S2040 - Active power of transformer No. 0 (110/10 kV, 40 MVA) and No. 9 (20/0,4 kV, 400 kVA

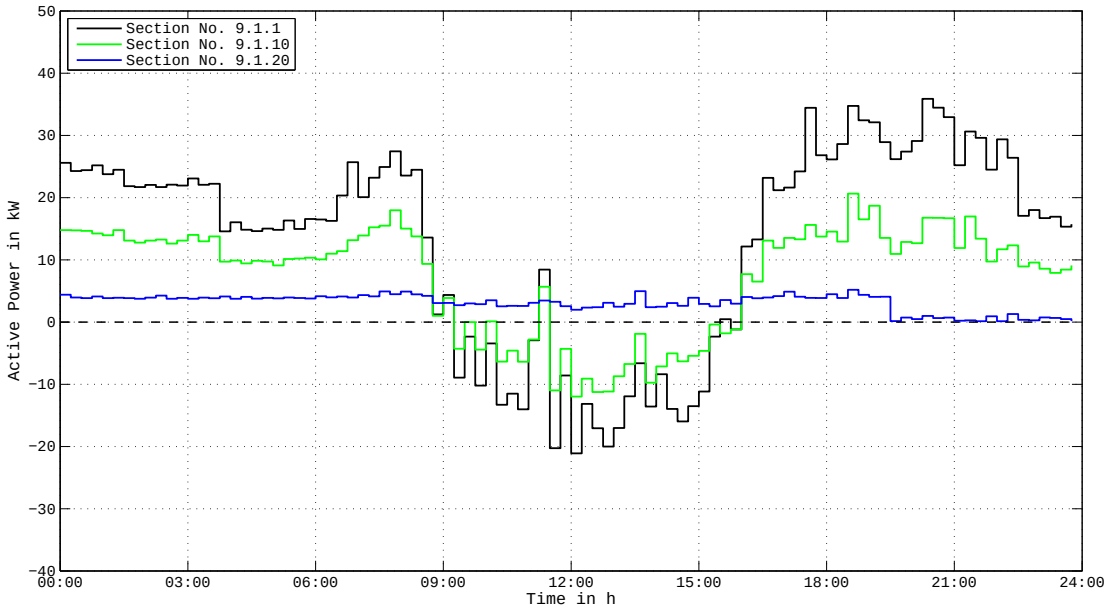

Figure A.18.: S2040 - Active power of section No. 9.1.1, No. 9.1.10 and No. 9.1.20

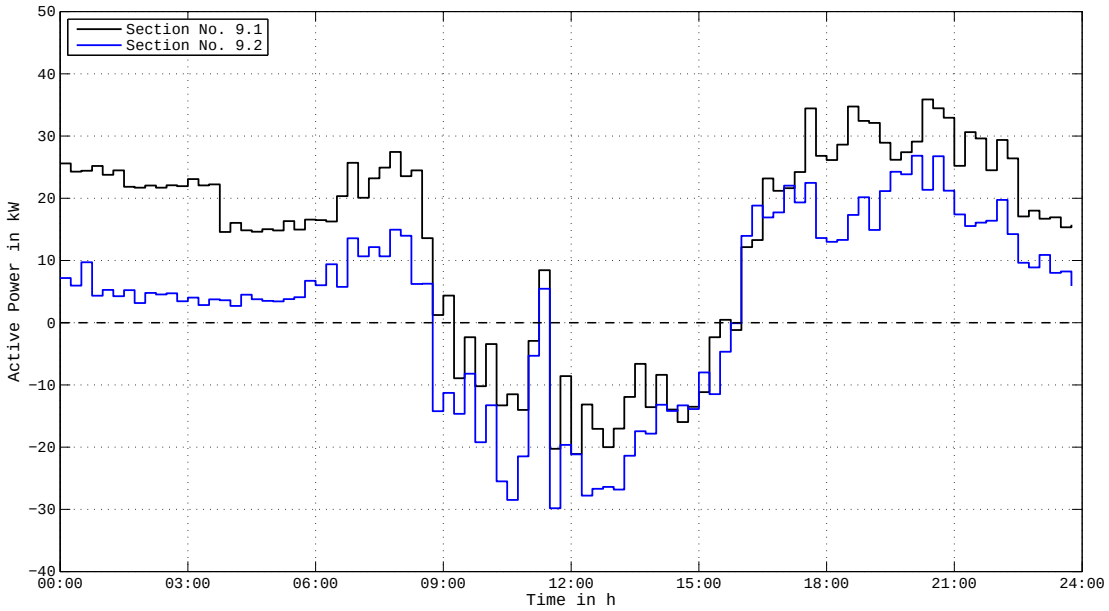

Figure A.19.: S2040 - Active power of feeder No. 9.1 and No. 9.2

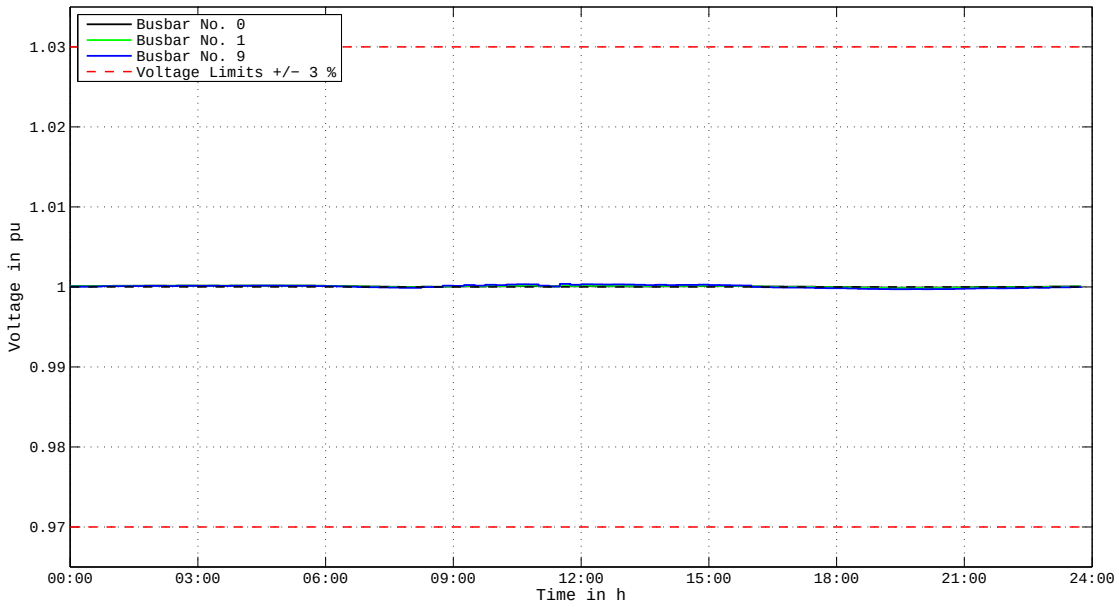

Figure A.20.: S2040 - Voltage of busbar No. 0, No. 1 and 9

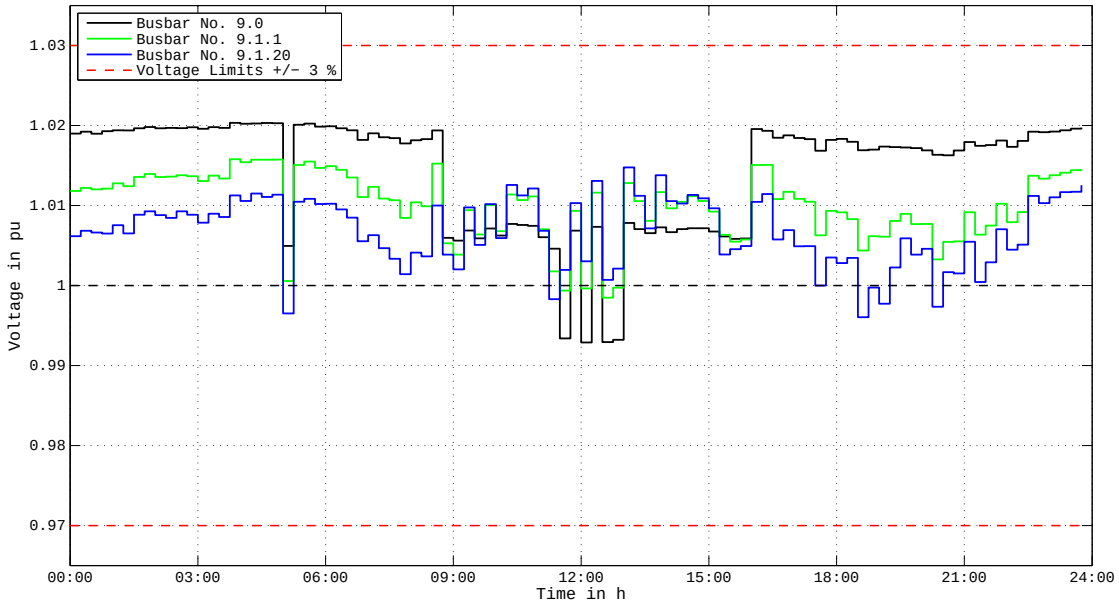

Figure A.21.: S2040 - Voltage of busbar No. 9.1., No. 9.1.1 and No. 9.1.20

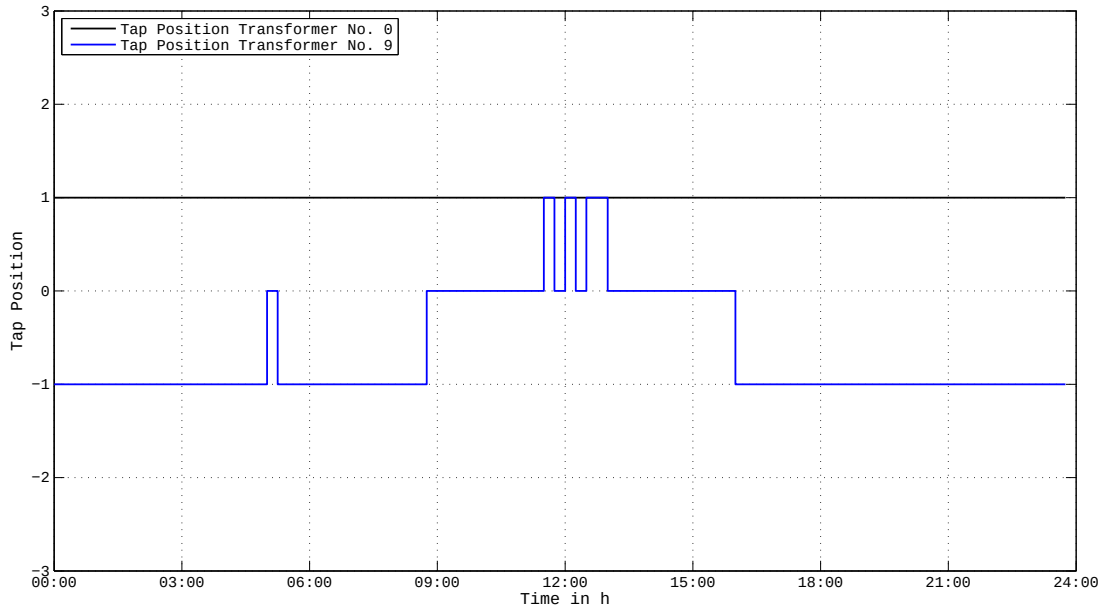

Figure A.22.: S2040 - Tap positions of transformer No. 0 (110/10 kV, 40 MVA) and No. 9 (20/0,4 kV, 400 kVA

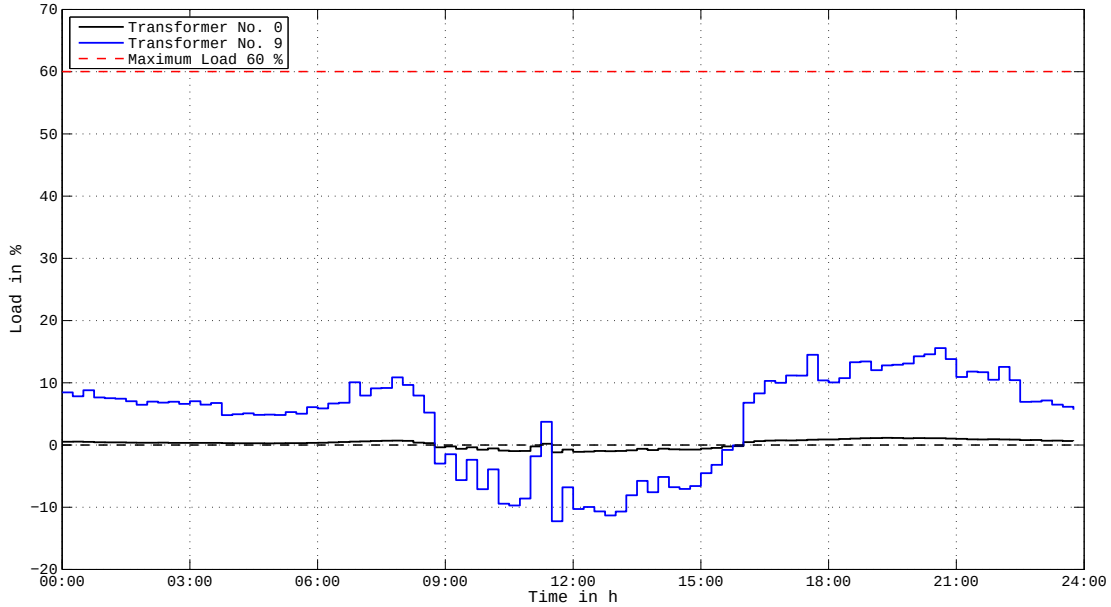

Figure A.23.: S2040 - Load of transformer No. 0 (110/10 kV, 40 MVA) and No. 9 (20/0,4 kV, 400 kVA

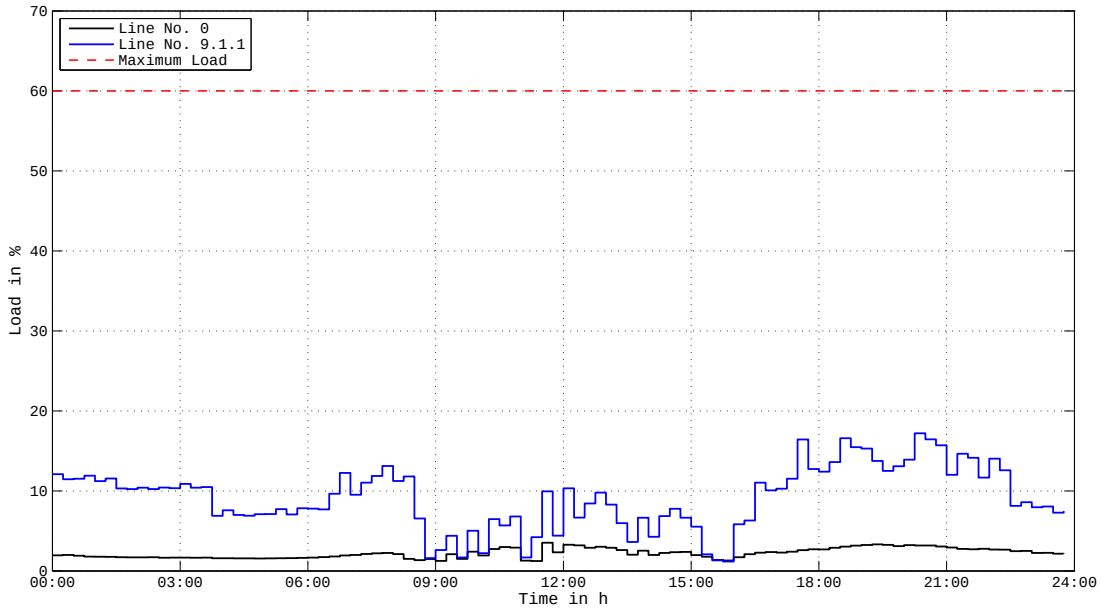

Figure A.24.: S2040 - Load of line No. 0 and No. 9.1.1

A.0.5. Scenario S-2020

In the scenario 2020 photovoltaic gains a share of 20%, electric mobility 10% and the household loads 20% above today's value. It is obvious if the scenario 2040 does not violate any limits, this current scenario will definitely not have a more massive impact than the scenario 2040.

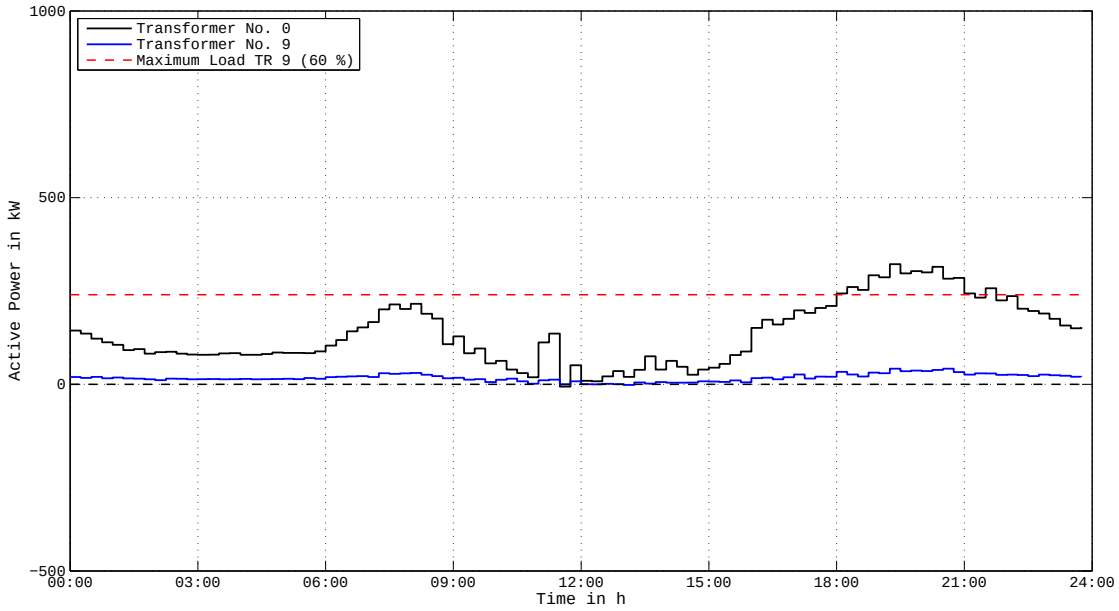

Figure A.25.: S2020 - Active power of transformer No. 0 (110/10 kV, 40 MVA) and No. 9 (20/0,4 kV, 400 kVA

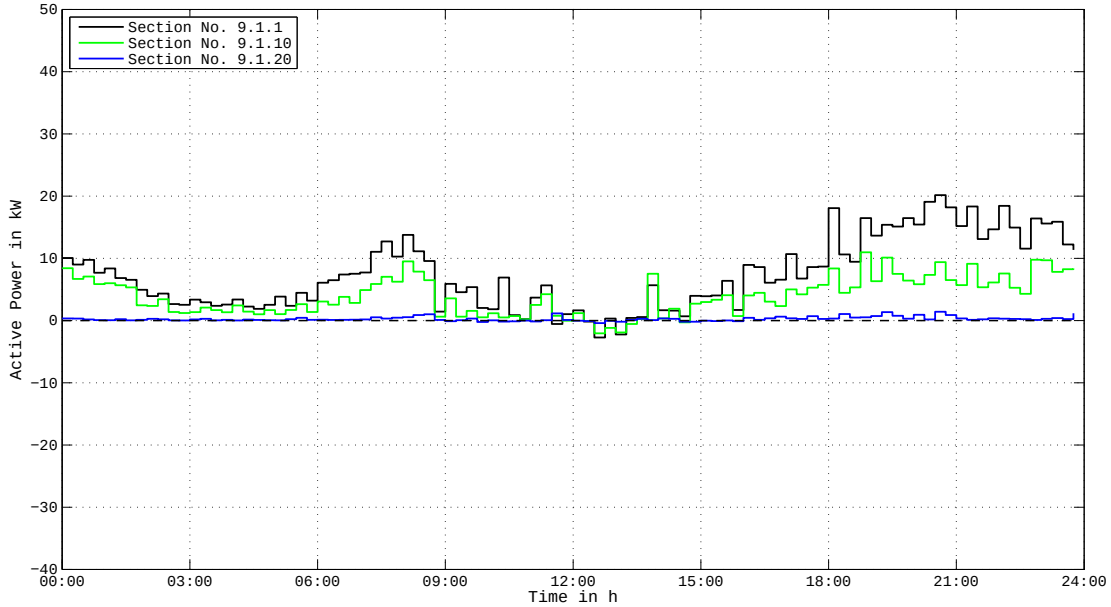

Figure A.26.: S2020 - Active power of section No. 9.1.1, No. 9.1.10 and No. 9.1.20

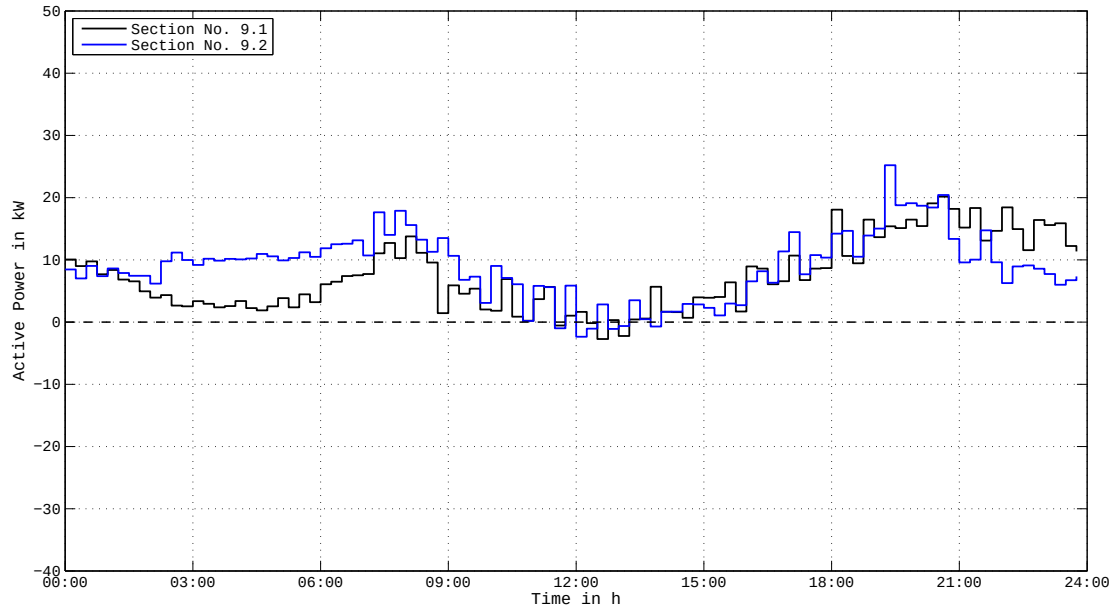

Figure A.27.: S2020 - Active power of feeder No. 9.1 and No. 9.2

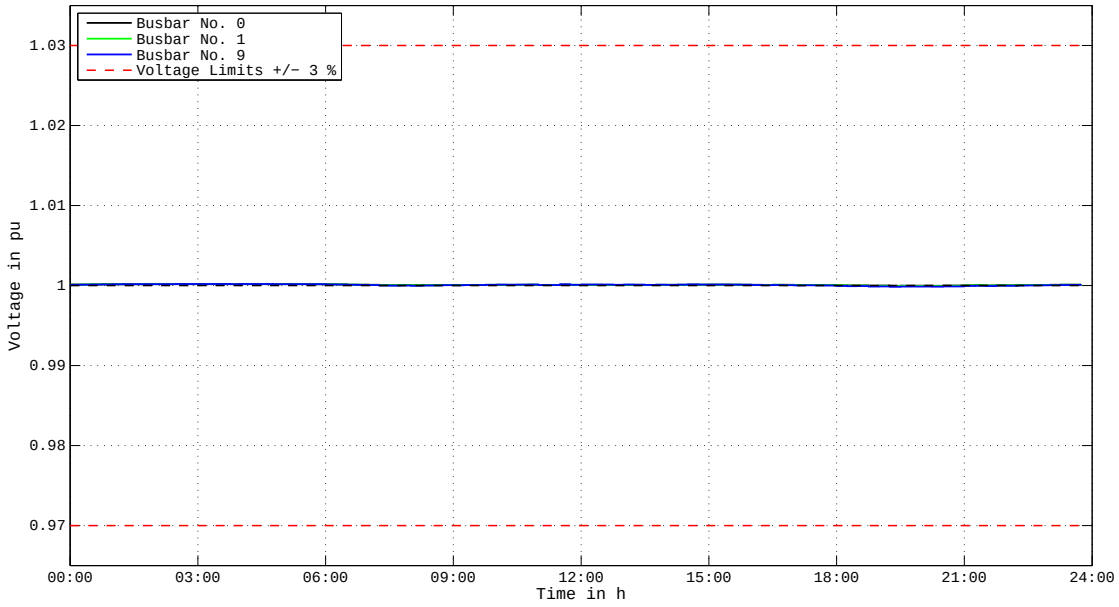

Figure A.28.: S2020 - Voltage of busbar No. 0, No. 1 and 9

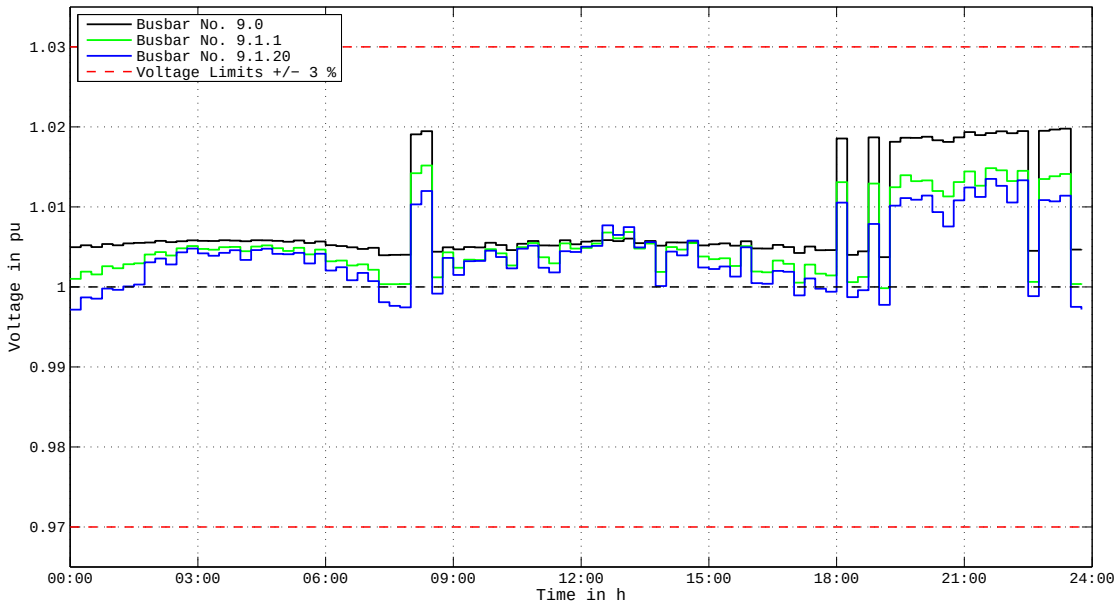

Figure A.29.: S2020 - Voltage of busbar No. 9.1., No. 9.1.1 and No. 9.1.20

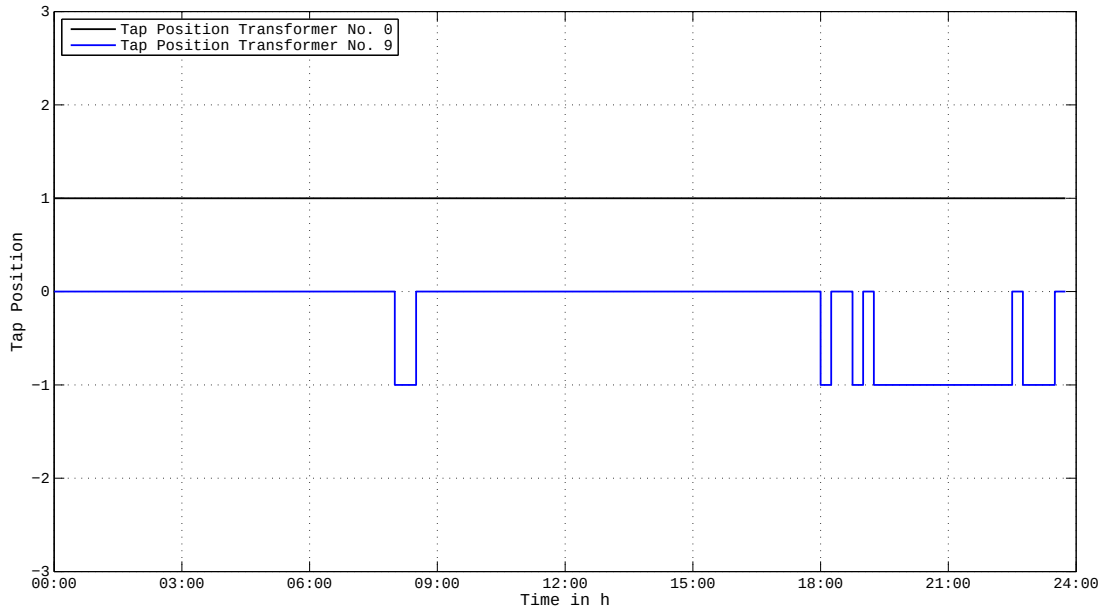

Figure A.30.: S2020 - Tap positions of transformer No. 0 (110/10 kV, 40 MVA) and No. 9 (20/0,4 kV, 400 kVA

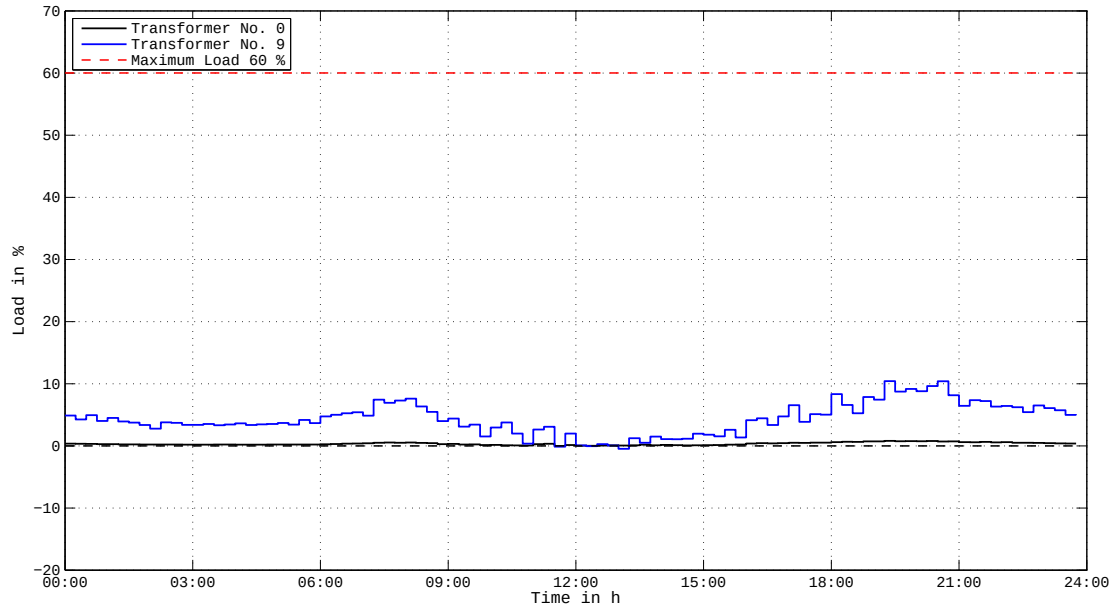

Figure A.31.: S2020 - Load of transformer No. 0 (110/10 kV, 40 MVA) and No. 9 (20/0,4 kV, 400 kVA

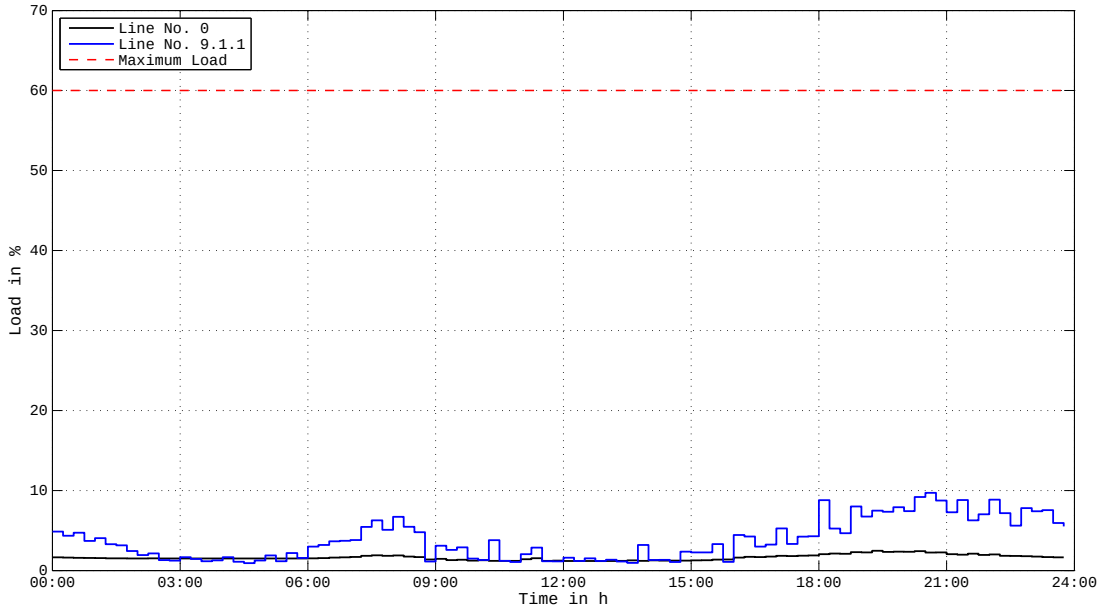

Figure A.32.: S2020 - Load of line No. 0 and No. 9.1.1

A.0.6. Scenario R-2040

In this scenario photovoltaic gains a share of 80%, electric mobility 40% and the household loads gain 50% above today's values. The simulation shows, that no load limits are violated neither the transformer nor the line loads. Only the voltage in figure A.36 is at the +3% limit for a short periods of time.

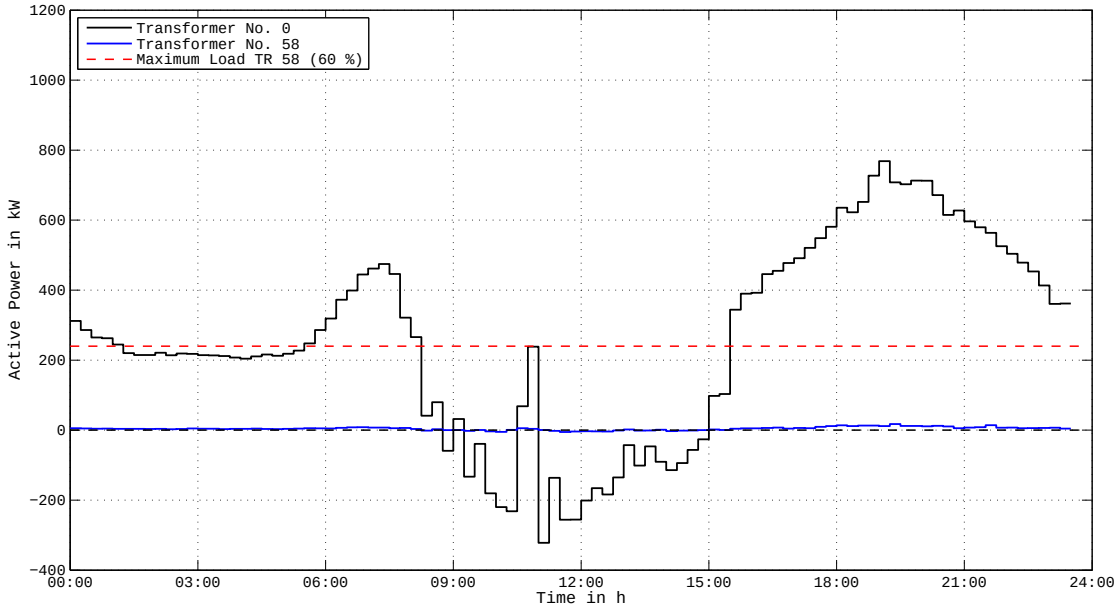

Figure A.33.: R2040 - Active power of transformer No. 0 (110/10 kV, 40 MVA) and No. 58 (110/20 kV, 400 kVA)

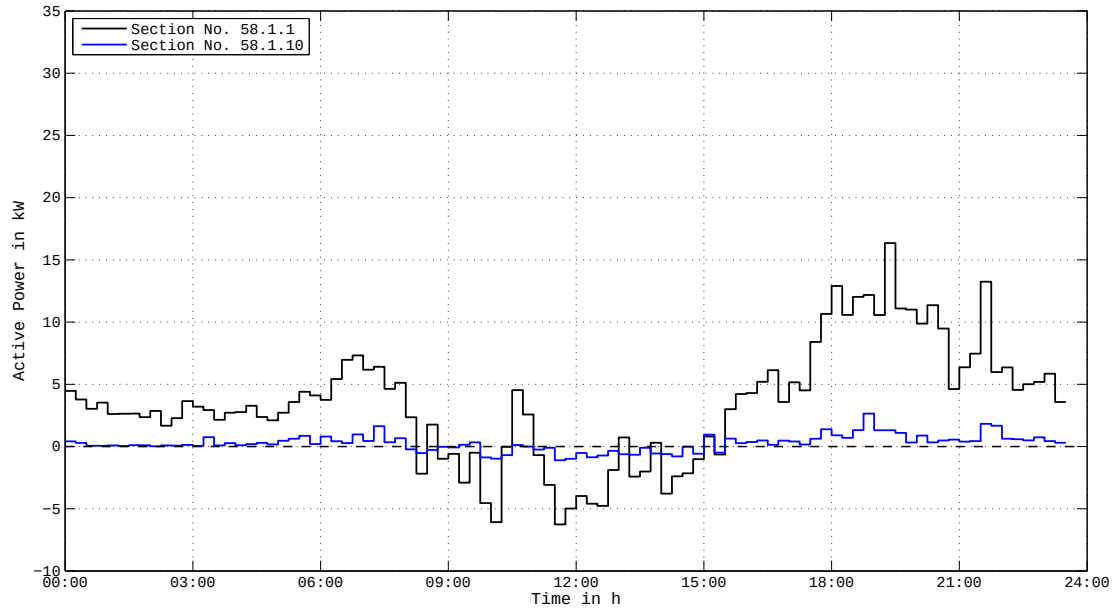

Figure A.34.: R2040 - Active power of section No. 58.1.1 and No. 58.1.10

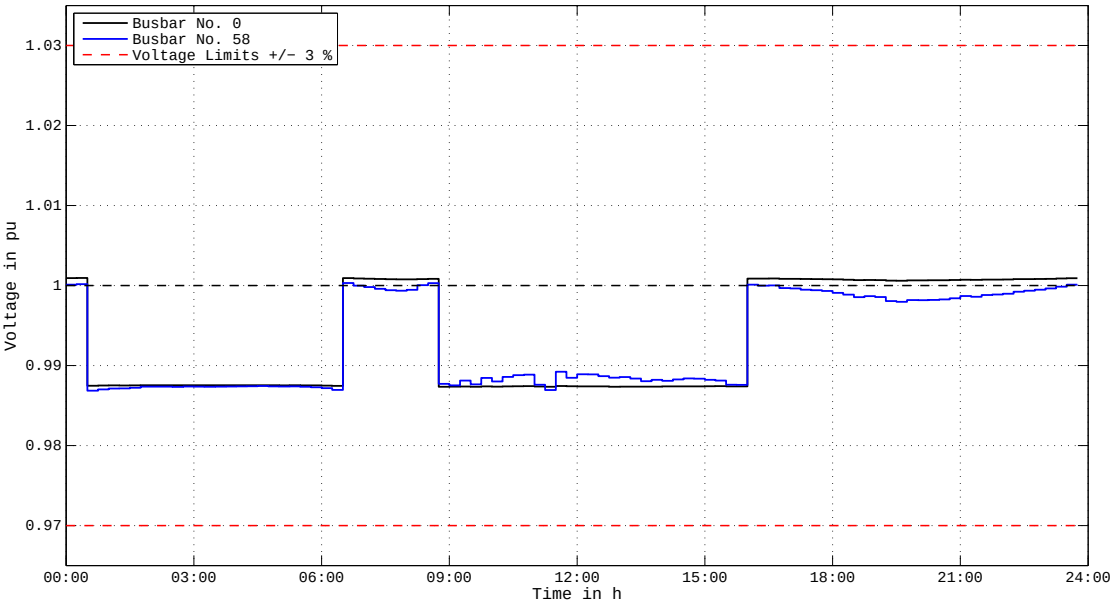

Figure A.35.: R2040 - Voltage of busbar No. 0, No. 58

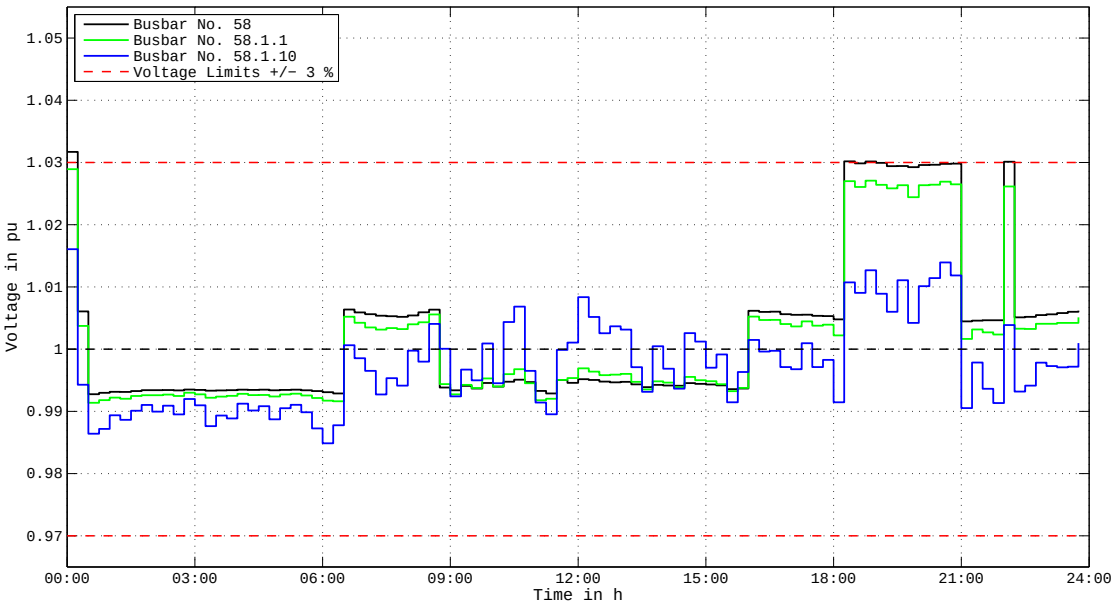

Figure A.36.: R2040 - Voltage of busbar No. 58.1., No. 58.1.1 and No. 58.1.10

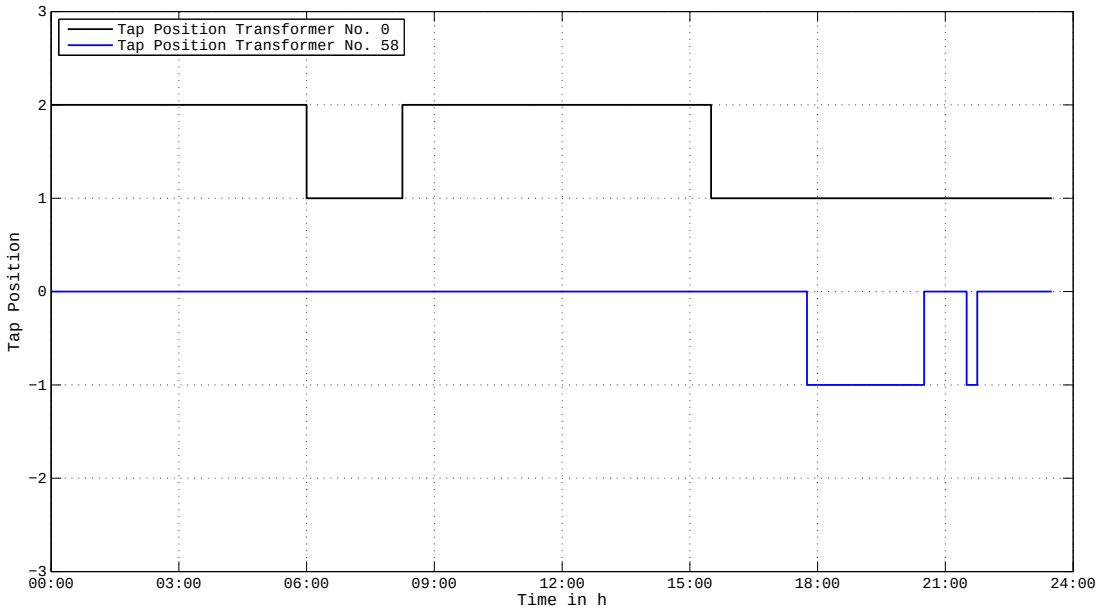

Figure A.37.: R2040 - Tap positions of transformer No. 0 (110/10 kV, 40 MVA) and No. 58 (110/20 kV, 400 kVA)

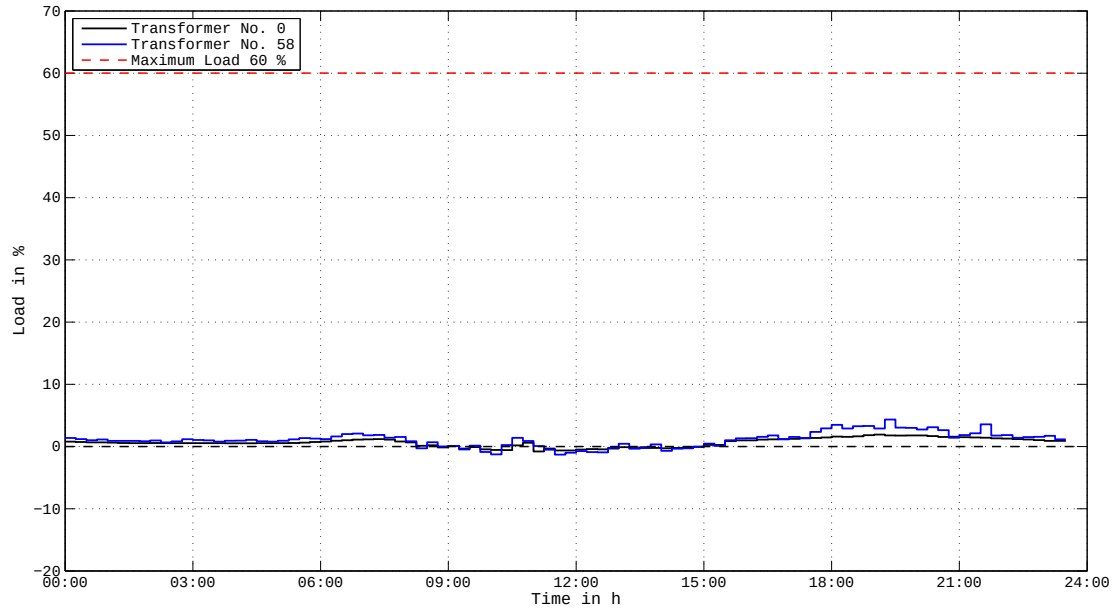

Figure A.38.: R2040 - Load of transformer No. 0 (110/10 kV, 40 MVA) and No. 58 (110/20 kV, 400 kVA)

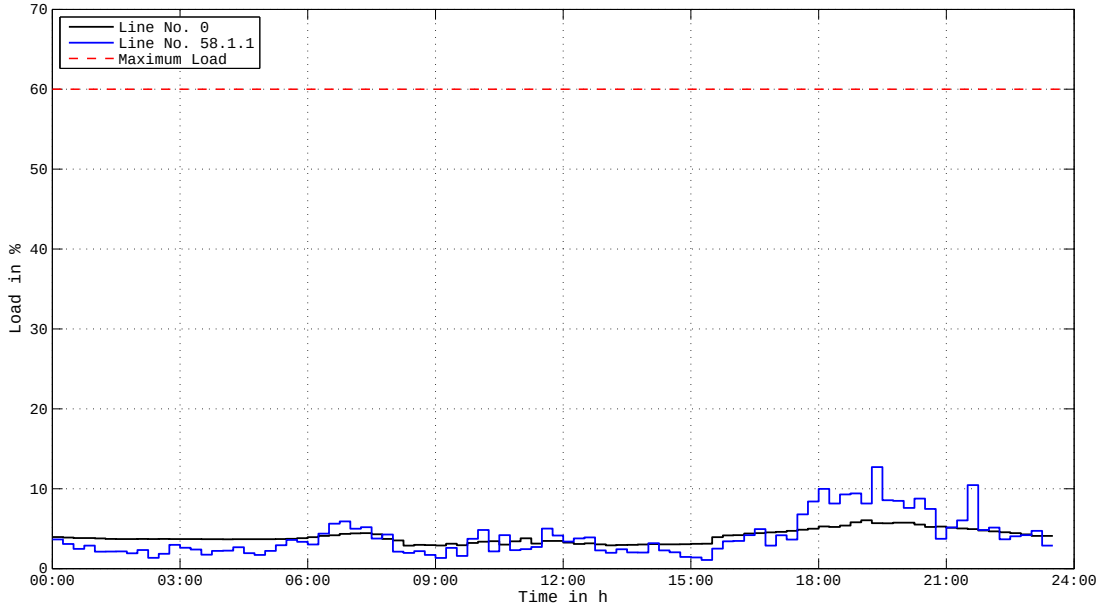

Figure A.39.: R2040 - Load of line No. 0 and No. 58.1.1

A.0.7. Scenario R-2020

In the scenario 2020 photovoltaic gains a share of 20%, electric mobility 10% and the household loads 20% above today's value. Figure A.41 indicates a highly fluctuating characteristic at the first feeder of subgrid No. 58 due to the probabilistic generation of these profiles. It is obvious if the scenario 2040 does not violate any load limits, this current scenario will definitely also not violate load thresholds. However, according to figure A.43 the voltage reaches its limit at 19:30 for half an hour.

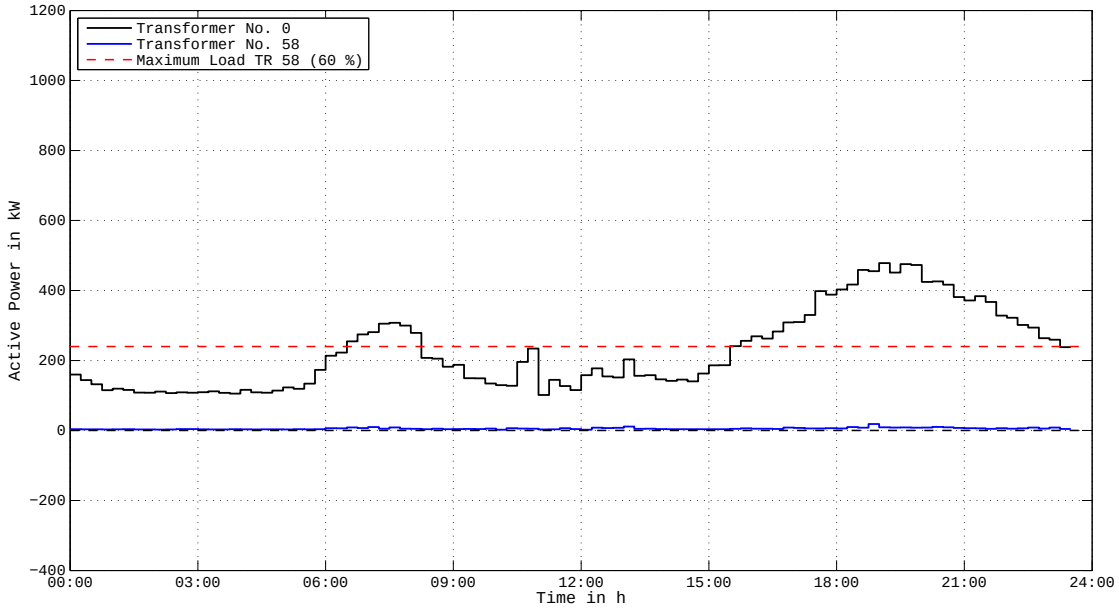

Figure A.40.: R2020 - Active power of transformer No. 0 (110/10 kV, 40 MVA) and No. 58 (110/20 kV, 400 kVA)

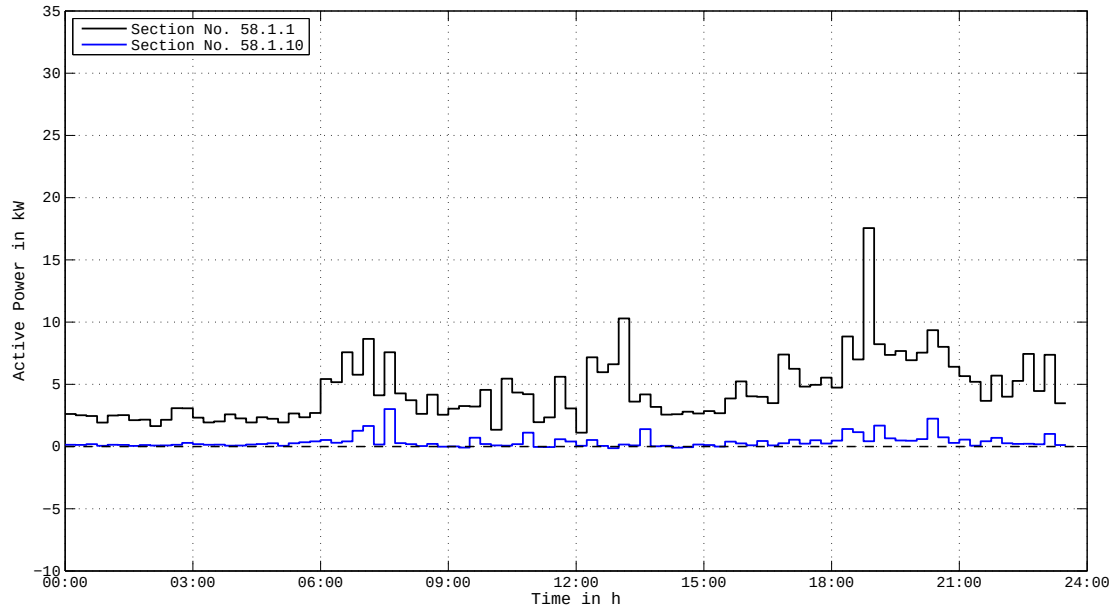

Figure A.41.: R2020 - Active power of section No. 58.1.1 and No. 58.1.10

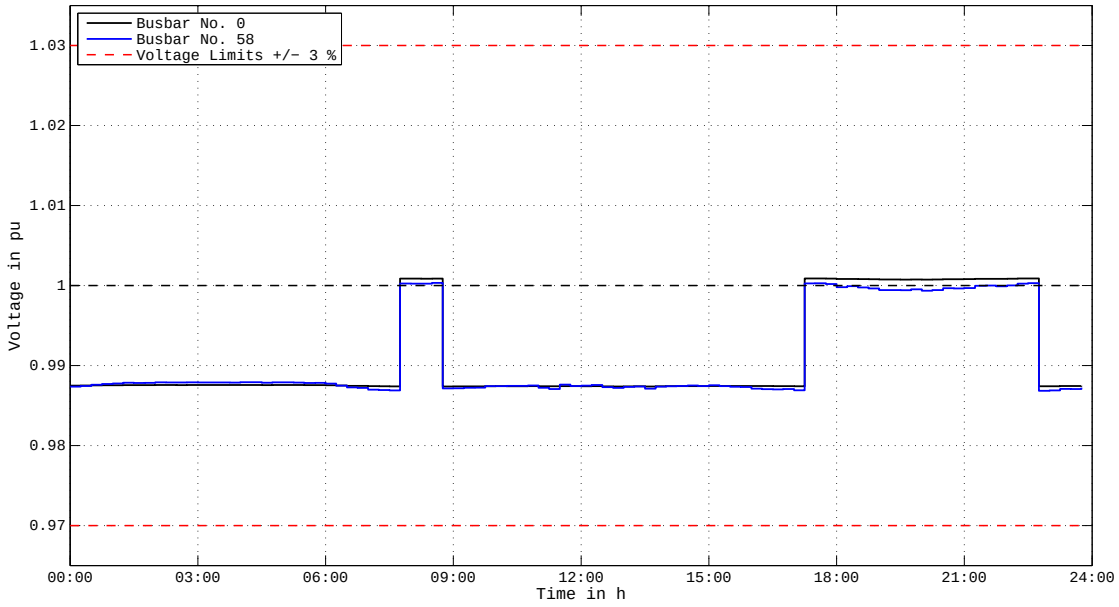

Figure A.42.: R2020 - Voltage of busbar No. 0, No. 58

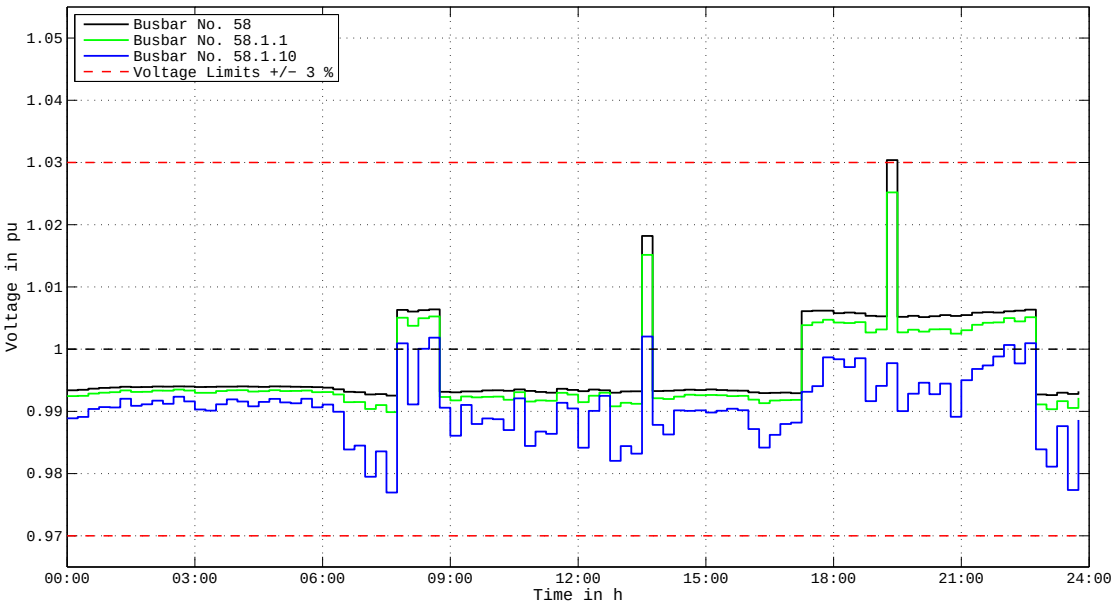

Figure A.43.: R2020 - Voltage of busbar No. 58.1., No. 58.1.1 and No. 58.1.10

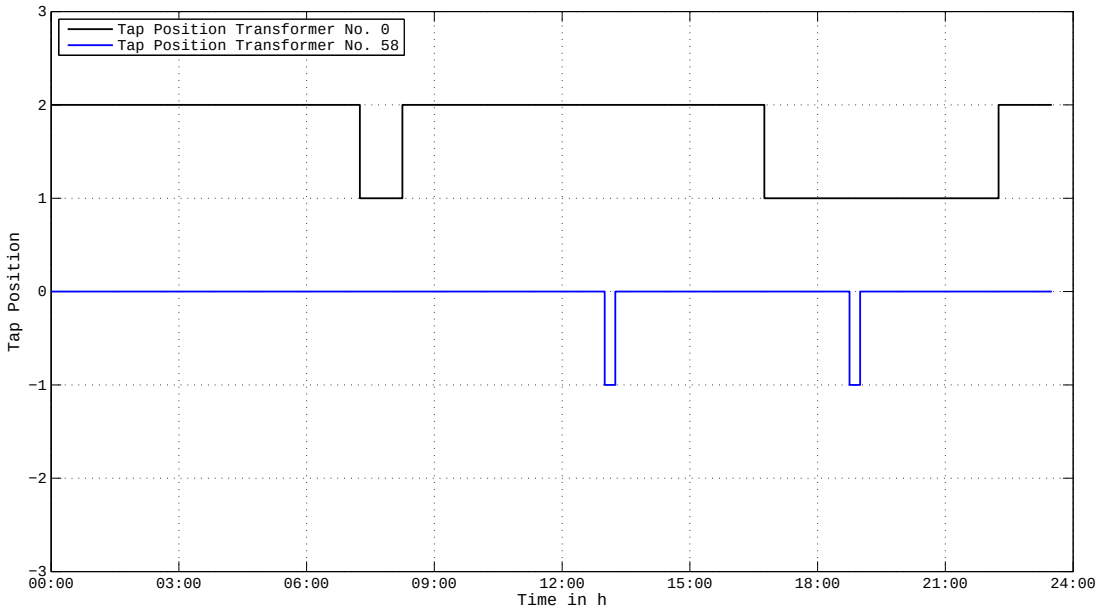

Figure A.44.: R2020 - Tap positions of transformer No. 0 (110/10 kV, 40 MVA) and No. 58 (110/20 kV, 400 kVA)

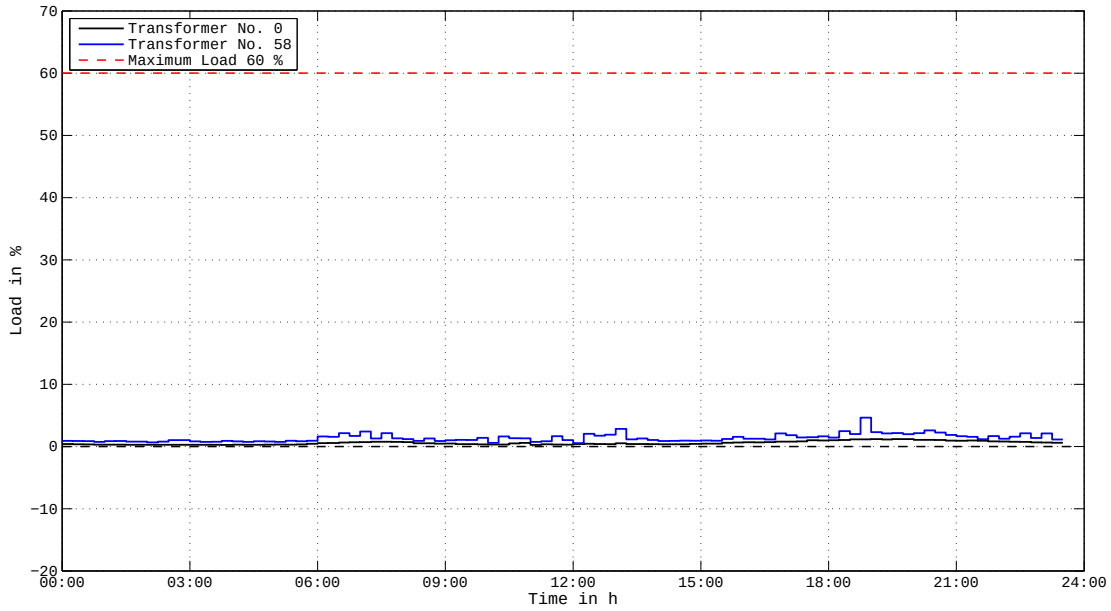

Figure A.45.: R2020 - Load of transformer No. 0 (110/10 kV, 40 MVA) and No. 58 (110/20 kV, 400 kVA)

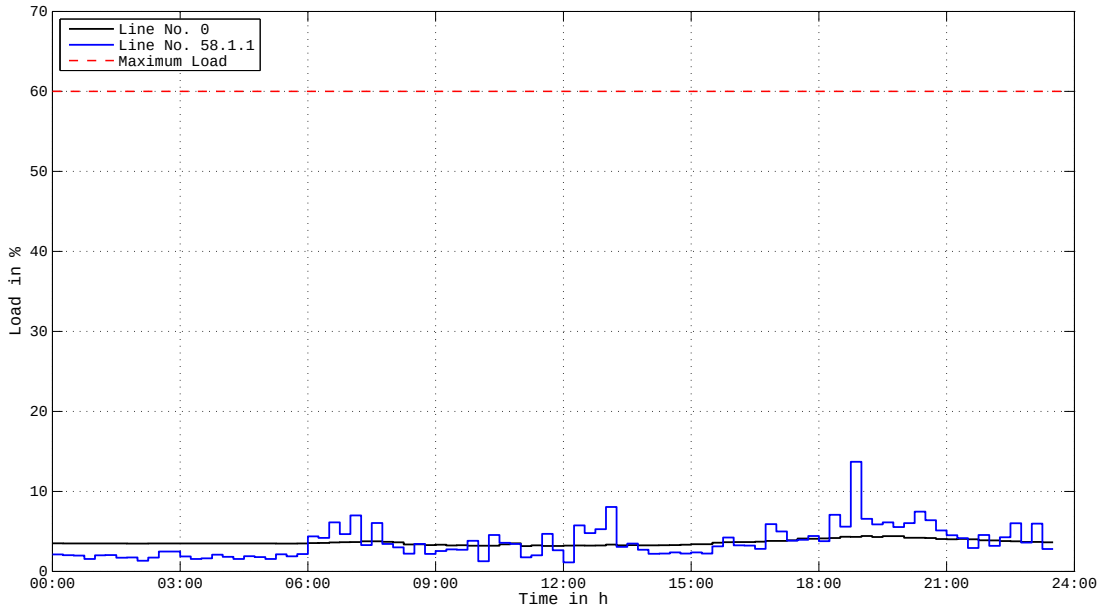

Figure A.46.: R2020 - Load of line No. 0 and No. 58.1.1